

# Book of Abstracts

## APMAS 2019



## **Disclaimer**

This book contains abstracts approved by the Congress Review Committee. Authors are responsible for the content and accuracy.

Opinions expressed may not necessarily reflect the position of the international scientific council of APMAS 2019.

## **Editorial Board**

Ahmet Yavuz Oral

Zehra Banu Oral

Mehmet Sezer

Mehmet Emre Aköz

Seda Kol

Onur Alp Aksan

Vala Can Aşkan

Gamze Sekicek

# **9<sup>th</sup> International Advances in Applied Physics & Materials Science Congress & Exhibition (APMAS 2019)**

**Oludeniz/Mugla - Turkey**

**October 22-28, 2019**

## Invited Speakers

Alexey Mironov	ISP SB RAS, Russian Federation
Andreja Bencan Golob	Jozef Stefan Institute, Slovenia
Andreja Gajovic	Ruđer Bošković Institute, Croatia
Arkady Zhukov	University of Basque Country, Spain
Bohdan Padlyak	University of Zielona Góra, Poland
Chanapa Kongmark	Kasetsart University, Thailand
Diya Alhaq Alsafadi	Royal Scientific Society, Jordan
Dong-Joo Lee	Yeungnam University, Republic of Korea
Farid Abed	American University of Sharjah, United Arab Emirates
Felix N. Chukhovskii	Shubnikov Institute of Crystallography, Federal Scientific Research Centre "Crystallography and Photonics", Russian Academy of Sciences, Russia
Gabriel Potirniche	University of Idaho, USA
George Kalosakas	University of Patras, Greece
Guillaume Nataf	University of Cambridge, UK
Guozhang Wu	East China University of Science & Technology, China
Hamza Cansever	Helmholtz Zentrum Dresden-Rossendorf- Institute of Ion Beam Physics and Materials Research, Germany
Hendrik Oktendy Lintang	Universitas Ma Chung, Indonesia
Illia Fedorin	National Technical University of Ukraine Igor Sikorsky Kyiv Polytechnic Institute, Ukraine
Jan Vcelak	CVUT UCEEB, Czech Republic
Jinyang Xu	Shanghai Jiao Tong University, China
Jiri Brozek	University of Chemistry and Technology Prague, Czech Republic
John Nicholas Karadelis	Coventry University, UK
Marjeta Maček Kržmanc	Jožef Stefan Institute, Slovenia
Marta Galbiati	Unité Mixte de Physique CNRS/Thales, France
Matsuo Masaru	Dalian University of Technology, China
Nasrin Al Nasiri	Imperial College London, UK
Nerija Zurauskiene	Center for Physical Sciences and Technology, Lithuania

Petar Petrov	Institute of Polymers – BAS, Bulgaria
Pinqiang Dai	Fujian University of Technology, China
Rashid K. Abu Al-Rub	Khalifa University, United Arab Emirates
Satoshi Kokado	Shizuoka University, Japan
Tatheer Zahra	Queensland University of Technology, Australia
Victor Rouco Gomez	CNRS Thales, Université Paris-Sud, France
Vitezslav Benda	Czech Technical University in Prague, Czech Republic
Yuan Yuan	Chongqing University, China
Yu-Qing Lou	Tsinghua University, China
Zhen Wu	Xi'an Jiaotong University, China
Zvezdana Bascarevic	Institute for Multidisciplinary Research Belgrade University, Serbia

<b>Chair</b>	
Ahmet Yavuz Oral	Gebze Technical University, Turkey

**Scientific Committee**

Andrei Turutin	National University of Science and Technology MISIS, Russia
Anouar Acheghaf	Abdelmalek Essadi university, Morocco
Brajesh Pandey	Symbiosis Institute of Technology, India
Claudio Rodrigo Cuevas Henríquez	Federal University of Pernambuco, Brazil
Danica Zmejkosk	University of Belgrade, Serbia
Didem Sen Karaman	Izmir Katip Celebi University, Turkey
Gabriel Potirniche	University of Idaho, USA
George Kalosakas	University of Patras, Greece
Guillaume Nataf	University of Cambridge, UK
Guozhang Wu	East China University of Science and Technology
Iftikhar Ahmad	King Saud University, Saudi Arabia
Illia Fedorin	National Technical University of Ukraine
Israel Sánchez Domínguez	UNAM, Mexico
Jianlin Wang	University of Science and Technology of China, China
Jianxin Geng	Beijing University of Chemical Technology, China
Jinyang Xu	Shanghai Jiao Tong University, China
Karen Ghazaryan	Institute of Mechanics of National Academy of Sciences, Armenai
Miroslav Cvetinov	University of Novi Sad, Serbia
Neeru Bhagat	Symbiosis Institute of Technology, India
Nerija Žurauskienė	Center for Physical Sciences and Technology, Lithuania
Rashid K. Abu Al-Rub	Khalifa University of Science and Technology, Abu Dhabi, UAE
Rizwan Ahmed Malik	Changwon National University, South Korea
Shafaqat Siddique	Technische Universität Dortmund, Germany
Silvester Tursiloadi	Indonesian Institute of Sciences, Indonesia
Tatheer Zahra	Queensland University of Technology, Australia

Tetiana Prikhna	National Academy of Sciences of Ukraine, Ukraine
Vitezslav Benda	Czech Technical University in Prague, Czech Republic
Weidong Song	Beijing Institute of Technology, China
Xavier Moya	University of Cambridge, UK
Xiaolong Liu	Chinese Academy of Sciences, China
Yuan Yuan	Chongqing University, China
Zhen Wu	Xi'an Jiaotong University, China
Zvezdana Bascarevic	Institute for Multidisciplinary Research, University of Belgrade, Serbia

## Organizing Committee

Ahmet Yavuz Oral	Gebze Technical University, Turkey
Ersin Kayahan	Kocaeli University, Turkey
M. Alper Sahiner	Seton Hall University, USA
Banu Oral	Gebze Technical University, Turkey
Bassim H. Hameed	Universiti Sains Malaysia, Malaysia
Tarik Talib Issa Al-Omran	University of Baghdad, Iraq
John Karadelis	Coventry University, UK

## INVITED SPEAKERS

**Id-1140**

### **$\beta$ -Relaxation Governs Damping Stability of Phenol/Acrylate Hybrids**

Guozhang Wu, Gaopeng Shi

Shanghai Key laboratory of Advanced Polymeric Materials, School of Materials Science and Engineering, East China University of Science & Technology, Shanghai 200237, China

Corresponding author: wgz@ecust.edu.cn

**Abstract:** The noncovalent bonding-induced self-assembly and multifunctionalization of small molecule/macromolecule hybrids are pivotal topics in recent scientific research. Hindered phenols have been reported effective to remarkably enhance the damping property of acrylic polymers. However, many of these small molecules easily self-aggregate and subsequently form complex crystals, which ultimately degrade the effectiveness of sound attenuation and vibration damping. In this work, the long-term stability of the novel damping materials was investigated and the results were correlated to hierarchical relaxation of the acrylic mixtures. We were surprised by the fact that  $\beta_{fast}$  relaxation of the mixture governs the damping stability. Further experimental results revealed that long distance diffusion of small molecules to self-aggregation and subsequent crystallization is determined by  $\beta_{JC}$  relaxation. It is  $\beta_{fast}$  relaxation that controls the anomalous diffusion within a limited spatial distance where the small molecules fluctuate to break down the intermolecular hydrogen bonding between the hydroxyl group of phenols and the carboxyl group of acrylates. These results not only provide a strategy for rapidly evaluating the service life of the new damping materials, but also help to clarify the mechanism of the small-molecule-enhanced damping.

**Keywords:** Polymeric Damping Materials;  $\beta$ -Relaxation; Long-term Stability

## INVITED SPEAKERS

Id-1154

**Computational Design of Novel High-Capacity Mg-Based Materials for Hydrogen Storage**

Zhen Wu, Chenhui QIAN, Zaoxiao Zhang

School of Chemical Engineering and Technology, Xi'an Jiaotong University, Xi'an, Shaanxi, 710049, P.R. China

Corresponding author: wuz2015@xjtu.edu.cn

**Abstract:** Today, energy crisis and environment pollution are serious challenges for human being. It becomes an urgent demand to develop a clean and renewable energy to replace the traditional fossil energy. Hydrogen, an ideal carrier of renewable energy, with the advantages of abundance on Earth, high energy density and pollution-free utilization. In view of intermittent of hydrogen energy for utilization, hydrogen storage technology plays an important role on achieving large-scale applications of hydrogen energy. Solid-state hydrogen storage, with the advantages of safety and efficiency, has been recognized as a practical approach. Mg-based hydride is expected to be one of the most promising solid-state hydrogen storage materials due to its good security, low cost, high capacity and volumetric density. However, Mg-based hydride has a serious drawback needed to be reckoned with, which is poor thermodynamic properties caused by the strong interactions between the atoms of Mg-based hydride. In order to improve the thermodynamic properties, the method of doping elements into Mg-based hydride has been performed using the first-principles study. In our work, several kinds of doping modes, including interstitially doping metalloid and nonmetal, doubly doping interstitial nonmetals and co-doping transition metal + nonmetal, have been attempted with the purpose of improving the thermodynamics of Mg-based hydride. Some novel Mg-based hydrides, such as Mg-Ni-B-H, Mg-Ni-N-H and Mg-Ni-B-N-H, are designed as hydrogen storage materials through the computational simulation. And the hydrogen storage properties of these novel materials are predicted based on the first-principles calculations. The calculation results show that the modified Mg-based hydrides always have the better hydrogen storage properties than the pristine counterpart. For example, the  $\text{Mg}_{0.8}\text{Ni}_{0.2}(\text{BH}_4)_{1.8}(\text{NH}_2)_{0.2}$  hydride could desorb about 9.7 wt.% of  $\text{H}_2$  at a moderate temperature (about 85 °C), which meets the required target of U.S. Department of Energy (DOE) for on-board hydrogen storage.

**Keywords:** Hydrogen storage; Computational design; Mg-based hydride; Element doping

## INVITED SPEAKERS

**Id-1184**

### **Topology States of Iso-Frequency Surfaces of a Hypercrystal with Ferrite and Semiconductor Layers**

Illia Fedorin

National Technical University of Ukraine "Igor Sikorsky Kyiv Polytechnic Institute", 37, Prosp. Peremohy, Kyiv  
03056, Ukraine

Corresponding author: fedorin.ilya@gmail.com

**Abstract:** Photonic hypercrystals are a class of artificial materials, which combines the most interesting features of hyperbolic metamaterials and photonic crystals. They are formed by alternating layers of hyperbolic medium and either a dielectric or metallic material. The hypercrystals allow a number of unique properties, like an unprecedented degree of control of light, subdiffraction-limit localization of light, etc. [1].

Recently, researchers have found that a comprehensive study of topology states of dispersion surfaces provides unique insight into the physics of materials. Interest in such research is even more increased since topological materials show promise in wide range of potential applications in the devices of photonics and optoelectronics, like in faster, more efficient computer chips or quantum computers in wide ranges of wavelengths [2].

Therefore, the main subject of the current paper is to study the properties of iso-frequency surfaces of the artificial photonic hypercrystal, which is composed of periodically arranged ferrite-dielectric and semiconductor-dielectric metamaterials. The system is placed into an external magnetic field parallel to the boundaries of the layers. The effective medium theory is applied in order to derive the effective permittivity and permeability tensor components of the constituent metamaterials and hypercrystal. Usually, characteristic resonance frequencies of ferrite and semiconductor layers are confined to the microwave and THz range, respectively. However, influence of the external magnetic field allows effective control over the properties of the constituent layers of the hypercrystal, including the location of ferromagnetic resonance frequency, plasma frequency and/or hybrid frequencies within the single frequency band under certain condition.

**Keywords:** Hypercrystals, photonic structures, metamaterials, semiconductors, ferrites

#### **References:**

- [1] I. Fedorin, Electrodynamic properties of a hypercrystal with ferrite and semiconductor layers in an external magnetic field, *Superlattices and Microstructures*, vol. 113, pp. 337-345, 2018.
- [2] T. Ozawa, H. M. Price, A. Amo, N. Goldman, M. Hafezi, L. Lu, M. C. Rechtsman, D. Schuster, J. Simon, O. Zilberberg, and I. Carusotto, *Topological photonics*, *Rev. Mod. Phys.* vol. 91, pp. 015006, 2019.

## INVITED SPEAKERS

**Id-1219**

### **Stress- induced Magnetic Anisotropy Enabling Engineering of Magnetic Softness and Domain Wall Dynamics of Fe-rich Amorphous Microwires**

Arcady Zhukov<sup>1,2,3</sup>, Paula Corte-Leon<sup>1,2</sup>, Mihail Ipatov<sup>1,2</sup>, Lorena Gonzalez-Legarreta<sup>1,2</sup>, Juan Maria Blanco<sup>2</sup>,  
Valentina Zhukova<sup>1,2</sup>

<sup>1</sup>Dept. Phys. Mater., University of Basque Country, UPV/EHU San Sebastián 20018, Spain

<sup>2</sup>Dpto. de Física Aplicada, EUPDS, UPV/EHU, 20018, San Sebastian, Spain

<sup>3</sup>IKERBASQUE, Basque Foundation for Science, 48011 Bilbao, Spain

Corresponding author: arkadi.joukov@ehu.es

**Abstract:** Amorphous glass-coated microwires can present excellent magnetic properties such as magnetic bistability, enhanced magnetic softness and Giant Magnetoimpedance (GMI) effect and fast domain wall dynamics. Excellent magnetic softness and GMI effect have been reported for Co-rich microwires, while Co belongs to critical materials. Therefore, Fe-rich microwires are preferable for the applications, but they exhibit high magnetostriction coefficient and hence present low GMI effect.

We present our recent experimental results on influence of stress- annealing on magnetic softness and GMI effect of Fe- rich glass-coated microwires.

We observed that stress-annealed at appropriate annealing conditions Fe-rich microwires (time, stress and temperature) can present low coercivity, considerable magnetic softening, enhanced GMI effect or extremely fast domain wall propagation.

For interpretation of observed changes of hysteresis loops after stress annealing, we considered internal stresses relaxation and different mechanisms of stress-induced anisotropy.

Observed versatile properties of stress annealed Fe-rich microwires make them suitable for technological applications.

**Keywords:** Magnetic microwires, domain wall propagation, magnetic anisotropy, internal stresses

#### **References:**

[1] A. Zhukov, M. Ipatov and V. Zhukova, Advances in Giant Magnetoimpedance of Materials, *Handbook of Magnetic Materials*, ed. K.H.J. Buschow, 24: chapter 2 (2015) 139-236.

## INVITED SPEAKERS

Id-1228

**Magnetic Materials Based on Dinuclear Copper (II) Trimethoxybenzoates**

Masahiro Mikuriya<sup>1</sup>, Chihiro Yamakawa<sup>1</sup>, Kensuke Tanabe<sup>1</sup>, Raigo Nukita<sup>1</sup>, Yuki Amabe<sup>1</sup>, Daisuke Yoshioka<sup>1</sup>,  
Ryoji Mitsunashi<sup>2</sup>, Hidekazu Tanaka<sup>3</sup>, Makoto Handa<sup>3</sup>

<sup>1</sup>School of Science and Technology, Kwansai Gakuin University, 669-1337, Sanda, Japan

<sup>2</sup>Institute of Liberal Arts and Science, Kanazawa University, 920-1192, Kanazawa, Japan

<sup>3</sup>Interdisciplinary Graduate School of Science and Engineering, Shimane University, 690-8540, Matsue, Japan

Corresponding author: junpei@kwansai.ac.jp

**Abstract:** Copper acetate compounds have attracted much attention from chemists and physicists for a long period because of their antiferromagnetic Cu<sub>2</sub> core and potential application to inorganic-organic composite materials [1,2]. Chain compound of copper(II) benzoate with pyrazine showed an antiferromagnetic coupling within the Cu<sub>2</sub> core and a gas-adsorption property for N<sub>2</sub> [3], where the aromatic benzoate groups made a hydrophobic micropore [4]. We have engaged in synthetic work on copper(II) benzoates with substituent groups in order to understand the magnetic properties and adsorption properties of this type of complexes [5,6]. In this study, we introduced three methoxy groups at the different positions of the benzoate group in order to examine the effects on the complex formation (Fig. 1). The isolated complexes were characterized by measurements of elemental analysis, IR and UV-vis spectra, and temperature dependence of magnetic susceptibility. Crystal structures were determined by the single-crystal X-ray diffraction method for the isolated compound. Gas-adsorption behavior was also investigated for N<sub>2</sub>. We will discuss on the magnetic and adsorption properties based on the crystal structures.

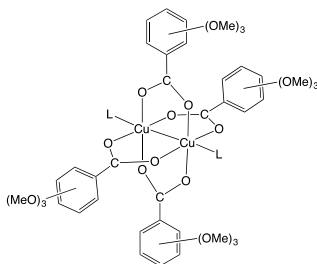


**Fig. 1.** Dinuclear copper(II) trimethoxybenzoate.

**References:**

- [1] M. Mikuriya, *Bull. Jpn. Soc. Coord. Chem.*, **2008**, *52*, 17-28.
- [2] M. Mikuriya R. Indrawati, R. Hashido, S. Matsubara, C. Nakamura, D. Yoshioka, K. Yokota, M. Fukuzaki, and M. Handa, *Magnetochemistry*, **2018**, *4*, 22.
- [3] R. Nukada, W. Mori, S. Takamizawa, M. Mikuriya, M. Handa, H. Naono, *Chem. Lett.*, **1999**, 367-368.
- [4] R. Nukada, M. Mikuriya, M. Handa, H. Naono, *The Proceedings of the 2nd International Porous and Powder Materials Symposium and Exhibition PPM 2015*, S. K. Ozdemir, M. Polat, M. Tanoglu, Eds. Izmir, Turkey, **2015**, pp. 77-81.
- [5] M. Mikuriya, C. Yamakawa, K. Tanabe, D. Yoshioka, R. Mitsunashi, H. Tanaka, and M. Handa, *J. Turkish Chem. Soc., Sect. A*, **2018**, *5(sp.is.1)*, 103-110.
- [6] M. Mikuriya, C. Yamakawa, N. Masuda, D. Yoshioka, S. Yamaguchi, H. Yamada, T. Mizuta, N.

Kawata, H. Tanaka, and M. Handa, *Open Chem. J.*, **2019**, 6, 19-26.

## INVITED SPEAKERS

Id-1296

### Designing Domain Walls in Bismuth Ferrite by Controlling the Type and Concentration of Defects

Andreja Bencan Golob<sup>1,2</sup>, G. Dražič<sup>1,2,4</sup>, Hana Uršič<sup>1,4</sup>, Maja Makarovič<sup>1,4</sup>, Matej Komelj<sup>3</sup>, Tadej Rojac<sup>1,4</sup>

<sup>1</sup> Electronic Ceramics Department, Jožef Stefan Institute, Ljubljana, Slovenia

<sup>2</sup> Jožef Stefan International Postgraduate School, 1000 Ljubljana, Slovenia

<sup>3</sup> Department for Nanostructured Materials, Jozef Stefan Institute, Ljubljana, Slovenia.

<sup>4</sup> Jožef Stefan International Postgraduate School, 1000 Ljubljana, Slovenia

Corresponding author: andreja.bencan@ijs.si

**Abstract:** Domain walls (DWs), which in ferroelectrics separate two domain regions of uniform spontaneous polarization, may exhibit a different local structure and functional properties to those of the matrix. For example, in otherwise insulating bulk BiFeO<sub>3</sub> (BFO), the ferroelectric DWs are known to possess high electrical conductivity. Local DW properties importantly influence the functional response of polycrystalline BFO, but even more intriguing is their use in “domain wall nanoelectronics” technology. Recently, an important step towards the understating of the DW conductivity in BFO was made. Using atomically resolved aberration-corrected scanning transmission electron microscopy (STEM), we explained the extrinsic nature of the DW conduction mechanism in BFO by identifying Fe<sup>4+</sup> charged defects, which segregate at the DWs along with Bi vacancies.

In this presentation we will show that DWs conductivity in bulk BFO can be tailored by controlling the type and concentration of point defects using different processing conditions (temperature, atmosphere, cooling rates). With the support of different microscopy methods down to the atomic level, and by applying the results of ab-initio calculations, we will explain how different processing conditions affect DW thickness, shape, local unit-cell distortion and the type and concentration of the defects at DW. We will correlate these structural features with local DW conductivity and finally with a macroscopic electro-mechanical response of bulk BFO.

**Keywords:** Bismuth ferrite, domain walls, point defects, scanning transmission electron microscopy

**Acknowledgements:** This work was supported by the Slovenian Research Agency within programs P2-0105, P2-0393 and projects J2-9253, PR-08298.

## INVITED SPEAKERS

Id-1319

## Heat Resistance of Conductive Filler-Polymer Composites Evaluated by Dynamic Tensile Modulus under Electric field and Dielectric Measurement

Masaru Matsuo, Yuezhen Bin

Department of Polymer Science and Materials, Dalian University of Technology, Dalian 116024, China

mm-matsuo@live.jp

**Abstract:** In attempt to study mechanical and structural stabilities of heat-resistant polymer and conductive filler composites by Joule heat, polyimide (PI)-vapor grown carbon fiber (VGCF) composites were fabricated by in situ polymerization to realize excellent dispersion of VGCFs in PI matrix. In addition to X-ray diffraction, dynamic tensile modulus was measured to investigate frequency-temperature dependence under electric field. As the results, the change in the storage modulus by Joule heat was almost equal to well-known change by external forced heating indicating that the PI-VGCF composites were very stable to Joule heat. The electric current mechanism was analyzed theoretically in terms of thermal fluctuation-induced tunneling conduction. To do so, the VGCF/PI boundary resistance must be evaluated. However, the measurement by DC current provides only the average resistance of the specimen system. Accordingly, the analysis was done by curve fitting for complex impedances between the experimental result and theoretical curve calculated using equivalent circuit model with a series arrangement of several units containing resistance and capacitance. Figure 1 shows an example for vapor-grown carbon fiber (VGCF) and polyimide (PI). Based on the good fitting between experimental and theoretical results about impedance as a function of frequency, the DC component at frequency  $\rightarrow 0$  provides electric current behavior in relation to the morphology of the composites, that is, interference resistance between electrode and composition, VGCF/PI boundary resistance and VGCF resistance. Based on the predicted VGCF/PI boundary resistance, the tunneling current is found to be governed by average surface area ( $A$ ) of the fillers over which most of tunneling occurs, rather than the gap distance ( $D$ ) between adjacent semi-conductive fillers (see Figure 2). No change in  $D$  against Joule heat indicated the good heat resistance of the composites.

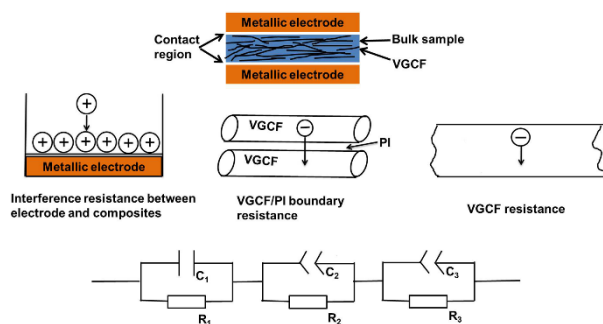


Figure 1

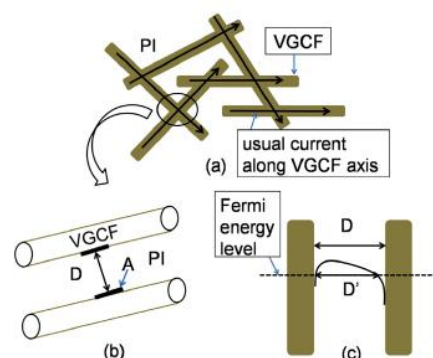


Figure 2

## INVITED SPEAKERS

**Id-1345**

### **Novel Types of Additively Manufactured Micro-architected Multifunctional Shell-Based Cellular Materials**

Rashid Abu Al-Rub<sup>1,2</sup>, Oraib Al-Ketan<sup>1</sup>, Rachid Rezgui<sup>3</sup>, Reza Rowshan<sup>3</sup>

<sup>1</sup>Advanced Digital & Additive Manufacturing Center, Khalifa University of Science and Technology, Abu Dhabi, UAE

<sup>2</sup>Aerospace Engineering Department, Khalifa University of Science and Technology, Abu Dhabi, UAE

<sup>3</sup>Core Technology Platforms, New York University Abu Dhabi, Abu Dhabi, UAE

Corresponding author: rashid.abualrub@ku.ac.ae

**Abstract:** In nature, biological systems exhibiting topological hierarchy that spans over multiple length scales show extraordinary multifunctional properties. Mimicking these architectural features can lead to the creation of man-made lightweight, yet mechanically robust and smart materials. Despite their complexity, the emergence of advanced fabrication techniques such as additive manufacturing (or 3D printing) that can achieve complex architectures at small scales (i.e., nanometer and micrometer) facilitated the fabrication of such topologies. In this work, the fabrication, characterization, mechanical testing, and modeling of novel types of micro-architected nature-inspired and periodic cellular materials (or lattices) are presented. The proposed lattices are based on the mathematically-known triply periodic minimal surfaces (TPMS). These shell-based micro-architected metamaterials with high geometrical complexity were fabricated with feature sizes in the order of several microns using the direct laser writing two-photon lithography technique. The material orientation in the TPMS-based lattices alternates between different geometrical segments providing much efficient load-bearing capacity as compared to strut-based lattices. These TPMS-based lattices are proved to be ideal candidates in many engineering applications such as catalytic substrates, electrodes for batteries, heat exchangers, heat sinks, cores of sandwich panels, etc. Such applications will be discussed in this work.

**Keywords:** Architected materials, 3D printing, metamaterials, mechanical properties

## INVITED SPEAKERS

**Id-1348**

### **Effect of the Silver on Enhancement of Luminescence of the RE<sup>3+</sup> Ions in Borate Glasses**

Bohdan Padlyak<sup>1,2</sup>, Ihor Kindrat<sup>1</sup>

<sup>1</sup>University of Zielona Góra, Institute of Physics, Division of Spectroscopy of Functional Materials, 4a Szafrana Str., 65-516 Zielona Góra, Poland

<sup>2</sup>Vlokh Institute of Physical Optics, Sector of Spectroscopy, 23 Dragomanov Str., 79-005 Lviv, Ukraine

Corresponding author: B.Padlyak@if.uz.zgora.pl

**Abstract:** The lithium tetraborate (Li<sub>2</sub>B<sub>4</sub>O<sub>7</sub>) glasses, co-doped with rare-earth (RE = Eu, Sm) and silver (Ag), as new luminescent materials were detailed investigated using conventional electron paramagnetic resonance (EPR) and optical spectroscopy techniques. The EPR, optical absorption, emission, and luminescence excitation spectra as well as luminescence decay kinetics of the Ag<sup>+</sup>, Eu<sup>3+</sup>, and Sm<sup>3+</sup> centres in the RE-Ag co-doped Li<sub>2</sub>B<sub>4</sub>O<sub>7</sub> glasses were detailed investigated and analysed [1,2]. Measured values of external quantum yield (QY) clearly show significant enhancement of the Eu<sup>3+</sup> (red emission) and Sm<sup>3+</sup> (orange-red emission) luminescence intensity in the Li<sub>2</sub>B<sub>4</sub>O<sub>7</sub>:Eu,Ag (QY = 26.1 %) and Li<sub>2</sub>B<sub>4</sub>O<sub>7</sub>:Sm,Ag (QY = 29.1 %) glasses in comparison with Li<sub>2</sub>B<sub>4</sub>O<sub>7</sub>:Eu (QY = 11.7 %) and Li<sub>2</sub>B<sub>4</sub>O<sub>7</sub>:Sm (QY = 20.4 %) glasses [1,2]. The observed relatively high values of the Eu<sup>3+</sup> and Sm<sup>3+</sup> quantum yield of luminescence in the Li<sub>2</sub>B<sub>4</sub>O<sub>7</sub>:Eu,Ag and Li<sub>2</sub>B<sub>4</sub>O<sub>7</sub>:Sm,Ag glasses have been explained by excitation energy transfer from Ag<sup>+</sup> ions and molecular-like Ag nanoclusters to the Eu<sup>3+</sup> and Sm<sup>3+</sup> ions as well as local field effects, induced by surface plasmon resonance of Ag nanoparticles. Potential applications of the Li<sub>2</sub>B<sub>4</sub>O<sub>7</sub>:Eu,Ag and Li<sub>2</sub>B<sub>4</sub>O<sub>7</sub>:Sm,Ag glasses as promising luminescent materials of the visible spectral range, including solar cells working in regions with intense UV radiation, are considered.

**Keywords:** Borate glasses, trivalent rare-earth ions (RE<sup>3+</sup>), silver ions and nanoparticles, EPR, luminescence, decay kinetics, energy transfer

#### **References:**

- [1] I.I. Kindrat, B.V. Padlyak, B. Kukliński, A. Drzewiecki, V.T. Adamiv, J. Lumin. 204 (2018) 122–129.  
[2] I.I. Kindrat, B.V. Padlyak, B. Kukliński, A. Drzewiecki, V.T. Adamiv, J. Lumin. 213 (2019) 290–296.

## INVITED SPEAKERS

**Id-1354**

### **Study on Microstructure and Properties of High-Entropy Alloys Prepared by Powder Metallurgy**

Pinqiang Dai<sup>1,2,3</sup>, Zhanjiang Li<sup>1</sup>

<sup>1</sup> College of Materials Science and Engineering, Fujian University of Technology, Fuzhou, 350118, China

<sup>2</sup> Fujian Provincial Key Laboratory of New Material Preparation and Forming Technology, Fuzhou 350108, China

<sup>3</sup> School of Materials Science and Engineering, Fuzhou University, Fuzhou 350116, China

Corresponding author: pqdai@126.com

**Abstract:** High entropy alloy (HEA) is a new kind of metal material developed in recent years, which usually shows superior properties to conventional alloys, such as high strength and toughness, high wear resistance, excellent thermal stability and so on. FeCoCrNiMn alloy is typical high entropy alloy with FCC structure. It has excellent ductility and fracture toughness. However, its strength and hardness are very low, which greatly limits its application as structural material. In present study, powder metallurgy technology was used to fabricate the FeCoCrNiMn system HEAs. The effect of additional elements (such as N, Ti, C and Al) on the microstructure and mechanical properties of the alloy was studied, and the mechanisms of phase formation and strengthening were revealed. This study will provide a theoretical and experimental basis for the engineering application of high-entropy alloys.

**Keywords:** High-entropy alloy, powder metallurgy, microstructure, mechanical property, strengthening mechanism

## INVITED SPEAKERS

Id-1358

**Theoretical Study on Anisotropic Magnetoresistance Effect for Ferromagnets**Satoshi Kokado<sup>1</sup>, Masakiyo Tsunoda<sup>2</sup><sup>1</sup>Graduate School of Integrated Science and Technology, Shizuoka University, Hamamatsu 432-8561, Japan<sup>2</sup>Graduate School of Engineering, Tohoku University, Sendai 980-8579, Japan

Corresponding author: kokado.satoshi@shizuoka.ac.jp

**Abstract:** The anisotropic magnetoresistance (AMR) effect is a fundamental phenomenon in which a resistivity depends on the relative angle between the current  $I$  and magnetization  $M$  directions [1-10]. The efficiency of the effect “AMR ratio” is defined by  $\Delta\rho/\rho = (\rho_{\parallel} - \rho_{\perp})/\rho_{\perp}$ , where  $\rho_{\parallel}$  ( $\rho_{\perp}$ ) is a resistivity for  $I//M$  ( $I \perp M$ ). The AMR ratio has been experimentally investigated for various ferromagnets (FMs) for the last 160 years. In particular, it has been reported that Fe [1], Co, and Ni exhibit positive AMR ratios, while Fe<sub>4</sub>N [1,2] and half-metallic FMs show negative AMR ratios. Systematic analyses for such AMR ratios, however, have been scarce so far. In addition, an intuitive explanation about the AMR effects has seldom been given.

In this study, we derived a general expression of the AMR ratio using the two-current model with all  $s$ - $d$  scattering processes [3-5]. The  $d$  states were obtained from a Hamiltonian with the spin-orbit interaction  $V_{SO}$ . Using the expression, we found a relation between the sign of the AMR ratio and the  $s$ - $d$  scattering process [3]. In addition, the AMR effects could be intuitively explained by using the  $d$  states, which are distorted by  $V_{SO}$  [4]. In a model with no crystal field, we also showed that the negative AMR ratio is a necessary condition for the half-metallic FMs [3-7].

**Keywords:** Anisotropic magnetoresistance, spin-orbit interaction, theory

**References**

- [1]. M. Tsunoda, Y. Komasaki, S. Kokado *et al.*, Appl. Phys. Express 2, 083001 (2009).
- [2]. M. Tsunoda, H. Takahashi, S. Kokado *et al.*, Appl. Phys. Express 3, 113003 (2010).  
S. Kokado, M. Tsunoda *et al.*, J. Phys. Soc. Jpn. 81, 024705 (2012).
- [3]. S. Kokado and M. Tsunoda, Adv. Mater. Res. 750-752, 978 (2013).
- [4]. S. Kokado, Y. Sakuraba, and M. Tsunoda, Jpn. J. Appl. Phys. 55, 108004 (2016).
- [5]. F. Yang, Y. Sakuraba, S. Kokado *et al.*, Phys. Rev. B 86, 020409 (2012).
- [6]. Y. Sakuraba, S. Kokado *et al.*, Appl. Phys. Lett. 104, 172407 (2014).
- [7]. T. Sato, S. Kokado *et al.*, Appl. Phys. Lett. 113, 112407 (2018).
- [8]. S. Kokado and M. Tsunoda, J. Phys. Soc. Jpn. 84, 094710 (2015).
- [9]. S. Kokado and M. Tsunoda, J. Phys. Soc. Jpn. 88, 034706 (2019).

## INVITED SPEAKERS

**Id-1373**

### **Tunnel Electroresistance in Superconducting/Ferroelectric Junctions**

Víctor Rouco<sup>1</sup>, R. El Hage<sup>1</sup>, A. Sander<sup>1</sup>, J. Grandal<sup>2</sup>, J. Briatico<sup>1</sup>, S. Collin<sup>1</sup>, J. Trastoy<sup>1</sup>, K. Bouzehouane<sup>1</sup>, A. I. Buzdin<sup>3</sup>, G. Singh<sup>4</sup>, N. Bergeal<sup>4</sup>, C. Feuillet-Palma<sup>4</sup>, J. Lesueur<sup>4</sup>, M. Varela<sup>2</sup>, J. Santamaría<sup>1,2</sup>, Javier E. Villegas<sup>1</sup>

<sup>1</sup>Unité Mixte de Physique, CNRS Thales, Université Paris-Sud, Université Paris Saclay, 91767 Palaiseau, France

<sup>2</sup>Grupo de Física de Materiales Complejos, Dpt. Física de Materiales, Universidad Complutense de Madrid, 28040 Madrid, Spain

<sup>3</sup>Univ Bordeaux, LOMA UMR CNRS 5798, F-33405 Talence, France

<sup>4</sup>Laboratoire de Physique et d'Etude des Matériaux, ESPCI Paris, Université PSL, CNRS, 75005 Paris, France

Corresponding author: vrouco@ucm.es

**Abstract:** Tunnel electroresistance (TER) is usually ascribed to the non-volatile, fast and reversible switching mechanism observed in junctions with ferroelectric barrier and different electrodes. This effect has greatly expanded electron tunneling applications such as novel memories and memristors for neuromorphic computing, and is explained by subtle mechanisms connected to the voltage-induced reversal of the ferroelectric polarization. Here we demonstrate that identical functional effects can be obtained in a much simpler geometry i.e. without any material barrier, considering an unrelated mechanism: reversible redox reaction and oxygen vacancy motion which modifies the oxide's ground-state of the electrodes.

We show that in junctions with a material barrier (ferroelectric or not), and even in systems without it (where two electrodes are in direct contact). To probe oxygen electromigration and redox reactions our junctions are based on a cuprate superconductor acting as an electrode. Its ground state is extremely sensitive to the oxygen stoichiometry and can be tracked in operando via changes in the tunnel conductance spectra. Furthermore, we extend the concept of electroresistance to the tunneling of superconducting quasiparticles, for which the switching effects increase more than one order of magnitude with respect the tunneling of normal electrons.

These results imply strong simplifications in the geometrical design of current resistive switching applications, and opens the way towards a new class of Josephson memories; a grail in the field of superconducting electronics.

**Keywords:** Ferroelectric tunnel junctions, oxygen vacancies

**Acknowledgements:** Work supported by the ERC grant N° 647100 and French ANR grant ANR-15-CE24-0008-01.

## INVITED SPEAKERS

Id-1376

### Giant Thermally Modulated and Stable Step Bunching on Epitaxially Grown SrTiO<sub>3</sub> Thin Films on Vicinal MgO (100) Terraces

Azza Hadj Youssef<sup>1</sup>, Gitanjali Kolhatkar<sup>1,2</sup>, C. Amaechi<sup>1</sup>, Alexandre Merlen<sup>3</sup>, Andreas Ruediger<sup>1</sup>

<sup>1</sup>Nanophotonics-Nanoelectronics, Centre Énergie Matériaux et Télécommunications, INRS, 1650 Lionel-Boulet

<sup>2</sup>Munich University of Applied Sciences, Department of Applied Sciences and Mechatronics, Lothstrasse 34, 80335 Munich, Germany

<sup>3</sup>IM2NP, UMR 7334 CNRS, Universités d'Aix Marseille and Toulon, France

Corresponding author: azza.hadj.youssef@emt.inrs.ca

**Abstract:** Perovskite oxides display a substantial variety of properties that have strongly impacted science and technology in the last decades because of their potential for device applications. It was early recognized that high quality thin film epitaxies could be achieved using single crystalline substrates. In addition, in the field of semiconductor technology, strain can be imposed on the deposited film through a lattice mismatch with the substrate in order to modify their physical and structural properties. Technological progress on integrating perovskite oxides in nanometric thin films requires an exhaustive control of the thin film growth, which largely depends on the substrate preparation, as well as on the growth conditions and control.

Here, we investigate the growth evolution of strontium titanate (SrTiO<sub>3</sub>) thin films on (100) magnesium oxide (MgO) substrates by tailoring and modulating the film surface morphology in order to design long-range and self-ordered nanostructures. More specifically, we grow 15 nm thin SrTiO<sub>3</sub> films on MgO (100) substrates by radio frequency-magnetron sputtering and subsequently modulate the film surface morphology by performing post-annealing at various time and temperature. The formation of smooth and highly regular steps of 15-unit cell high and about 1 μm width of organized nanostructures is obtained by performing a controlled post-annealing at 900°C and 700°C for 1 hour each under oxygen flow.

Our thin film morphology design presents a versatile template for selective thin film deposition allowing 2D nanostructures growth, but also efficient surface activity for catalytic applications and two-dimensional (2D) electron gases.

**Keywords:** Strontium titanate, growth evolution, surface modulation, self-ordered nanostructures, annealing

## INVITED SPEAKERS

**Id-1389**

### **Nanostructured Lanthanum Manganite Films Grown by Pulsed-Injection MOCVD: Tuning the Magnetoresistive Properties for Magnetic Field Sensors Applications**

Nerija Zurauskiene<sup>1,2</sup>, Voitech Stankevici<sup>1,2</sup>, Skirmantas Kersulis<sup>1</sup>, Valentina Plausinaitiene<sup>1,3</sup>, Milita Vagner<sup>1,3</sup>,  
Vakarlis Rudokas<sup>1</sup>, Saulius Balevicius<sup>1</sup>

<sup>1</sup>Department of Functional materials and Electronics, Center for Physical Sciences and Technology,  
Sauletekioave. 3, LT-10257 Vilnius, Lithuania

<sup>2</sup>Faculty of Electronics, Vilnius Gediminas Technical University, Naugarduko 41, LT-03227 Vilnius, Lithuania

<sup>3</sup>Institute of Chemistry, Faculty of Chemistry and Geosciences, Vilnius University, Naugarduko 24, LT-03225  
Vilnius, Lithuania

Corresponding author: nerija.zurauskiene@ftmc.lt

**Abstract:** An increasing demand of magnetic field sensors with high sensitivity in a wide range of magnetic fields and operating temperatures has resulted in numerous investigations of physical phenomena in advanced materials and fabrication of novel magnetoresistive devices. The commercialized magnetic sensors based on so-called xMR magnetoresistive effects (anisotropic AMR, giant GMR and tunnelling TMR) [1] are becoming one of the mostly important components in information technologies as well as for application areas in medical and consumer electronics. Recently it was demonstrated that colossal magnetoresistance (CMR) effect can be employed for the development of magnetic field sensors which measure the magnitude of magnetic fields up to megagauss (B-scalar sensors) [2]. The existing commercial pulsed magnetic field meters based on xMR or Hall sensors [1,3] could measure the magnetic field magnitude with high accuracy only when field direction is known in advance. However, such sensors cannot be applied in pulsed magnetic field cases if both the magnitude and the direction of the field may change simultaneously. In such case a three-axis combination of the sensors can be used, but it limits frequency range of the meter. The demand for fast high magnetic field B-scalar sensors which can measure the magnitude of magnetic fields is increasing rapidly due to the development of advanced scientific and industrial devices and techniques such as non-destructive pulsed-field magnets, pulsed-field joining, forming and welding apparatus, mass acceleration, plasma monitoring, contactless high current measurement techniques, etc. Each application has specific requirements for the sensor fabrication, its specifications, magnetic field and temperature ranges of operation and accuracy.

It has been demonstrated that CMR-B-scalar sensors based on nanostructured (polycrystalline with nanosized grains) lanthanum manganite films can be successfully used for the development of CMR-B-scalar sensors, which are capable to measure the magnitude of pulsed magnetic fields in very small volumes ( $10^{-2}$  mm<sup>3</sup>) [4]. Such sensors were used to measure the magnetic diffusion processes in railguns [5] and the distribution of magnetic fields in non-destructive pulsed-field magnets [6].

In this study, the main physical properties of nanostructured  $\text{La}_{1-x}\text{Sr}_x(\text{Mn}_{1-y}\text{Co}_y)_z\text{O}_3$  films grown by pulsed injection MOCVD technique, and examples of their applications for the development of CMR-B-scalar

sensors will be described. It will be demonstrated that CMR behaviour in such films significantly depends on the properties of nanosized crystalline grains and intergrain boundary material. The structure and morphology of the films, the obtained magnetoresistance values, magnetoresistance anisotropy, and relaxation processes will be analysed in order to have possibilities to tune the main properties of nanostructured films for the development of magnetic field sensors operating in a wide magnetic field range at room as well as cryogenic temperatures. Finally, the hybrid manganite-graphene magnetic field sensor which operation is based on negative CMR effect in manganite and Lorentz force induced positive magnetoresistance effect in graphene will be presented. Such hybrid sensor exhibits higher sensitivity to magnetic field in comparison to individual manganite or graphene sensors.

**Keywords:** Lanthanum manganite thin films, colossal magnetoresistance, magnetic field sensors

#### References

- [1]. Ch. Zheng, K. Zhu, S. Cardoso de Freitas *et al.*, *IEEE Trans. Magn.* **55**, 0800130 (2019).
- [2]. S. Balevicius N. Zurauskiene, V. Stankevici, S. Kersulis, V. Plausinaitiene, A. Abrutis, S. Zherlitsyn, T. Herrmannsdoerfer, J. Wosnitza, F. Wolff-Fabris, *Appl. Phys. Lett.* **101**, 092407 (2012).
- [3]. L. Jogschies, D. Klaas, R. Kruppe, J. Rittinger, P. Taptimthong, A. Wienecke, L. Rissing and M. C. Wurz, *J. Sens. Actuator Netw.* **2**, 85 (2013).
- [4]. T. Stankevič, L. Medišauskas, V. Stankevič, S. Balevičius, N. Žurauskienė, O. Liebfried, and M. Schneider, *Rev. Sci. Instrum.* **85**, 044704 (2014).
- [5]. M. Schneider, O. Liebfried, V. Stankevič, S. Balevičius, N. Žurauskienė, *IEEE Trans. Magn.* **45**, 430 (2009).
- [6]. S. Balevičius, N. Žurauskienė, V. Stankevič, T. Herrmannsdörfer, S. Zherlitsyn, Y. Skourski, F. Wolff-Fabris, J. Wosnitza, *IEEE Trans. Magn.* **49**, 5480 (2013).

## INVITED SPEAKERS

Id-1404

### Ferromagnetic Resonance Detection in Magnetic Single Objects via a Novel Microresonator and Microantenna Approach

Hamza Cansever<sup>1</sup>, Kilian Lenz<sup>1</sup>, Rysard Narkowicz<sup>1</sup>, Ewa Kowalska<sup>1</sup>, Jürgen Fassbender<sup>1,2</sup>, Alina M. Deac<sup>1</sup>,  
Jürgen Lindner<sup>1</sup>

<sup>1</sup>Helmholtz-Zentrum Dresden-Rossendorf, Institute of Ion Beam Physics and Materials Research, Bautzner  
Landstraße 400, 01328 Dresden, Germany

<sup>2</sup>Technische Universität Dresden, Institute of Solid State Physics, 01069 Dresden, Germany

Corresponding author: h.cansever@hzdr.de

**Abstract:** Ferromagnetic resonance has been commonly used as a spectroscopic technique investigating the fundamental properties of ferromagnetic materials, such as magnetization, g-factor, magnetic anisotropy and damping (relaxation) parameters [1-4]. Conventionally, an FMR spectrometer is operating at a fixed microwave frequency to detect the microwave absorption of the magnetic object by sweeping an external magnetic field through the resonance. The sensitivity of this weak absorption process is typically enhanced by using a microwave bridge setup. However, for a reliable quantification of key magnetic parameters like the g-factor or spin relaxation times, the measurements should be performed within a broad range of frequencies. This is achieved by broadband FMR spectrometers which employ vector network analyzers (VNA) that detect the microwave transmission or reflection parameters of the sample [5-6]. However, neither conventional cavities nor broadband FMR spectrometers are able to detect signals of micro/nano size samples due to the tiny sample volume. To achieve optimal sensitivity for small objects, planar microresonators were introduced for electron paramagnetic resonance (EPR) experiments [7]. Microresonators have been used to investigate magnetization dynamics of magnetic object to understand uniform and spin wave modes [8], as well as the spin-Seebeck effect in magnetic tunnel junctions [9.] The microresonator approach allows producing rf magnetic fields homogeneously concentrated inside a metallic loop, thereby increasing the filling factor of the resonator. Here, we explain the novel microresonator approach in detail and introduce moreover a microantenna approach which allows to perform experiments in the range of 8-18 GHz employing a co-planar layout. We investigate magnetization dynamics within Permalloy (Ni80Fe20) wires by using both, microresonator and microantenna approach.

**Keywords:** Ferromagnetic resonance, microresonator, microantenna

#### References

- [1]. P. E. Wigen, C.F. Kooi, M. R. Shanaberger, T. R. Rosing, Phys. Rev. Lett. 9, 206, 1962.
- [2]. P. E. Wigen, Z. Zhang, Braz. J. Phys. 22, 267, 1992.
- [3]. M. Farle, "Rep. Prog. Phys. 61, 755, 1998.
- [4]. J. R. Fermin, A. Azevedo, F. M. Aguiar, B. Li, S. M. J. Rezende, Appl. Phys. 85, 7316, 1999.
- [5]. M. Vroubel, Y. Zhuang, B. Rejaei, J. N. Burghartz, J. Appl. Phys. 99, 08P506, 2006.
- [6]. C. Nistor, K. Sun, Z. Wang, M. Wu, C. Mathieu, M. Hadley Appl. Phys. Lett. 95, 012504, 2009.
- [7]. R. Narkowicz, D. Suter, I. Niemyer, Rev. Sci. Instrum. 79, 084702, 2008.

- [8]. A Banholzer, R Narkowicz, C Hassel, R Meckenstock, S Stienen, O Posth, D Suter, M Farle, J Lindner, *Nanotechnology*, 22, 295713, 2011.
- [9]. H. Cansever, R. Narkowicz, K. Lenz, C. Fowley, L. Ramasubramanian, O. Yildirim, A. Niesen, T. Huebner, G. Reiss, J. Lindner, J. Fassbender, A. M. Deac, *J. Phys. D: Appl. Phys.* 51, 22400

## INVITED SPEAKERS

Id-1410

**Challenges of the Inverse Problem of the X-Ray Diffraction Topo-Tomography. Theory, Formulas and Computer Iterative Algorithms towards the 3D Recovery of Elastic Static Displacement Field around the Point-Defects in a Crystal**

Felix Chukhovskii, Petr Konarev, Vladimir Volkov,

Shubnikov Institute of Crystallography, Federal Scientific Research Centre "Crystallography and Photonics",  
Russian Academy of Sciences, Moscow, 119333 Russia

Corresponding author: f\_chukhov@yahoo.ca

**Abstract:** In the recent 10 years, the X-ray diffraction tomography (XRDT) is widely applied to the structural analysis of real crystals. In the XRDT method (see, e.g., [1]), the crystal plate is rotated around an axis perpendicular to the reflecting planes net, usually the rotation axis  $OX$  is selected along the diffraction vector  $\mathbf{h}$ . Then, the 2D-projection tomography set is collected for different rotation (inclination) angles  $\Phi$ , each of which is related to some inclination of the diffraction X-ray plane with respect to the intrinsic coordinate system of the crystal sample, the axis  $OS$  is along the wave vector  $\mathbf{k}_h$  of the diffracted wave (see Fig. 1).

An idea of the computer restoration of the spatial defect positions in a crystal and, what is more important, the local 3D static displacement fields around defects in crystalline materials according to the XRDT data is of a special interest. Clearly (see, [1, 2]), such a problem is equally, if not more, directly related to the quantitative interpretation of defect imaging on the 2D-projections in the XRDT method. The latter is due to the different defect imaging mechanisms in the near and far regions surrounding the crystal lattice defects.

In the present report, the semi-kinematic analytical solution of the dynamical Takagi-Taupin equations for the diffracted wave amplitude  $E_h(\mathbf{r})$  is built that allows in general to develop the consequent theoretical approach for resolving the inverse XRDT problem. As an example, using the one 2D-projection tomography data with inclination angles  $\Phi = 0$ , the results of the computer restoration of the 3D displacement field function  $f(\mathbf{r}-\mathbf{r}_0) = \mathbf{h} \cdot \mathbf{u}(\mathbf{r}-\mathbf{r}_0)$  around the Coulomb-type point defect in crystal Si(111) are reported and discussed (diffraction vector  $\mathbf{h} = [\bar{2}22]$ , the X-ray  $\text{MoK}\alpha_1$ -radiation, the wavelength  $\lambda=0.071$  nm. The Bragg angle  $\theta_B = 10,65^\circ$ .  $\mathbf{u}(\mathbf{r}-\mathbf{r}_0)$  is the near field of elastic static displacements around the Coulomb-type point defect at the point  $\mathbf{r}_0$ ). Respectively, to computer restoration of the 3D displacement field function  $f(\mathbf{r}-\mathbf{r}_0)$  the simulated annealing [3] and quasi-Newton gradient descent algorithms [4] are applied to our problem. To obtain a good solution convergence, some physical constrains onto the type of functions  $\{f(\mathbf{r}-\mathbf{r}_0)\}$  searched are imposed. The 2D-projection numerically simulated and then, used for the computer 3D restoration of the theoretical function  $f(\mathbf{r}-\mathbf{r}_0)$  is shown in Fig. 2.

By using the quasi-Newton descent algorithm, the cross-section pictures of the theoretical function  $f(\mathbf{r}-\mathbf{r}_0)$  and the ones restored from the 2D-projection in Fig. 3 in planes  $z=\text{const.}$ .  $z$ (dimensionless units)=: (A) 6, (B) 8, (C) 10, in are depicted in Fig. 3. The case (B) is related to the mid-thickness of Si(111) plate.

**Keywords:** 3D diffraction X-ray topo-tomography, Takagi-Taupin equations, semi-kinematic analytical approach, the simulated annealing algorithm, the quasi-Newton gradient descent algorithm

**References**

- [1]. Besedin, I.S., Chukhovskii, F.N., Asadchikov, V.E. Crystallography Reports. 2014, Vol. 59, № 3, pp. 323-330. [www.eiseverywhere.com/retrieveupload.php?c3VibWlzc2lubi80NzU1N18zNTQ2MMDMu](http://www.eiseverywhere.com/retrieveupload.php?c3VibWlzc2lubi80NzU1N18zNTQ2MMDMu)
- [2]. Authier A. Dynamical theory of X-ray diffraction. Oxford: University press, 2003. 513 pp.
- [3]. Kirkpatrick, S., Gelatt C. D., Vecchi, M. P. Science. 1983. Vol. 220, pp. 671– 680.
- [4]. Gill, P. E., Murray, W. & Wright, M. H. Practical Optimization. London: Academic Press. 1981, 401p.

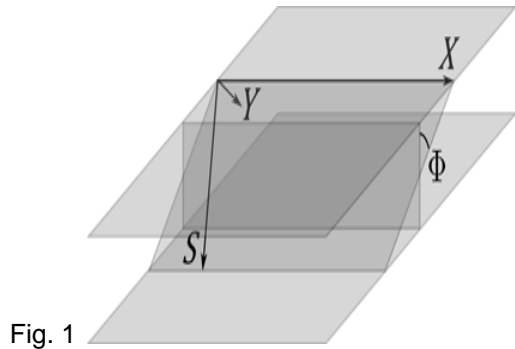


Fig. 1

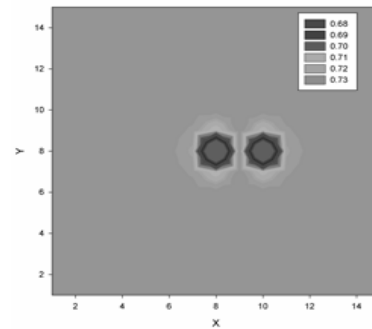
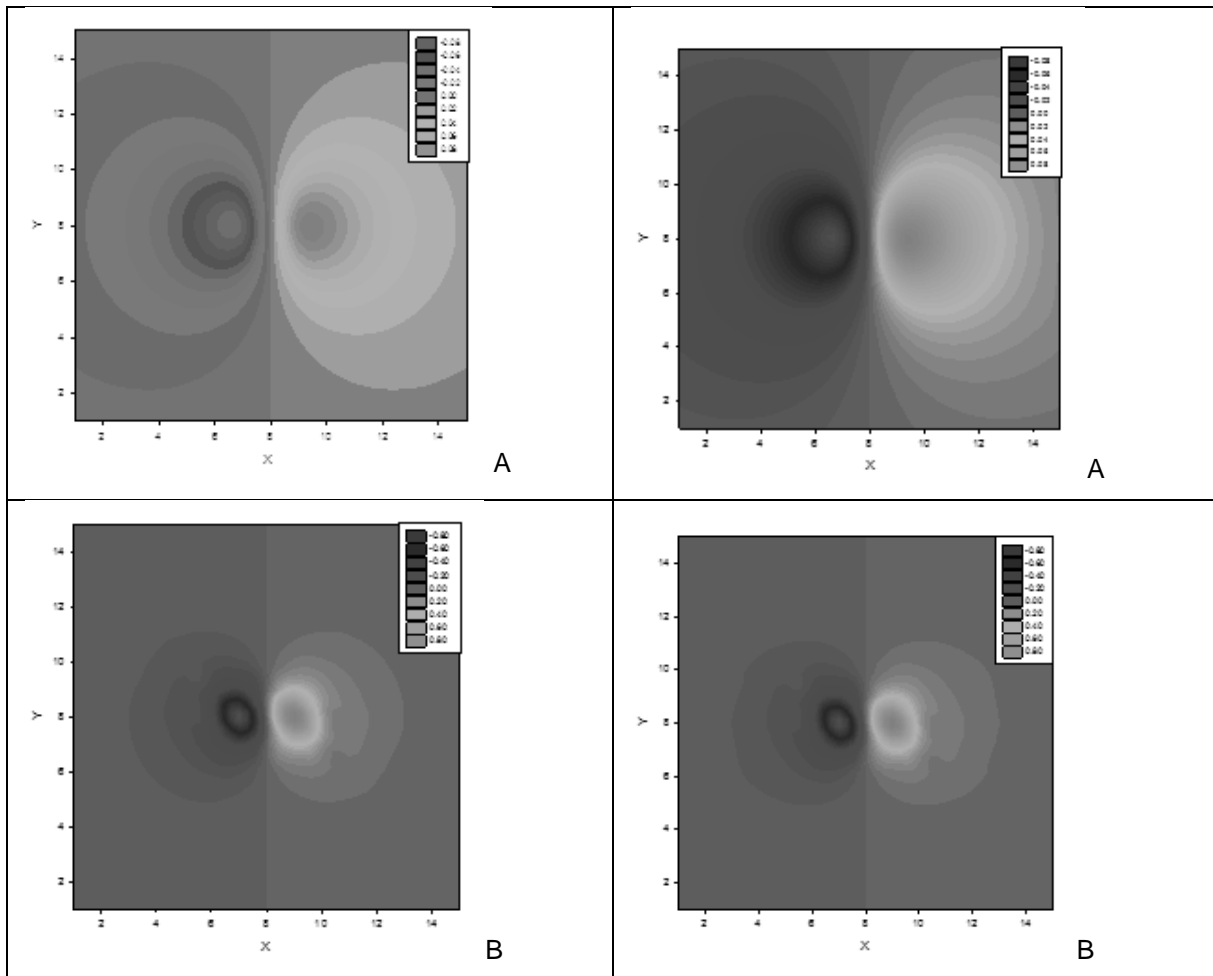


Fig.2



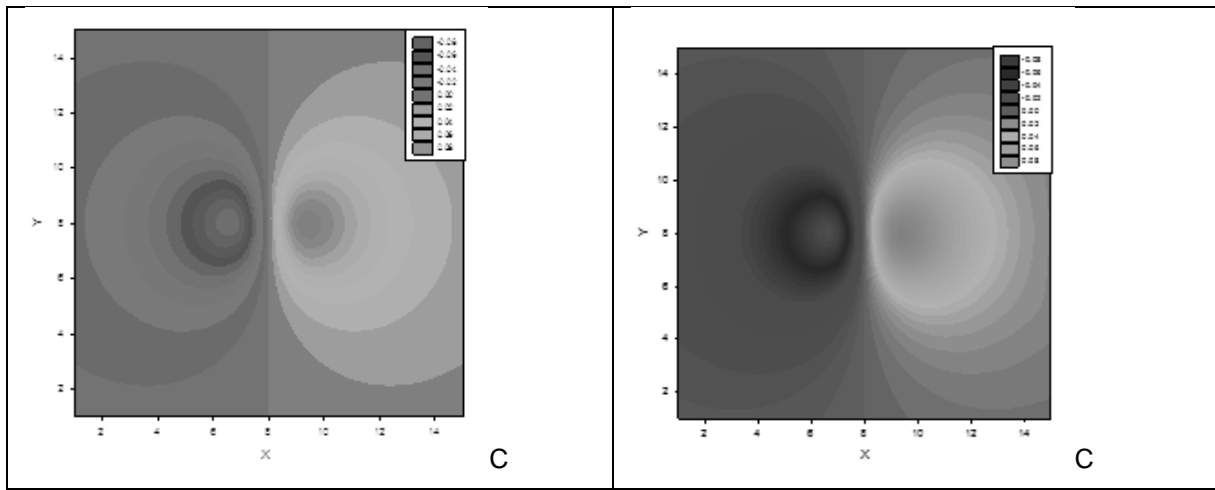


Fig. 3

**INVITED SPEAKERS****Id-1422****Effects of Perforation on Thin Superconducting Films**

Alexey Mironov

ISP SB RAS, Russian Federation

Corresponding author: mironov@isp.nsc.ru

**Abstract:** We present the results of the experimental study of low-temperature transport properties of perforated superconducting and superinsulating TiN and NbTiN film. Nanopatterning transforms a thin initially superconducting film into an array of superconducting islands coupled by weak links. The island's sizes vary randomly or made the same throughout the film. Nanopatterning drives the superconducting films closely to superconductor-insulator transition. As result, we can observe patterning-driven superconductor-superinsulator transition. Appearance of the superinsulator is detected by the changes from the monotonic to threshold behavior of current-voltage characteristics evidencing formation of the zero-conducting state at finite temperature. Note, that transformation into superinsulator depends on only from initial disordering of the superconducting film and doesn't depends on randomness of weak links or sizes of islands. Both in the superconducting and superinsulating state, we observe the periodic dependence of the resistance upon the external magnetic field, with the period  $B_0$  corresponding to the magnetic flux quantum per unit cell. In the superconducting state we also find oscillations of the differential resistance with positive and negative amplitude. For superconducting films with initially positive amplitude of the differential resistance we observed the transition where minima of the differential resistance at rational frustrations  $f = B/B_0$  reverse into maxima upon increasing the current, while magnetoresistances maintain minima at rational  $f$  at any currents. The observed transition is similar to the vortex Mott insulator-to-metal transitions observed in regular arrays. For superconducting films with initially negative amplitude of the differential resistance we observed multiple transition between positive and negative amplitude of the differential resistance and magnetoresistance with increasing current. Moreover, we show that oscillations of magnetoresistance are observed at any current. This behavior may be due to the negative energy of the Josephson coupling. Also, we observed magnetic field induced oscillations of the threshold voltage in the superinsulating state with the period  $B_0$  corresponding to the magnetic flux quantum per unit cell. The observed oscillations indicate the defining role of Josephson energy in formation of the superconducting and superinsulating states.

**Keywords:** Superconductor, nanostructures, vortex, superinsulator

## INVITED SPEAKERS

**Id-1423**

### **Magnetic Catalysts and Their Applications**

Raed Abu-Reziq

Institute of Chemistry, Casali Center for Applied Chemistry, Center for Nanoscience and Nanotechnology, The Hebrew University, Jerusalem 91904, Israel

Corresponding author: Raed.Abu-Reziq@mail.huji.ac.il

**Abstract:** Homogeneous and heterogeneous catalysis are key techniques in modern synthesis and play a central role both in academic and industrial research. Homogeneous catalysts have the advantages of being selective and reactive, but their separation from the reaction mixtures is a difficult process. In contrast, heterogeneous catalysts are less selective and reactive, but they can be easily separated from the reaction medium and recycled. Selective, reactive and recyclable catalyst can be considered as an ideal catalyst and very attractive for various applications. In order to achieve such ideal catalysts, there is a quest to develop new catalytic systems that can bridge between homogeneous and heterogeneous catalysis.

In this talk, new methods for immobilization of catalysts that combine the advantages of homogeneous and heterogeneous catalysts will be described. For example, a method that is based on supporting rhodium catalysts on the surface of magnetic nanoparticles will be described. The performance of magnetically separable rhodium-based catalysts in selective hydroaminomethylation will be discussed. After application in catalytic reactions, these new catalysts can be easily separated from the reaction medium by applying external magnetic field. Furthermore, the design, preparation and applications of catalytic systems based on magnetically separable nano- and microreactors will be also presented.

**Keywords:** Magnetic materials, nanocatalysis, nano- and microreactors, sol-gel chemistry, interfacial polymerization

## INVITED SPEAKERS

Id-1428

### Production of Biodegradable Plastic Polyhydroxyalkanoates from Low-Cost Substrates for Industrial Applications

Diya Alsafadi

Royal Scientific Society, P.O.Box 1438, Amman 11941 Jordan

Corresponding author: Diya.safadi@rss.jo

**Abstract:** A currently hot topic is the disastrous pollution of the oceans, the origin of all life, by more than ten million tons of toxic petroleum-derived plastics entering the oceans every year, mainly from rivers and coastal populations worldwide [1]. Bioplastics have been considered as sustainable solution to reduce the environmental burden by partially replacing petroleum-derived plastics. Bioplastics polyhydroxyalkanoates (PHAs) are a family of polyesters that intracellularly accumulated as carbon and energy sources by several bacteria and archaea under unfavorable conditions (excess carbon and depletion of essential nutrients such as nitrogen and oxygen) [2]. PHAs have similar properties to petroleum-based plastics such as polypropylene and polyethylene, but PHA also biodegradable, biocompatible, water resistant and non-toxic. Thus, PHAs can be used in a variety of disposable packaging goods (such as plastic bags, containers) and may also have high-value applications in medicine and pharmaceutical fields (such as fields of artificial blood vessels, drug delivery vehicles and bone replacement) [3].

The high production cost of PHAs compared to that of traditional plastic prevents further market penetration [4]. A cost reduction in PHAs biosynthesis process could be obtained by using inexpensive carbon sources and developing new PHAs accumulation process with cheap and simple purification steps.

The extreme halophiles, microorganisms thrive in extreme environments of ~4.5 M salt, [5] are promising candidates with increasing interest for the economical large scale production of PHA.

In our research work we present an effective cultivation processes for the production of PHA by extreme halophile, *Haloferax mediterranei* from different local and inexpensive carbon sources such as olive mill wastewater [6], date palm fruit waste and sesame seed wastewater. The obtained biopolymer was extracted from microbial biomass by cheap and easy purification steps with minimal quantities of toxic solvents. For industrial applications, the chemical composition, molecular weight, thermal and mechanical properties of the produced PHA polymers were also determined.

**Keywords:** Biodegradable plastic, polyhydroxyalkanoates, carbon sources, thermal and mechanical propertie

#### References

- [1]. Laineza, M., González, J. M., Aguilarc, A. and Velad, C., 2017, Spanish strategy on bioeconomy: Towards a knowledge based sustainable innovation: *New Biotechnology*, **40**, 87-95.
- [2]. Scarlat, N., Dallemand, J-F., Monforti-Ferrario, F. and Nita, V., 2015, The role of biomass and bioenergy in a future bioeconomy: policies and facts: *Environmental Development*, **15**, 3-34.

- [3]. Reddy, C., S., Ghai, R., Rashmi and Kalia V., C. 2003, Polyhydroxyalkanoates: an overview: Bioresource Technology, **87**, 137-146.
- [4]. Venkateswar, Reddy., M., Mawatari, Y., Onodera, R., Nakamura, Y., Yajima, Y. and Chang, Y. C., 2017, Polyhydroxyalkanoates (PHA) production from synthetic waste using *Pseudomonas pseudoflava*: PHA synthase enzyme activity analysis from *P. pseudoflava* and *P. palleronii*: *Bioresource Technology*, **234**, 99-105.
- [5]. Isafadi D, Khalili F, Juwhari H, Lahlouh B. Purification and biochemical characterization of photo-active membrane protein bacteriorhodopsin from *Haloarcula marismortui*, an extreme halophile from the Dead Sea. *Int J Biol Macromol* 2018; 118:1942-1947.
- [6]. Alsafadi, D. and Almashqbah, O., 2016, A one-stage cultivation process for the production of poly-3-(hydroxybutyrate-co-hydroxyvalerate) from olive mill wastewater by *Haloflex mediterranei*: *New Biotechnology*, **43**, 47-53

## INVITED SPEAKERS

**Id-1443**

### Photovoltaic Cells and Modules for Future Energy Systems

Vitezslav Benda

Czech Technical University in Prague, Department of Electrotechnology, Technicka 2, 166 27 Praha 6, Czech Republic

Corresponding author: [benda@fel.cvut.cz](mailto:benda@fel.cvut.cz)

**Abstract:** Photovoltaics (PV) is expected to play a key role in the future global energy system.

Progress in technology has resulted in impressive reduction with the price of PV modules and other parts of photovoltaic power systems, so that the cost of electrical energy produced by PV systems decreased close to long-term cost of electrical energy over the grid.

PV conversion can be done with a wide range of materials, device architectures and technologies.

The key components are PV modules representing basic devices, which are able operate for a long time in outdoor conditions. PV modules can be realized from different materials by different fabrication technologies. There are some criteria that can be supporting or limiting a successful placement of particular technologies to the market. They are:

- **Efficiency of solar irradiation to electrical energy conversion.** It depends on physical construction of the cell (module) and it is limited by the cell material, construction and technology tools
- **Module (cell) cost.** It is usually presented as a cost for a unit of electrical power generated under the standard irradiance (1000 W/m<sup>2</sup>, spectrum AM1.5) at temperature 25°C. This cost depends on input materials costs and costs of technological operations, and also on the scale of production, supply chain efficiency, standardisation level, etc.
- **Photovoltaic system cost.** It consists of costs of system components, photovoltaic modules, and BOS (inverters, supporting constructions, protections, transformers, monitoring and other accessories) and also cost of mountings (including overheads) and cost of used area.
- **The cost of electricity produced by PV systems.** It is the most important criterion for the technology's success. The Levelized Cost of Energy (LCOE) method takes into account the investment cost, the operating and recycling costs, and the total energy produced during the system service life that can be a factor influencing acceptability of particular technologies.

A categorisation in three generations of PV cell and module technology groups has been used frequently over the past 15 years. The first generation was represented by wafer-based crystalline silicon cells, the second generation, represented by one junction thin film cells and the term "third generation PV" was then used for emerging technologies having a potential to bring a combination of high efficiency and low fabrication cost (tandem cells, DSSC, organic and polymeric cells, perovskite cells, quantum dot cells). In this paper, the main features of individual technology groups are discussed from the view of criteria above.

At present, the wafer based crystalline silicon technologies have fitted best to above criteria and they have the role of workhorse of present PV power generation, representing nearly 95% of total module

production due to their high efficiency, low cost and a high service time. Thin film CdTe and CIGS technologies have still reserves in both fabrications cost and efficiency, but their expansion is limited by some resource restrictions. Very prospectus may be PV modules based on perovskites, if they reach an acceptable service life and overcome the commercial valley of death by scaling up rapidly to the volume needed for competitiveness.

**Keywords:** Photovoltac cells, photovoltaic modules, efficiency, service life, crystalline silicon cells and modules, thin film cells and modules, perovskites, PV module cost, PV system cost, LEOC

## INVITED SPEAKERS

**Id-1450**

### **Machining Challenges and Solutions to Aerospace Grade Composite-Titanium Stacks**

Jinyang Xu

School of Mechanical Engineering, Shanghai Jiao Tong University, Shanghai 200240, PR China

Corresponding author. xujinyang@sjtu.edu.cn

**Abstract:** Multilayer composite/metal stacks constituted by carbon fiber reinforced polymers (CFRPs) and titanium alloys are advanced high-performance materials being widely used in the modern aerospace industry due to their improved mechanical/physical properties and enhanced structural functionalities. Due to the different properties of each stacked material, machining of these hybrid composite stacks has posed significant challenges to the manufacturing community. The invited talk reports the existing challenges faced by the current machining industries and then presents the potential solutions by lecturing the innovative works carried out by the speaker's research group. The fundamental mechanisms of the chip removal process and defects formation of CFRP/Ti6Al4V stacks are firstly introduced. Issues of hole quality attributes and tool wear progression during the stack drilling are discussed. Performances of several innovative cutting methods involving the MQL machining and the vibration assisted drilling to improve the stack machinability are illustrated. Eventually, the future developments in the fields of high-quality machining of aerospace grade CFRP/Ti6Al4V stacks are put forward.

**Keywords:** CFRP/Ti6Al4V Stacks, machining, challenges, cutting strategies, drilling quality, tool wear.

**Acknowledgments:** The work was funded by the National Natural Science Foundation of China (Grant No.51705319) and the Shanghai Pujiang Program (Grant No.17PJ1403800).

## INVITED SPEAKERS

Id-1453

### Compositional Engineering of (Ba, Ca)TiO<sub>3</sub>-Based Solid-Solution Plates: Piezoelectric Characteristics and Phase Transitions Behaviour

Marjeta Maček Kržmanc<sup>1</sup>, Hana Uršič<sup>2</sup>, Nina Daneu<sup>1</sup>, Špela Kunej<sup>1</sup>, Matjaž Spreitzer<sup>1</sup>, Romana Cerc Korošec<sup>3</sup>,  
Ioana Dorina Vlaicu<sup>4</sup>

<sup>1</sup>Advanced Materials Department Jožef Stefan Institute, Jamova 39, Ljubljana 1000, Slovenia

<sup>2</sup>Electronic Ceramics Department, Jožef Stefan Institute, Jamova 39, Ljubljana 1000, Slovenia

<sup>3</sup>Faculty of Chemistry and Chemical Technology, University of Ljubljana, Večna pot 113, Ljubljana 1001, Slovenia

<sup>4</sup>National Institute of Materials Physics, Atomistilor Str. 405A, Magurele, 077125, Romania

marjeta.macek@ijs.si

**Abstract:** Preferentially oriented and aligned perovskite plates are important for enhancement of dielectric and piezoelectric performance of polymer+ceramic composites and preferentially oriented ceramics, respectively. The preferential orientation of grains in certain crystallographic direction (so called texturing) is achieved by template grain growth, where the perovskite plates serve as the template to seed oriented grain growth in ceramics [1]. The direction of maximal piezoelectric response depends on chemical composition, crystal structure and temperature. For tetragonal (Ba,Ca)TiO<sub>3</sub> ceramics the highest piezoelectric response at room temperature was reported to be along the polar axis (i.e. along [001]) [2]. For preparation of textured (Ba,Ca)TiO<sub>3</sub> ceramics with this preferential orientation, (001) oriented (Ba,Ca)TiO<sub>3</sub> plates will ensure better consistency of chemical composition with precursor matrix powder than the template plates with other compositions.

In this research the topochemical conversion (TC) of Bi<sub>4</sub>Ti<sub>3</sub>O<sub>12</sub> to (001) oriented (Ba,Ca)TiO<sub>3</sub> solid-solution plates in molten salt (900 °C) was studied. The main focus was on controlling of solid-solution compositions, crystal and domain structure and further on the study of their correlations with the piezoelectric characteristics and phase transitions behaviour (orthorhombic-to-tetragonal (O-T) and tetragonal-to-cubic (T-C)). It was found that the incorporation of Ca in the (Ba,Ca)TiO<sub>3</sub> plates is limited and that the elimination of Bi is lower (2 at. %) than in the case of the TC to BaTiO<sub>3</sub> plates (≤1 at. %). According to X-ray diffraction (XRD) analysis, clear (001)/(100) tetragonal splitting, typical for **a**- and **c**-domains, was observed for the compositions with Ca:Ba up to 0.05:0.95. Piezo-response-force microscope (PFM) examination of the plates revealed the presence of ~500-nm-sized domains and local  $d_{33}$  values of 50–180 pm/V. High resolution (HR) scanning transmission electron microscopy (STEM) of plate's cross-section showed highly ordered single crystalline structure with homogeneous distributions of Ca and Bi in the perovskite matrix. The deviation from typical composition was observed around Ca-rich dislocations and nanosized Bi-rich inclusions.

The substitution of A-site cation in BaTiO<sub>3</sub> is known to influence the O-T and T-C phase transitions temperatures and thus define the width of temperature range of tetragonal phase stability, what consequently determine the temperature dependence of piezoelectric coefficients. The O-T and T-C phase transitions behaviour for studied (Ba,Ca)TiO<sub>3</sub> plates were investigated by means of low- and high-temperature XRD, respectively and by differential scanning calorimetry (DSC).

The understanding of influence of composition on the piezoelectric properties and on O-T and T-C phase transition is of high importance for maximization of piezoelectric performance of the plates and oriented (Ba,Ca)TiO<sub>3</sub>-based ceramics, what further widen their application potential.

**Keywords:** Perovskites, ferroelectrics, piezoelectrics, plate-like particles, phase transitions

**References**

- [1]. S. F. Poterala et al., Chem. Mater., 22 (2010) 2061-2068.
- [2]. A. B. Haugen et al., J. Appl. Phys. 116 (2014) 134102.

## INVITED SPEAKERS

**Id-1460**

### **Improvement of the Sulfur Corrosion Resistance of Copper Windings by Using Grain Boundary Engineering (GBE) and Its Effect for Oil-paper Insulation**

Yuan Yuan<sup>1,2</sup>, Zhou Jiang<sup>2</sup>

<sup>1</sup>School of Material Science and Engineering, Chongqing University, Chongqing, China

<sup>2</sup>State Key Laboratory of Power Transmission Equipment and System Security and New Technology, Chongqing

University, Chongqing, China

Corresponding author: yuany@cqu.edu.cn

**Abstract:** Corrosive sulfur in insulating oil has been identified to cause sudden and unexpected failures of several transformers and reactors in recent years. In this study, the sulfur corrosion resistance of copper windings was improved by using “Grain Boundary Engineering” (GBE). The microstructure of the copper windings was investigated. Results shows that the special grain boundaries could restrain and delay the expanding and combination of corrosion pits. The content of copper in oil decreased dramatically from 3660 ug/kg to 2.47 ug/kg. Meanwhile, the physical and chemical and electrical properties of oil-paper insulation are promoted obviously, and aging degree reduced.

**Keywords:** Sulfur corrosion resistance, copper winding, grain boundary engineering, oil-paper insulation

## INVITED SPEAKERS

**Id-1469**

### **Advanced Polymeric Materials and Preserving of Polymer Objects**

Jiří Brožek, Kalousková Radka, Benešová Václava, Jaroslav Minář, Malinová Lenka

Department of Polymers, University of Chemistry and Technology Prague, Technická 5, CZ 166 28 Prague 6,  
Czech Republic

Corresponding author: jiri,brozek@vscht.cz;

**Abstract:** Synthetic polymers are more stable and affordable than natural polymers and have virtually displaced them from many applications. The goal of material research is to prepare materials with improved mechanical properties, stability, and more easily degradable on the other side.

Our efforts are therefore focused on the preparation of polymer materials containing layered fillers such as graphene oxide and layered silicate. The properties of such materials are determined both by the chemical structure of the filler and by the polymer matrix and the method of preparation. Another interesting research topic is the synthesis of polymers with different sensitivity to degradation or even compostable materials.

On the other hand, we are also faced with the difficult task of preserving polymeric objects, that documents development and technological advances in museum and library collections. Within the project, we solve the extent of damage of the book covers made from soft PVC during storage under different conditions.

**Keywords:** Polymeric materials, characterization, preserving polymeric objects

**Acknowledgement:** This work was supported from research program DG18PO2OVV001 (NAKI II).

## INVITED SPEAKERS

**Id-1477**

### **Processing, Characterisation and Testing of Environmental Barrier Coatings for SiC/SiC CMCs**

Nasrin Al Nasiri

Centre for Advanced Structural Ceramics, Department of Materials, Imperial College London, Royal School of  
Mines, Prince consort Road, London SW7 2BP, United Kingdom

Corresponding author: n.al-nasiri10@imperial.c.uk

**Abstract:** The need to increase the cycle efficiency and reduce noise and NO<sub>x</sub> emissions from jet engine turbine has promoted the development of ceramic matrix composites (CMC) such as silicon carbide fibre-reinforced silicon carbide (SiC-SiC). Use of CMCs will lead to a significant improvement in fuel consumption and thrust-to-weight ratio compared to metal alloys. In addition, the low density of CMCs allows weight savings of up to 30% compared to Ni-based super alloys equating to about 1000kg/engine thus leading to vastly improved fuel consumption. However, silicon (Si)-based ceramics such as SiC-SiC have poor environmental durability in high velocity combustion environments. Si-based ceramics have excellent oxidation resistance due to formation of a protective silica layer on reacting with dry air making them stable at temperatures up to 1200°C for long-term application. On the other hand, the same silica layer will react with water vapour to form gaseous silicon hydroxide, leading to high recession and component failure. To avoid this behaviour, a prophylactic environmental barrier coating (EBC) is required. A variety of EBCs have been developed in the past, which consists of a minimum of 4 layers requiring a costly application method such as plasma spraying. In this work, five rare earth monosilicates are being examined as potential EBCs: Y<sub>2</sub>SiO<sub>5</sub>, Yb<sub>2</sub>SiO<sub>5</sub>, Lu<sub>2</sub>SiO<sub>5</sub>, Gd<sub>2</sub>SiO<sub>5</sub> and Er<sub>2</sub>SiO<sub>5</sub>. Their performance in steam environments is being studied at 1200-1350°C for different times as a first step to determine which EBC candidate is most promising for protecting SiC-SiC CMCs in the jet engine environment. The main aim of this study is to develop a reliable single layer of EBC instead of multilayers and to develop a low cost method of applying the EBC.

**Keywords:** EBCs, CMCs coatings

## INVITED SPEAKERS

**Id-1478**

### **Uniaxial Compression and Buckling of Graphenes**

George Kalosakas

Department of Materials Science, University of Patras, Rio, GR-26504, Greece

Corresponding author: georgek@upatras.gr

**Abstract:** The mechanical response of single- and multi-layer graphenes [1], as well as of graphene nanoribbons of various lengths and widths [2], under uniaxial compression is presented. Molecular dynamics simulations are used to calculate compressive stress-strain curves and critical buckling values. The dependence of the critical buckling on the size of graphenes is discussed. In graphene nanoribbons, a single master curve describes the variation of the critical buckling with the aspect ratio of the nanostructure. The obtained results are compared with the predictions of the continuum elasticity theory [3-5].

**Keywords:** Graphene, compression, buckling

#### **References**

- [1]. A.P. Sgouros, G. Kalosakas, C. Galiotis, and K. Papagelis: *Uniaxial compression of suspended single and multilayer graphenes*, 2D Mater. **3**, 025033 (2016).
- [2]. A.P. Sgouros, G. Kalosakas, K. Papagelis, and C. Galiotis: *Compressive response and buckling of graphene nanoribbons*, Sci. Rep. **8**, 9593 (2018).
- [3]. S. Timoshenko and J.M. Gere: *Theory of elastic stability*, Dover Publications, 2009.
- [4]. D.W.A. Rees: *Mechanics of Optimal Structural Design: Minimum Weight Structures*, John Wiley & Sons Ltd, 2009.
- [5]. J.C. Houbolt and E.Z. Stowell: *Critical stress of plate columns*, Natl. Advis. Comm. Aeronaut. Tech. Note 2163 (1950).

## INVITED SPEAKERS

**Id-1485**

### **Advances in Polymer Enriched Concrete for Strengthening Concrete Roads and Airfields. The Case of Green Overlays**

John Nicholas Karadelis

Faculty of Engineering Environment and Computing, School of Energy Construction and Environment, Sir John Laing Building, Coventry University, Coventry, CV1 5FB, UK

Corresponding author: john.karadelis@coventry.ac.uk

**Abstract:** This research was part of an ambitious investigation aiming to develop a 'green' pavement overlay in the form of steel fibre reinforced, roller compacted (bonded), polymer modified concrete (SFR-RC-PMC) with special workability properties, to facilitate placement by an asphalt paver and compaction with a vibrating roller. The essential problems for strengthening concrete pavements with structural overlays were scrutinised. A cost effective, minimal disruption, sustainable and environmentally friendly alternative to the wholesale demolition, removal and complete reconstruction of the existing structural concrete pavement, has been accomplished.

A large number of laboratory tests (more than 500 specimens overall) were carried out aiming to improve the "compactability" and "placeability" of fresh, and the mechanical properties of hardened concrete via a series of carefully **designed mixes**. In the absence of a suitable compaction process, the modified light compaction method was conceived, developed and verified experimentally with a number of coarse and fine aggregates, polymer types and steel-fibres. Preliminary bond performance was examined by block splitting tests and cylinder direct shear tests. The results were promising.

The efficacy of steel fibres in the roller compacted concrete (RCC) was scrutinised. It was found that the **flexural strength** of steel fibres in Polymer Modified, Roller Compacted Concrete (PMRCC) is superior to that in conventional concrete. The "size" effect was also investigated by establishing that the size of the ligament affects the strength of the specimen.

Under repeated traffic loads (rocking effect), shear failure is also profound, leading eventually to reflection cracking. There is evidence that high compressive strengths (existent in the PMC mix) cannot always guarantee high **shear strengths**, despite the fact that codes of practice preach that the latter is always proportional to the former. To this end, all plain (unreinforced) PMC and OPCC (ordinary Portland cement concrete) beams failed abruptly in a brittle manner. In contrast, steel fibre reinforced PMC beams continued to carry loads even after the appearance of cracks (1% of steel fibre by vol. fraction increased shear strength by 58%) displaying the required ductility.

Any early age gain in strength has a dramatic impact on cost savings, disruption to traffic, road users convenience, etc. The 3-day shear strength of SFRPMC beams was recorded to be even higher than the corresponding 28-day OPCC strength.

The **Interfacial Delamination** study focussed on achieving effective horizontal shear transfer across the interface of the new and old concrete as well as maximum fracture resistance. It also looked at the progressive fracture and de-bonding processes at discontinuities, under intrinsic deformation of the overlay. The study utilised the classical constrained Extreme Vertices Design (EVD) approach.

Essentially, it was found that the interface restraint capacities (delamination driving energy) against delamination, increase with overlay thickness and relative stiffness values. That is, as the delamination coefficient becomes smaller, continuously increasing driving energy is needed to initiate, or propagate delamination along the plane of the interface.

As a final point, the performance of **composite** (OPCC-base PMC-overlay) **beams on elastic foundation** was examined. Two types of foundation were considered: A rubber foundation (RF) and a cement stabilized aggregate foundation (CF). It was established that the elastic solid foundation model is suitable for modelling composite beams on elastic foundations.

It was verified, this time from a different perspective, that increasing overlay thickness can effectively reduce the susceptibility to shear failure and reflective cracking and minimise the differential displacement at underlying joints or cracks.

It was recognised that the fibre bridging effect in combination with the enhanced mechanical properties of the Styrene Butadiene Rubber (SBR) and Polyvinyl Alcohol (PVA) polymer enriched overlay, have a significant advantage over their OPCC rival, in controlling deformation and stress concentration at a crack tip.

Finally, one should stress that the chief advantages of our “green” PRSS (Pavement Repair & Strengthening System) against the conventional systems are seen in the construction process, durability, toughness and structural integrity that lead to safety for the road user. PRSS does not require formwork, rebars, long curing/strengthening times. It is free of maintenance and repairs and guarantees a long life span compared to its flexible rivals.

**Keywords:** polymers, concrete, overlays, design-mixes, flexural, shear, delamination, composites

## INVITED SPEAKERS

**Id-1487**

### **Development of Computational Simulation Tools for Fatigue and Creep-Fatigue Crack Growth in Metallic Alloys at Elevated Temperatures**

Gabriel Potirniche, Jose Ramirez, Nicholas Shaber, Martin Taylor, Robert Stephens, Indrajit Charit  
University of Idaho, USA

Corresponding author: gabrielp@uidaho.edu

**Abstract:** Fatigue and creep-fatigue crack growth are two important failure modes of metallic components subjected to a combination of mechanical loads and elevated temperatures. Robust computational methods have been developed over the last decades for the prediction of fatigue crack growth under variable amplitude loading. On the other hand, models for creep-fatigue crack growth are still needed to be developed, especially due to the complex interaction between creep and fatigue loads. The objective of this work is to develop reliable computational models to simulate fatigue and creep-fatigue crack growth. To achieve this, two computational methods have been employed.

The first method uses the strip-yield modelling technique. In this method, the crack surfaces behind the crack tip and plastic zone ahead of the advancing crack tip are meshed with bar elements undergoing elastic, plastic and creep deformations. Crack opening displacements, crack-tip plastic zone and contact stresses between crack surfaces are computed at every step in a loading cycle using the weight function method. Factors that determine crack growth rates (i.e., load ratio, ratio of applied stress to yield stress, and duration of creep dwell time) are modelled by computing the crack opening and closing due to the plasticity-induced crack closure phenomenon. Fatigue crack growth rates are predicted using the computed effective stress intensity factor range, while creep crack growth rates are computed using the applied stress intensity factor during the creep dwell time.

The second computational method used to predict crack growth is the finite element method. Crack growth was modelled in the finite element software ABAQUS using the node release scheme. The crack is advanced by removing constraints from each element ahead of the crack tip every two applied cycles. The crack surfaces are modelled using contact elements using a penalty function with an augmented Lagrange contact algorithm. Plasticity-induced crack closure was quantified by computing crack-tip opening stresses. The crack-tip opening stresses and crack growth rates computed with the finite element method were similar to those obtained from the strip-yield modelling, for both fatigue and creep-fatigue loading scenarios.

Predictions of crack growth rates under fatigue and creep-fatigue loading scenarios from the two computational techniques were compared with experimental results in several metallic alloys, such as ferritic-martensitic steels, austenitic stainless steels, Ni-base alloys, and aluminium alloys. The comparison between the experimental results and computational predictions of crack growth rates was excellent. A detailed description of an experimental testing program of crack growth is presented in the case of austenitic stainless-steel Fe-25Ni-20Cr (Alloy 709), a material used in power plant applications. High temperature testing of crack growth rates under fatigue and creep-fatigue loading was performed. Specimen fractography was performed using optical microscopy, scanning electron microscopy and

electron back-scatter diffraction. The mechanisms of microstructure damage and crack propagation were identified. The computational methods validated by experimental results represent a useful tool in predicting crack growth and service life of structural components under various load and temperature conditions.

**Keywords:** Fatigue, creep, crack growth

## INVITED SPEAKERS

**Id-1493**

### **Role of Auxetic Composites in Protection of Building Materials and Structures**

Tatheer Zahra

Queensland University of Technology, 2 George St, Brisbane, QLD 4000, Australia, Ph. (+61) 7 31385327,

Corresponding author: t.zahra@qut.edu.au

**Abstract:** Common building materials including concrete, masonry and mortar are brittle in nature and fractured due to dissipation of energy under extreme loads caused by impact, blast and seismic forces. The structures made of these materials are required to be protected against brittle collapse by minimising the energy dissipation. The strengthening and protection to these materials can be realised using high energy absorbing materials that can reduce the damage and hence the loss of lives and repair costs. Auxetic composites by virtue of having negative Poisson's ratio are unique and exhibit high energy absorption, high shear modulus and high bonding properties. Negative Poisson' ratio (NPR) means these expand or contract laterally when subjected to longitudinal tension and compression respectively. This property enables these composites to bond strongly to the parent brittle material and prevents their fracture and dispersion under loading. Their application in medical, sports and defence industries has been explored by many researchers, however, their role in building materials and infrastructure protection has been studied sparingly. This research aims to demonstrate the application of auxetic composites in building materials and construction industry as a protective render. For this purpose, mortar-auxetic foam prisms and mortar-auxetic fabric render beams were developed in the lab. The prism samples were tested under compression, whilst render samples were tested under out-of-plane bending for variable strain rates ranging from 1mm/min to 150mm/min. Experimental program concluded that mortar-auxetic composites exhibited high energy absorption and high bonding strength with the mortar in comparison to the common fibre reinforced polymer (FRP) composites used for strengthening of the building materials. Further, their application in protecting and strengthening the masonry walls under eccentric compression and impact load was studied through finite element modelling method. Drystack or mortarless walls rendered with mortar-auxetic fabric composites were analysed under eccentric compression and their behaviour was compared with traditional mortared masonry. It was inferred that mortar-auxetic render provided adequate strength to the mortarless masonry walls in resisting the eccentric compression loads. Similarly, rendered masonry walls performed better in resisting the lateral impact in comparison to unrendered walls. The lateral displacement was reduced by around 22% and energy absorption was increased 8 folds. These findings conclude that auxetic fabric composites can be employed as protective renders in building materials and structures to increase their energy absorption capabilities and reduce brittleness.

**Keywords:** Auxetic composites, negative poisson's ratio (NPR), masonry, eccentric compression, impact, energy absorption, failure

## INVITED SPEAKERS

**Id-1502**

### **Effects of Material Constituent and Magnetic Field on Mechanical Properties of Magnetorheological Elastomers**

Dong-Joo Lee, Vineet Kumar

School of Mechanical Engineering, Yeungnam University, Gyongsan, Gyungbuk, Korea.

Corresponding author: djlee@yu.ac.kr

**Abstract:** Magnetorheological elastomers (MREs) have gained a considerable attention recently because of their prospects for application in various smart systems. The main advantages of MRE are better durability, the time-dependent and reversible variation of damping characteristics for better control of engine mount, suspension bushing & body mounts, etc. For example, the bushing using MRE can control more effectively the brake shudder phenomenon than hydraulic suspension for longer period. In this presentation, magnetorheological effects will be discussed as functions of an external magnetic field, filler particles and matrix types. The study is performed by measuring the compressive modulus, the response rate and magnitude in the presence and absence of magnetic field up to 2 Tesla. The used filler particles are 2 types (carbonyl and electrolyte) of iron particles (IPs) with 4 different sizes and content up to 80 phr, and carbon nanotubes (CNTs) up to 3 phr. The elastomers as the matrix are room-temperature-vulcanized (RTV) silicone rubber, natural rubber (NR) and acrylonitrile butadiene rubber (NBR).

The aim of this study was to increase the knowledge on the reinforcing mechanisms, and the filler distribution and orientation mechanism for better understanding of MREs as polymer composites. The most important parameter influencing the composite behavior is the average particle size, shape and content of the filler. Particle wetting and distribution are also important factors since metallic particles located in soft matrix. The focus was to clarify those mechanisms and microstructural changes in the elastic and damping properties of studied types of MREs when subjected to magnetic field. Since many published papers are limited to one type of rubber and IP, the understanding of MRE as composite was very limited. Also, the applied magnetic field strengths of those studies are less than 1.0 Tesla during the specimen vulcanization. In this study, the influence of the alignment of the magnetic particles on the composite properties with and without applied magnetic field up to 2 Tesla was studied. The elastic and damping properties are compared based on the filler distribution and filler orientation mechanism depending on the matrix types. The results show that the elastic and damping properties of both isotropic and aligned MREs can be modified significantly by applying external magnetic field up to 1.5 Tesla. Those properties depend on the particle alignment, distribution and interfacial condition in the composite.

**Keywords:** Composite, magnetorheological elastomers, filler, matrix

## INVITED SPEAKERS

**Id-1507**

### **Introducing 2D Materials for Magnetic Tunnel Junctions**

Marta Galbiati<sup>1,2</sup>, Victor Zlatko<sup>1</sup>, Maëlis Piquemal-Banci<sup>1</sup>, Regina Galceran<sup>1</sup>, Florian Godel<sup>1</sup>, Marie-Blandine Martin<sup>1</sup>, Sabina Caneva<sup>2</sup>, Robert Weatherup<sup>2</sup>, Stephan Hofmann<sup>2</sup>, Stephane Xavier<sup>3</sup>, Bernard Servet<sup>3</sup>, Richard Mattana<sup>1</sup>, Abdelmadjid Anane<sup>1</sup>, Frederic Petroff<sup>1</sup>, Albert Fert<sup>1</sup>, Bruno Dlubak<sup>1</sup>, Pierre Seneor<sup>1</sup>

<sup>1</sup>Unité Mixte de Physique, CNRS, Thales, Univ. Paris-Sud, Université Paris-Saclay, Palaiseau 91767, France

<sup>2</sup>Univesidad de Valencia, Instituto de Ciencia Molecular, Paterna, 46980, Spain

<sup>3</sup>Thales Research and Technology, 1 av. A. Fresnel, Palaiseau 91767, France

<sup>4</sup>Univesidad de Valencia, Instituto de Ciencia Molecular, Paterna, 46980, Spain

Corresponding author: marta.galbiati@cnrs-thales.fr

**Abstract:** The recent discovery of graphene, and other 2D materials, has opened novel exciting opportunities in terms of functionalities and performances for spintronics devices. While to date, it is mainly graphene properties for efficient spin transport which have been put forward, we will present here experimental results on another avenue for 2D materials in spintronics. We showed that a thin graphene passivation layer can prevent the oxidation of a ferromagnet and unveil new ALD processes. Importantly, beyond allowing to preserve a highly surface sensitive spin current polarizer/analyzer behavior, the use of graphene on ferromagnets unveiled a new enhanced spin filtering property [1,2]. We will present results concerning 2D materials, from atomically thin insulator h-BN to TMDCs. We will show how ferromagnet metal hybridization can transform an insulating 2D monolayer into a metal [3] and how spin physics may impact 2D based spin valves. These different experiments unveil the promises of 2D materials for spintronics [4] in 2D-MTJ.

**Keywords:** Spintronics, magnetic tunnel junctions, 2D materials, graphene

**References:**

- [1]. Dlubak et al. *ACS Nano* **6**, 10930 (2012) ; Weatherup et al. *ACS Nano* **6**, 9996 (2012)
- [2]. Martin et al. *ACS Nano* **8**, 7890 (2014) & *APL* **107**, 012408 (2015)
- [3]. Piquemal-Banci et al. *APL* **108**, 102404 (2016) & *ACS Nano* **12**, 4712 (2018)
- [4]. **Review:** Piquemal-Banci et al. *J. Phys. D: Appl. Phys.* **50**, 203002 (2017)

## INVITED SPEAKERS

**Id-1515**

### **Methods to Improve Fly Ash Reactivity and Increase Its Reuse Potential in Construction Materials Industry**

Zvezdana Bascarevic

Institute for Multidisciplinary Research Belgrade University, Kneza Viselava 1, 11030 Belgrade, Serbia

Corresponding author: zvezdana@imsi.bg.ac.rs

**Abstract:** Fly ash, a by-product from coal combustion in thermal power plants, is one of the most abundant anthropogenic materials. It is estimated that between 500 and 750 million tonnes of this material is generated worldwide annually. Various recycling and reuse options have been recognized for a long time now, with the highest quantities of fly ash being used in construction industry, either as a raw material or as an additive in cement and concrete industry. Current utilization rates of fly ash are assessed to be around 90 % in EU, 70 % in China and 40 % in USA, but with global average at only 25 %. Very often, possibilities to reuse local fly ash are limited by its properties, i.e. reactivity. Particle size distribution, chemical and mineralogical compositions are the most important properties of a fly ash sample that influence its reuse potential.

This works shows the effects of mechanical and chemical activation of several fly ash samples from several power plants on the properties of the fly ash and the properties of different construction materials based on the fly ash. Mechanical activation of the fly ash samples was done in a planetary ball mill. Optimization of the activation process was performed by gradual decrease in the grinding balls to fly ash ratio, thus decreasing the energy used for the process. It was found that even with very low ball-to-powder ratio, such as 3, it was possible to achieve drastic improvement in fly ash properties, in terms of particle size distribution and specific surface area.

Both starting and mechanically activated fly ash samples were used as raw materials for synthesis of geopolymers (binder materials made 100 % of fly ash) and hybrid binders (high volume fly ash binders, in which up to 70 mass % of Portland cement was substituted by fly ash). Also, suitability of the fly ash samples as cement replacement material in concrete was evaluated. It was found that with proper chemical activation of the fly ash samples it was possible to produce binder materials with mechanical properties comparable, or even superior, to traditionally used Portland cement.

**Keywords:** Building materials, fly ash

## INVITED SPEAKERS

Id-1519

**Modified TiO<sub>2</sub> Based Nanostructures for Photocatalysis**

Andreja Gajović<sup>1</sup>, Milivoj Plodinec<sup>2</sup>, Vedran Kojić<sup>1</sup>, Marko Rukavina<sup>3</sup>, Nikša Krstulović<sup>4</sup>, Blažeka Damjan<sup>4</sup>,  
Salamon Krešimir<sup>1</sup>, Luka Radetić<sup>5</sup>, Marc Willinger<sup>6</sup>, Miran Čeh<sup>7</sup>, Ivana Grčić<sup>5</sup>

<sup>1</sup>Ruđer Bošković Institute, Bijenička 54, HR-10000 Zagreb, Croatia

<sup>2</sup>Fritz-Haber-Institute der Max-Planck-Gesellschaft, D-14195 Berlin, Germany

<sup>3</sup>Graduate student at University of Zagreb, Faculty of Chemical Engineering and Technology, Marulićev trg 19,  
HR-10000 Zagreb, Croatia

<sup>4</sup>Institute of Physics, Bijenička 46, HR-10000 Zagreb, Croatia

<sup>5</sup>University of Zagreb, Faculty of Geotechnical Engineering, Hallerova aleja 7, HR-42000 Varaždin, Croatia

<sup>6</sup>ETH Zürich, Otto-Stern-Weg 3, 8093 Zürich, Switzerland

<sup>7</sup>Jožef Stefan Institute, Jamova 39, SI-1000 Ljubljana, Slovenia

Corresponding author: gajovic@irb.hr

**Abstract:** Increasing awareness of harmful consequences of persistent organic pollutants in water makes development of cheap and stable photocatalysts for their degradation one of significant goals in environmental engineering. Materials based on nanostructured TiO<sub>2</sub> are among the most prominent materials of the last 40 years that have been studied for the purpose of use in photocatalysis. One of the main limitations for the application of TiO<sub>2</sub> in materials photocatalysis is a wide energy bandgap,  $E_g = 3.2$  eV, so its application is limited to UV radiation. In order to increase the efficiency of the TiO<sub>2</sub> nanostructure as a photocatalyst and expand the spectral range in which the photocatalyst is activated, different approaches to modifications of the synthesized nanoparticles of TiO<sub>2</sub> were applied.

In this study the photocatalytic degradation of water pollutant will be examined using different nanostructures of TiO<sub>2</sub>-based photocatalysts. The strategies used for the improvement of their photocatalytic activity in UV region as well as broadening of their activity in visible and near IR light, will be presented.

The synthesis of TiO<sub>2</sub> nanostructures (nanotubes-NT, and nanoparticles-NP) was obtained by electrochemical oxidation in organic electrolyte and hydrothermal syntheses for preparation of NT, or by pulsed laser ablation (PLA) for preparation of NP. Surface modification and decoration with silver nanoparticles was done by photo-reduction, while decoration with FeOOH/Fe<sub>2</sub>O<sub>3</sub> was achieved by hydrothermal synthesis. The additional processing in reduction atmosphere was also occasionally applied. The structural properties of studied photocatalysts were investigated by X-ray powder diffraction (XRD), Raman spectroscopy, scanning and transmission electron microscopy (SEM and TEM), while the photocatalytic degradation was studied using different model pollutants from simple dyes as methylene blue, or caffeine to serious industrial and pharmaceutical pollutants as 2,5-dihydroxybenzoic acid, or salicylic acid.

It was shown that the photocatalytic activity of studied nanostructures was considerably increased by optimization of the TiO<sub>2</sub>-based materials bandgap to obtain absorption in the visible and near-IR regions of the solar irradiation by decoration with Ag or FeOOH/Fe<sub>2</sub>O<sub>3</sub> nanoparticles, and/or by introducing defects in reduction atmosphere. The improvement of photocatalytic properties of TiO<sub>2</sub> nanoparticles

prepared by PLA were obtained by increase of the active surface by decreasing the size of TiO<sub>2</sub> photocatalyst nanoparticles and by introducing some content of TiO<sub>2</sub> of Magneli phases. The shift of the photocatalytic activity in the visible and near-IR regions of the spectrum would allow the work of photocatalytic reactors for purification of the water using only sun light without appliance of additional UV lamps. The photocatalytic properties of the synthesized photocatalysts will be discussed considering the morphology, crystal structure and the atomic percentage of the decoration.

**Keywords:** TiO<sub>2</sub>, nanostructures, structural characterization, photocatalysis

**Acknowledgment:** This work has been supported in part by Croatian Science Foundation under the project IP-2018-01-5246, and by the European Union funds under the project "Unlocked solar cells and modules through research and development activities".

## INVITED SPEAKERS

**Id-1524**

### **Effect of Dynamic Strain Aging on Thermomechanical Response of High Strength Steels**

Farid Abed

Department of Civil Engineering, American University of Sharjah, United Arab Emirates (UAE), P. O. Box: 26666

Corresponding author: fabled@aus.edu

**Abstract:** Experimental investigation of the thermomechanical behavior of several high strength steel alloys such as AISI4140, MMFX bars, C45 and EN8 under different temperatures and strain rates is presented in this paper. Quasi-static and dynamic tests were conducted at a range of temperatures between 298°K and 923°K and for strain rates up to  $10^3 \text{ s}^{-1}$  using universal testing machines, drop-hammer and Split-Hopkinson bar tests. The true stress true strains for the different combinations of strain rates and temperatures are presented and discussed. Scanning electron microscopy (SEM) images were also utilized to quantify the density of micro-cracks and voids of fractured specimens. Particular attention was paid to key features related to the significant effect of dynamic strain aging and its connection to the coupling effect of temperatures and strain rates. The flow stresses of C45, EN8, AISI 4140 and MMFX steels showed almost insignificant dependence on the quasi-static strain rate at room temperature. However, the strain rate sensitivity increases as the temperature increases with very active regions of dynamic strain aging (DSA) encountered at higher temperatures. The tests results were then utilized to verify the Voyiadjis-Abed (VA) model and describe the flow stress of these alloys for finite element modeling and applications, and to simulate different structural responses of these steel alloys.

**Keywords:** High strength steel, temperature, strain rate, DSA

## INVITED SPEAKERS

**Id-1525**

### **Multiferroic Domain Walls in Ferroelastic Materials**

Guillaume Nataf<sup>1</sup>, Dominique Martinotti<sup>2</sup>, Claire Mathieu<sup>2</sup>, Raphaël Haumont<sup>3</sup>, Patrick Hicher<sup>3</sup>, Mael Guennou<sup>4</sup>,  
Ludovic Torteche<sup>5,6</sup>, Jens Kreisel<sup>4</sup>, Nick Barrett<sup>2</sup>

Department of Materials Science, University of Cambridge, 27 Charles Babbage Road, Cambridge CB3 0FS, UK

<sup>2</sup>SPEC, CEA, CNRS, Université Paris-Saclay, CEA Saclay, 91191 Gif-sur-Yvette Cedex, France

<sup>3</sup>ICMMO, Université Paris-Sud, 91405 Orsay, France

<sup>4</sup>Physics and Materials Science Research Unit, University of Luxembourg, 41 Rue du Brill, L-4422 Belvaux,  
Luxembourg

<sup>5</sup>CEA Saclay, IRAMIS, NIMBE (UMR 3685), LICSEN, 91191 Gif-sur-Yvette, France

<sup>6</sup>Sorbonne Universités, UPMC Univ Paris 06, Institut Parisien de Chimie Moléculaire (UMR CNRS 8232), Paris,  
France

Corresponding Author: gn283@cam.ac.uk

**Abstract:** There is a growing interest for structural and electric properties of ferroelectric and ferroelastic domain walls, within the emerging field of domain boundary engineering [1,2], which holds the promise of using distinct functional properties of domain walls in and as devices. In particular, there has been a search for ferroelectric domain walls in non-ferroelectric materials [3–6].

Here, we report a study of ferroelastic domain walls in non-ferroelectric, non-polar CaTiO<sub>3</sub>. We use a low energy electron microscope (LEEM) to observe domain walls in CaTiO<sub>3</sub> and provide direct in-situ evidence of their polar nature and as such of their possible multiferroic character (ferroelastic and ferroelectric). In a second step, we study the manipulation of surface charges at domain walls upon electron injection, realized by increasing the energy of the incoming electron beam of the LEEM [7].

**Keywords:** Domain walls

#### **References**

- [1]. G. Catalan, J. Seidel, R. Ramesh, and J. F. Scott, *Rev. Mod. Phys.* **84**, 119 (2012).
- [2]. E. Salje and H. Zhang, *Phase Transitions* **82**, 452 (2009).
- [3]. Y. Frenkel, N. Haham, Y. Shperber, C. Bell, Y. Xie, Z. Chen, Y. Hikita, H. Y. Hwang, E. K. H. Salje, and B. Kalisky, *Nat. Mater.* **16**, 1203 (2017).
- [4]. D. Pesquera, M. A. Carpenter, and E. K. H. Salje, *Phys. Rev. Lett.* **121**, 235701 (2018).
- [5]. H. Yokota, S. Matsumoto, E. K. H. Salje, and Y. Uesu, *Phys. Rev. B* **98**, 104105 (2018).
- [6]. P. Tolédano, M. Guennou, and J. Kreisel, *Phys. Rev. B* **89**, 134104 (2014).
- [7]. G. F. Nataf, M. Guennou, J. Kreisel, P. Hicher, R. Haumont, O. Aktas, E. K. H. Salje, L. Torteche, C. Mathieu, D. Martinotti, and N. Barrett, *Phys. Rev. Mater.* **1**, 074410 (2017).

## INVITED SPEAKERS

**Id-1548**

### **Functional Block Copolymer Nanocarriers of Natural Polyphenols**

Petar Petrov

Institute of Polymers, Bulgarian Academy of Sciences, Akad. G. Bonchev St. 103 A, 1113 Sofia, Bulgaria

ppetrov@polymer.bas.bg

**Abstract:** Functional polymeric nanocarriers have attracted considerable attention for application in drug and gene delivery due to their favourable properties such as biocompatibility, longevity, high loading capacity and *in vivo* stability, controlled drug release profile, and capability to accumulate in target zones of the body. In particular, functional block copolymer micelles have great potential to overcome the existing pharmaceutical and clinical limitations of many hydrophobic bioactive substances.

This contribution describes the fabrication of functional polymeric nanocarriers by self- and co-assembly of amphiphilic block copolymers. Various biocompatible and biodegradable copolymers were obtained via controlled polymerization techniques and click chemistry. In the next step, nano-sized micelles of tailored structure, composition and functionality were formed by (cooperative) self-assembly of block copolymers in aqueous media using the solvent evaporation method. The micelles were then loaded with the biologically active substances curcumin and caffeic acid phenethyl ester. The colloid stability, release profile, encapsulation efficiency, and cytotoxicity of micellar nanocarriers were assessed. In vitro experiments revealed a sustained release profile and an enhanced antitumor and antioxidant activity of the micellar formulation as compared to the free drugs. A multifunctional system exhibited great potential for targeted delivery of anti-cancer drugs in mitochondria, thus causing programmed tumor cell death.

**Keywords:** Nanocarriers, blok copolymers

**Acknowledgements:** This work was supported by the Bulgarian National Science Fund (Grant DN 09/1 - 2016).

## INVITED SPEAKERS

Id-1555

## Formation Mechanism, Structure, Magnetic and Photocatalytic Properties of Aluminate and Ferrite Spinels

Chanapa Kongmark<sup>1,2</sup>, Thanit Tangcharoen<sup>3</sup>, Pongtanawat Khemthong<sup>2,4</sup><sup>1</sup>Department of Materials Science, Faculty of Science, Kasetsart University, Bangkok 10900, Thailand<sup>2</sup>Research Network of NANOTEC—KU on NanoCatalysts and NanoMaterials for Sustainable Energy and Environment, Kasetsart University, Bangkok 10900, Thailand<sup>3</sup>Department of Basic Science and Physical Education, Faculty of Science at Sriracha, Kasetsart University, Sriracha Campus, Chonburi 20230, Thailand<sup>4</sup>National Nanotechnology Center (NANOTEC), National Science and Technology Development Agency (NSTDA), Pathumthani 10900, Thailand

Corresponding author: chanapa.k@ku.th

**Abstract:** Metal oxide nanoparticles with spinel-type crystal structure have gained considerable attention for a wide range of applications such as gas sensors, catalysts, supercapacitors, ceramic coating, optical and electronic devices. Knowledge on structural properties of the spinel is the key to the development of this class of material because it can dictate the characteristic properties of these materials. A summary of our recent research on the formation mechanism, the relationship between structure, magnetic and photocatalytic properties of aluminate and ferrite spinels will be presented.

The reaction mechanism during the formation of CuFe<sub>2</sub>O<sub>4</sub> spinel nanoparticles from Cu(II) and Fe(III) nitrate precursors in the confined space of SBA-15 at high temperature was monitored by in-situ X-ray absorption spectroscopy (XAS) using the synchrotron radiation (at SLRI, Thailand). The new formation mechanism was observed, the intermediate processes were elucidated [1].

Spinel ferrite nanoparticles (MFe<sub>2</sub>O<sub>4</sub>; M = Ni, Mn, and Cu), which are well-known for potential applications as magnetic catalysts, were successfully synthesized via sol-gel auto-combustion method. The cation distribution and valence state of these ferrites were probed by Ni, Mn, Cu, and Fe K-edge XAS. The relationship between the local atomic structure of metals and the magnetic properties of these materials has been illustrated [4].

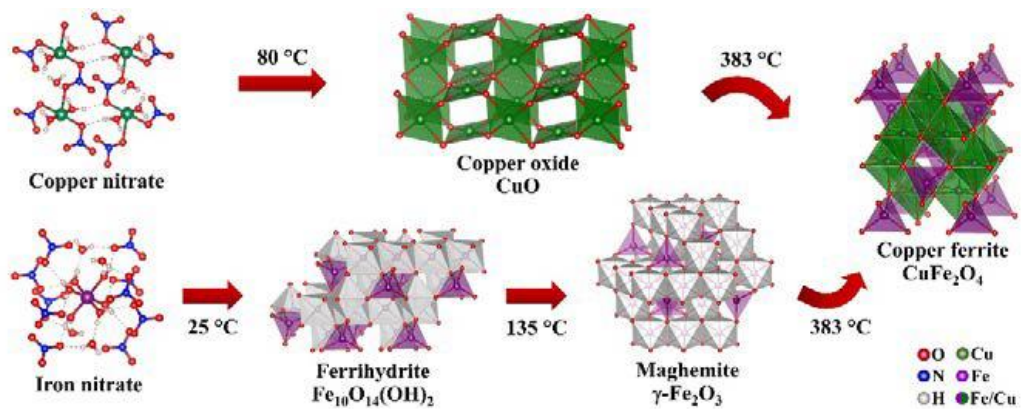
Nanocrystalline aluminate spinels (MAI<sub>2</sub>O<sub>4</sub>; M = Ni, Cu, and Zn) were obtained with various crystallite sizes (40–60 nm) and distinct band gap energies, *E<sub>g</sub>* (3.0–5.5 eV). The photocatalytic activity of these materials were evaluated by the decomposition of four types of pollutants: phenol rhodamine B, heteropolyaromatic methylene blue, azoic methyl orange, and methyl red under ultraviolet irradiation. The photocatalytic degradation efficiencies of all organic dyes by aluminate spinels reach 80–95% within 100 min. These results suggested that NiAl<sub>2</sub>O<sub>4</sub>, CuAl<sub>2</sub>O<sub>4</sub> and ZnAl<sub>2</sub>O<sub>4</sub> can serve as photocatalysts for the degradation of a wide range of organic pollutants in environment [2,3].

**Keywords:** Aluminate spinel, Ferrite spinel, Formation, Photocatalysis.

### References

- [1]. P. Khemthong, C. Kongmark, N. Kochaputi, S. Mahakot, S. Rodporn, K. Faungnawakij, Inorg. Chem. 58 (2019) 6584-6587.
- [2]. T. Tangcharoen, W. Klysubun, C. Kongmark, J. Mol. Struct. 1182 (2019) 219-229.

- [3]. T. Tangcharoen, J. T-Thienprasert, C. Kongmark, J. Mater. Sci.: Mater. Electron. 29 (2018) 8995-9006.
- [4]. T. Tangcharoen, W. Klysubun, C. Kongmark and W. Pecharapa, Phys. Status Solidi A 211 (2014) 1903-1911.



Formation mechanism of CuFe<sub>2</sub>O<sub>4</sub> spinel in the confined space of SBA-15 [1].

## INVITED SPEAKERS

Id-1557

### **Mesoporous Silica Nanocomposites for Advanced Luminescent Chemosensor Materials: Design, Synthesis, Fabrication and Applications**

Hendrik Oktendy Lintang

Department of Chemistry, Faculty of Science and Technology, Universitas Ma Chung, Villa Puncak Tidar N-01,  
Malang 65151, East Java, Indonesia, Tlp.

Corresponding author: hendrik.lintang@machung.ac.id

**Abstract:** Porous nanomaterials such as mesoporous silica have been widely used for many applications due to the presence of uniform pores or channels and a large pore size as well as the properties of its surface. As chemosensor materials, nanocomposites of mesoporous silica consisting functional organic groups as a sensing site have been designed, synthesized and fabricated based on their desired functions for high sensing capability. In this lecture, advanced mesoporous silica nanocomposites with two types of organic functional groups from sol-gel [1] and grafting methods reveal as luminescent chemosensor materials [2] for the selective detection of metal ions. The first approach utilized mesoporous silica nanocomposite from sol-gel method where thin film consisting of one-dimensional columnar assembled gold(I) pyrazolate complex was successfully prepared for the detection of silver (Ag<sup>+</sup>) ions. In particular, when thin film composite was simply dipped into a tetrahydrofuran solution of 10 to 100  $\mu$ M silver triflate, the resulting composite showed a new luminescent peak centered at 486 nm (excitation at 276 nm) from a weak Au(I)–Ag(I) heterometallic interaction with a blue-green emission (at dark room with excitation at 254 nm). In addition, the original peak at 693 nm from a weak Au(I)–Au(I) monometallic interaction with a red emission (at dark room with excitation at 254 nm) was decreased at the same time. In 30 mins, the original emission intensity was quenched in 82%. The thin film composite can be reused by washing with cetyltrimethylammonium chloride in chloroform. Such sensing phenomenon is due to the permeation of silver ions to the silicate nanochannels to induce intra-columnar energy transfer [1]. The second approach utilized mesoporous silica nanocomposite from grafting method where Schiff base *N*-(5-nitro-2-oxindolin-3-ylidene)thiophene-2-carbohydrazide as a ligand was successfully grafted via an aminopropyl linker to the silica surface for the binding of iron (Fe<sup>3+</sup>) ions. In the range of 50 to 200  $\mu$ M for aqueous solution of Fe<sup>3+</sup> ions, the resulting powder composite showed a quenching phenomenon of its original emission peak at 533 nm (excitation at of 277 and 370 nm) up to 84%. The powder composite can be reused by binding to potassium thiocyanate in hydrochloric acid (pH = 1). Such sensing phenomenon is due to the interaction of Fe<sup>3+</sup> ions to C=O and C-S, C=N and C=O, and N-H and C=O sites of the ligand in the surface [2].

**Keywords:** Chemosensor, mesoporous silica, nanocomposite, organic functional group, sensor

**Acknowledgements:** This research was financially supported through World Class Research (WCR) Grant 2019 with a contract number of 012/MACHUNG/LPPM/SP2H-LIT-MULTI/III/2019, Ministry of Research, Technology and Higher Education, The Republic of Indonesia.

#### **References**

- [1]. Hendrik O. Lintang, Kazushi Kinbara, Takashi Yamashita and Takuzo Aida, *Chemistry – An Asian Journal* **2012**, 7, 2068-2072.
- [2]. Muhammad Riza Ghulam Fahmi, Adroit T.N. Fajar, Nurliana Roslan, Leny Yuliaty, Arif Fadlan, Mardi Santoso, Hendrik O. Lintang, *Open Chemistry* **2019**, 17, 438-447.

## INVITED SPEAKERS

**Id-1575**

### **Magnetized Relativistic Pulsar Winds**

Yu-Qing Lou

Tsinghua University, Physics Department and Tsinghua Center for Astrophysics, Tsinghua University-National Astronomical Observatories of China joint Research Center for Astrophysics, Department of Astronomy, Beijing, 100084 China

**Abstract:** We present a theoretical model for relativistic magnetohydrodynamic (RMHD) fluctuations in magnetized pulsar wind from a fast spinning radio pulsar involving electron-positron pair plasma. We advance a physical scenario for RMHD pulsar wind in the context of Crab Nebula involving RMHD shocks, magnetic reconnections, acceleration of pair particles, and high-energy photons. We also describe various MHD tidal waves in the thin magnetized plasma ocean in fast spinning neutron star and pertinent possible diagnostics.

**Keywords:** Relativistic magnetohydrodynamic, magnetized pulsar wind, Crab Nebula, MHD tidal waves

## REGULAR SESSIONS

Id-1190

### Self-Propagating High-Temperature Synthesis of $\text{Fe}_2\text{TiSn}_{1-x}\text{M}_x$ (M= Hf, V, Zr, Si) Heusler alloys with Following Spark Plasma Sintering

Zhanna Yermekova<sup>1</sup>, Sedegov Aleksey<sup>1</sup>, Moskovskikh Dmitry<sup>1</sup>, Novitskii Andrei<sup>2</sup>, Taranova Anastasiia<sup>2</sup>,  
Voronin Andrei<sup>2</sup>, Khovaylo Vladimir<sup>2</sup>,

<sup>1</sup>Russia, Moscow, Leninsky ave. 4, National University of Science and Technology MISIS, Research Center of Functional Nanoceramics

<sup>2</sup>Russia, Moscow, Leninsky ave. 4, National University of Science and Technology MISIS, Academic Research Center for Energy Efficiency

Corresponding author: ifjanna@gmail.com

**Abstract:** Sustainable energy concept is very important since the human population and basic energy demand are continuously growing. Such class of materials as thermoelectrics (TE) are able to convert heat energy directly into electricity and vice versa which makes them an essential component for development of efficient energy consumption strategy [1-4].

Repeated melting of mixed pure metals followed by annealing is a conventional approach for production of TE materials. In some cases additional pre- and post-treatment procedures [5] are also involved. Such approach is energy consuming and hard-to-adopt for large-scale production of nanostructures TE materials. Alternatively, several new techniques were suggested. Self-propagating high-temperature synthesis (SHS) could be a most promising approach for the direct single-phase TE material production at a minimal cost and on the timescale of seconds [6].

In a present work microstructure evolution of the materials were investigated for the  $\text{Fe}_2\text{TiSn}_{1-x}\text{M}_x$  (M = Hf, V, Zr, Si) component alloys. Thermoelectrical properties as a function of the doping element concentration were shown. Comparative analysis of the thermoelectric properties and structure evolution were performed as a function of the fabrication approach. Mechanical activation (MA), SHS followed by spark plasma sintering (SPS) and volume combustion synthesis approaches were considered for better material synthesis.

**Keywords:** Thermoelectric materials, Heusler alloys, self-propagating high-temperature synthesis, spark plasma sintering, mechanical activation.

#### References

- [1]. Yinhang Zhang, Young-Jung Heo, Mira Park, Soo-Jin Park (2019) Recent Advances in Organic Thermoelectric Materials: Principle Mechanisms and Emerging Carbon-Based Green Energy Materials, *Polymers* 11(1), 167. doi:10.3390/polym11010167
- [2]. R. Rodriguez, M. Preindl, James S. Cotton, Ali Emadi (2019) Review and Trends of Thermoelectric Generator Heat Recovery in Automotive Applications. *IEEE Transactions On Vehicular Technology*, accepted for publication doi:10.1109/TVT.2019.2908150
- [3]. Liu X and Wang Z (2019) Printable Thermoelectric Materials and Applications. *Front. Mater.* 6:88. doi: 10.3389/fmats.2019.00088

- [4]. S. Sinha, G. A. Vinayak, S.S. John, S. Kundu (2018) DC DC Boost Converter for Thermoelectric Energy Harvesting. Proceedings of the 2018 International Conference on Current Trends towards Converging Technologies, doi: 10.1109/ICCTCT.2018.8551039
- [5]. T. Mori (2017) Novel Principles and Nanostructuring Methods for Enhanced Thermoelectrics, *Small*. 13 1702013. doi:10.1002/smll.201702013.
- [6]. Y. Xing, R. Liu, Y.-Y. Sun, F. Chen, K. Zhao, T. Zhu, S. Bai, L. Chen (2018) Self-propagation high-temperature synthesis of half-Heusler thermoelectric materials: reaction mechanism and applicability, *J. Mater. Chem. A*. 6 19470–19478. doi:10.1039/C8TA07411A.

**REGULAR SESSIONS****Id-1196****ReRAM based on Water Soluble Polymer Nano Composite**

Sreedevi Vallabhapurapu

School of Computing, University of South Africa, Johannesburg 1710, South Africa

Corresponding author: vallas@unisa.ac.za

**Abstract:** Polymer nano composite based ReRAM has shown great potential among all other emerging memories for non-volatile memory applications. This is because of its simple structure and easy processing. The resistive switching layer used in the ReRAM devices is in general, nano particle incorporated polymer nano composite. In this context using a water soluble polymer nano composite as the active layer is interesting. Polyvinyl alcohol (PVA) is a water soluble material, which can be used for a memory device because it is less expensive and easy film formation. Inadequate work has been carried out so far in this particular material [1]. It is interesting to look into this material with different dispersion of nanomaterials for memory switching behaviour. In this context ReRAM with Polyvinyl alcohol (PVA) nanocomposite matrix (PVA and nano materials like Aluminium doped ZnO (AZO)) was developed, using simple drop casting on aluminium foil. Aluminium doped zinc oxide (AZO) nanoparticles with size ranging from 20 nm- 30 nm was prepared by chemical pyrophoric method, which was described elsewhere [2]. The top electrode is silver. We observed high switching ratio (> 3 orders of magnitude), between the high resistive state (HRS) and low resistive state (LRS) The switching mechanism involved in this organic computer memory was studied by modelling and analysing the switching characteristics.

**Keywords:** Nano composites, ReRAM, Polyvinyl alcohol (PVA)

**Acknowledgements:** We acknowledge University of South Africa for partial financial support. Experimental facilities and measurements at University of Hyderabad, India are acknowledged.

**Reference**

- [1]. Sreedevi Vallabhapurapu, L.D. Varma Sangani, M. Ghanashyam Krishna, V.V. Srinivasu, C. Du, S. Du and A. Srinivasan, *Materials Today: Proceedings* 9, 615 (2019)
- [2]. J. Das, D.K. Mishra and V.V. Srinivasu, *Journal of Alloys and Compounds* 704, 237 (2017)

## REGULAR SESSIONS

Id-1197

## Low field Microwave Absorption in Metal Nanoparticles Embedded Conducting Polymers

Vijaya Srinivasu Vallabhapurapu

Department of Physics, University of South Africa, Johannesburg 1710, South Africa.

**Abstract:** Low field microwave absorption (LFMA) in conducting polymers is very intriguing because it is completely different as compared to magnetic systems [1,2]. As an attempt to understand LFMA phenomenon in the conducting polymers, we choose a model system, namely, the conducting polyaniline (PANI) polymer and iron nanoparticles (NPs) embedded polyaniline nanofibres (PANI-Fe) composite systems. Then we systematically studied LFMA in this system. Synthesis of PANI-Fe composite nanofibers was described elsewhere [3]. Through our LFMA studies, we are able to establish that LFMA is absent in pure PANI, in spite of PANI being non-degenerate conducting polymer. On the other hand, LFMA was observed in bare Fe NPs systems and Fe NPs embedded PANI nanofibers. Key features are (a) Presence of minor hysteresis in LFMA, as compared to the substantial magnetization hysteresis (b) LFMA derivative peaks not having any correlation with the M-H loop anisotropy and coercive fields. This rules out the conventional interpretation of LFMA arising from the low field spin magnetization processes as reported in the literature. (c) microwave absorption in PANI-Fe system has a maximum at zero field and decreases with increasing applied magnetic field. This also rules out the predicted behaviour of polaron-bipolaron based mechanism for the LFMA origin. It is to be noted that in such a mechanism, the microwave absorption has a minimum at zero field and increases with the field in the case of non-degenerate conducting polymers, which was earlier reported in literature. Our work shows that LFMA correlates well with the magnetoresistance data for the PANI-Fe composite nanofibers system. This indicates that LFMA in this system is actually governed by magneto transport and not exactly by the low field magnetization process itself. We then compare our results with LFMA in various magnetic and multiferroic systems and try to give a generalized picture of understanding.

**Keywords:** Low field Microwave Absorption, conducting polymers, nano composites

### References

- [1]. V.V. Srinivasu, S.E. Lofland, S.M. Bhagat, K. Ghosh, S.D. Tyagi, Temperature and field dependence of microwave losses in manganite powders, *J. Appl. Phys.* 86 (1999) 1067.
- [2]. T.S. Mahule, V.V. Srinivasu, J. Das, Observation of low field microwave absorption in co-doped ZnO system, *Solid State Commun.* 243 (2016) 60.
- [3]. Madhumita Bhaumik, Arjun Maity, T.S. Mahule, V.V. Srinivasu, Low field microwave absorption in iron nanoparticles embedded polyaniline nanofibers composite, *Synthetic Metals*, 249 (2019) 63.

## REGULAR SESSIONS

Id-1216

### Vortex Motion of an Incompressible Polymeric Liquid

Roman Semenko, Alexander Blokhin

Novosibirsk State University, Sobolev Institute of Mathematics SB RAS, 630090, Novosibirsk, Russian Federation

Corresponding author: r.semenko@g.nsu.ru

**Abstract:** The dynamics of liquid polymers is rapidly developing modern field of applied physics due to the importance of polymeric materials and additive technologies. However, mathematically the modeling of polymer dynamics is challenging problem because of complex molecular structure of these materials. A number of different models of polymer hydrodynamics were introduced since the middle of XX century but from the mathematical point of view the most advanced and promising models are relatively poorly studied and their properties are mostly unclear.

The main goal of our research is to study one relatively recent rheological model of liquid polymers which is the mesoscopic Pokrovskii-Vinogradov model. We are focusing on various types of vortex motions within this model. This kind of motions have well-studied analogues for viscous Newtonian fluids which allows us to use the techniques developed for Navier-Stokes equations theory.

We are studying two types of flows. First one is the vortex motion of polymeric liquid in cylindrical near-axial zone. We are considering both stationary and non-stationary solutions with fixed and free boundary of axial zone. We also study this type of flow at the presence of magnetic field. Second type of flow is vortex motion of viscoelastic polymeric liquid above the rotating infinite disc. Here we are constructing the analogue of the well-known von Karman model of rotating viscous fluid.

**Keywords:** Liquid polymers, vortex motion, magnetohydrodynamics

## REGULAR SESSIONS

**Id-1217**

### **Affinity-Based Performance Analysis of Heterojunction p-i-n PV Cells**

Samed Halilov, Ahmer Baloch, Sergey Rashkeev, Noar Tabet, Fahhad Alharbi

QEERI, HBKU, Doha, Qatar

Corresponding author: samed.halilov@gmail.com

**Abstract:** Effect of the band alignment on the performance of hetero-junction p-i-n solar cell is investigated in the framework of 1D transport model. An affinity-based approach is introduced in order to identify a set of material parameters and doping levels which would result in lower series resistance  $R_s$ , higher open-circuit voltage  $V_{oc}$  and higher fill factor  $FF$ . The search reveals key ingredients of the hetero-junction optimized design. On one hand, certain band alignment determined by affinity-related quantities has to be observed to ensure the case of staggered gaps, once the dimensional requirements in the absorber and in the charge collectors are met. On the other hand, an affinity-based constraint is shown to control the potential profile which mitigates the adverse effect of barriers and accumulation regions at the junction interfaces. The constraint is shown to result in lower  $R_s$  and thus higher  $FF$ . Analytical approach reveals a whole region in the affinity space where the reverse saturation current  $J_0$  is at minimum, which also strongly overlaps with the constraints pinning down  $R_s$ . It is concluded that the performance figures are featured with shallow minima as functionals in roughly same region of the affinity space, where those numbers are also relatively stable. The findings aim at making material screening more feasible and widens significantly the options in the design of new p-i-n cells.

**Keywords:** Affinity discontinuity, Band alignment, Material Screening Descriptors, Closed-form expressions, Heterojunction solar cell.

## REGULAR SESSIONS

**Id-1303**

### **On the Choice of the Geometrical Extrapolation Models for the Mg-Al-Sr System Based on Experimental Investigation**

Mohammad Aljarrah, Atif Alkhazali

Industrial Engineering Department, Faculty of Engineering, The Hashemite University,

P.O. Box 150459, Zarqa 13115, Jordan

Corresponding author: maljarrah@hu.edu.jo

**Abstract:** Choice symmetry/asymmetry extrapolation model is proposed in the current study. solidification curves were deduced from DSC curves using heat transfer model as well as solidification curves predicted from different extrapolation models based on thermodynamic properties of binary sub-systems are presented. It was found that Kohler gives a better agreement than Muggianu (symmetric model). Moreover, treating Sr alone and taking it as single out gives the best prediction for solidification curves for all tested alloys. It has been shown that solidification curves calculated using Toop model for the ternary system, where Al or Mg is asymmetric, gives the poorest fit solidification curves deduced from DSC data.

**Keywords:** Symmetric/asymmetric model, Heat transfer model (HTM).

## REGULAR SESSIONS

Id-1324

### Blister Formation in Tungsten by Deuterium Ion Irradiation: Energy and Fluence Dependent Study

Asha Attri<sup>1</sup>, Arun Zala<sup>2</sup>, Ratnesh Kumar<sup>2</sup>, Anil Tyagi<sup>1,3</sup>, Sudhirsinh Vala<sup>2</sup>, Shishir Deshpande<sup>2,3</sup>

<sup>1</sup>ITER-India, Institute for Plasma Research, Bhat, Gandhinagar-382428, India

<sup>2</sup>Institute for Plasma Research, Bhat, Gandhinagar-382428, India

<sup>3</sup>Homi Bhabha National Institute, Training School Complex, Anushaktinagar, Mumbai 400094

Corresponding author: asha-pdf@iter-india.org

**Abstract:** Gaseous ion irradiation induced blister formation in plasma facing materials is one of the undesirable and unavoidable phenomenon in nuclear reactors. Presence of different type of impurities and lattice imperfection in material during its fabrication processes lead to increase the accumulation of gaseous atoms inside the host material. Formation of blisters severely impair mechanical strength and threat for its lifetime due to flaking/erosion of surface. Understanding the behavior and mechanism of blister formation in radiation environment is required to elucidate their properties as well as mitigate irradiation damage. Different energy and fluence dependent studies are required to set a template for blister formation and understand the phenomenon in detail.

In the present experiment polycrystalline tungsten (W) foils of thickness 0.1 mm, procured from Princeton Scientific Corporation, USA. Annealing of W foils were done at temperature 1838 K. Deuterium (D) ion irradiation with three different energies i.e. 5 keV, 10 keV and 15 keV D were done on tungsten foils at room temperature. Two different fluence  $5 \times 10^{17}$  ions/cm<sup>2</sup> and  $5 \times 10^{18}$  ions/cm<sup>2</sup> were selected for individual energies. Surface morphological studies with high resolution scanning electron microscope (FE-SEM), X-ray Diffraction and transmission electron microscopy (TEM) characterizations of W foils were done pre and post irradiation. Transfer of energy from the incoming ion to the lattice via electron phonon coupling provides required nano-scale modifications. Variation in surface morphology and difference in size of blisters on the surface confirms that except grain boundaries other trapping site exists, supporting accumulation of D atoms.

**Keywords:** Ion irradiation, blister, tungsten, FE-SEM, TEM

#### References:

- [1]. R. Neu, Tungsten as a Plasma Facing Material, (2003).
- [2]. W. Hu, F., Luo, Z., Shen, L., Guo, Z., Zheng, Y., Wen, Y., Ren. (2015) Hydrogen bubble formation and evolution in tungsten under different hydrogen irradiation conditions, Fusion Eng. Des. 90, 23–28.

## REGULAR SESSIONS

**Id-1335**

### **Prediction of Fatigue Lives of Aluminum Alloys Using Crystal Plasticity Framework**

Vidit Gaur<sup>1</sup>, Fabien Briffod<sup>2</sup>, Manabu Enoki<sup>2</sup>

<sup>1</sup>Department of Mechanical and Industrial Engineering, Indian Institute of Technology,  
Roorkee 247667, Uttarakhand, India

<sup>2</sup>Department of Materials Engineering, The University of Tokyo, 7-3-1 Hongo, Bunkyo-ku, Tokyo, 113-8656,  
Japan

Corresponding Author: viditgaurfme@iitr.ac.in

**Abstract:** This study aims to formulate a crystal plasticity framework for the prediction of fatigue lives of aluminum 5xxx alloy (FCC polycrystal). Al-5083 plates were welded using two different filler materials, Al-5183 and Al-5.8%Mg. EBSD analyses of weld bead revealed isotropic texture in all three directions with nearly equi-axed grains but different average grain sizes (5083/5183: ~60  $\mu\text{m}$  and 5083/Al-5.8%: ~90  $\mu\text{m}$ ). Low-cycle fatigue tests were run on cylindrical specimens of  $\phi 5$  mm using triangular waveform for different strain amplitudes (0.35%, 0.5%, 0.8%) but constant strain rate,  $10^{-3}$  sec<sup>-1</sup>. The data was used to calibrate the crystal plasticity parameters. Fully reversed high-cycle fatigue tests were run using the sinusoidal waveform at 30 Hz on similar shaped specimens. Physically short-crack growth tests were run on specially made dog-bone shaped flat specimens. The data obtained was compiled together and compared with the simulated results. Several 2D polycrystalline aggregates were generated using the home-made algorithm. The grain size and shape distribution was extracted from EBSD data by fitting each grain to an approximate ellipse. The poles figures obtained from these synthetic microstructures were compared with the experimental ones. Finite element simulations using a crystal plasticity model were performed under cyclic uniaxial tension-compression condition. A critical-plane fatigue indicator parameter (FIP) based on Tanaka-Mura model for crack initiation and Hobson model for microstructurally short-crack growth was proposed and combined with the experimental crack growth data for the prediction of total fatigue life and its scattering. The predicted results were in good agreement and will be discussed.

**Keywords:** Crystal plasticity, Fatigue, Finite element, Fatigue indicator parameter

## REGULAR SESSIONS

Id-1352

### A Computational Model of Chemical Reactions Occurring during Thermal Desorption Spectroscopy

Ján Dugáček, Pavel Šťáhel

CEPLANT – R&D Centre for Low-cost Plasma and Nanotechnology Surface Modifications, Masaryk University,  
Kotlářská 2, 611 37 Brno, Czech Republic

Corresponding author: jan.dugacek@gmail.com

**Abstract:** Thermal desorption spectroscopy is an analytical method where a thin film is slowly heated in high vacuum, causing a desorption of gases. The desorbed compounds' partial pressures are measured as a function of temperature using a mass spectrometer. The process not only provides information about the sample's chemical composition, but also about the strength of the bonds that hold the desorbed particles in the film. However, determining the activation energy with acceptable precision is currently a difficult task. Empirical formulas like the Redhead method exist, but the data rarely fits the expected curves and the results are imprecise. They can be used to distinguish between physisorption and chemisorption, but are not accurate enough to determine the type of chemical bonds. To address this problem, we have developed a novel method of determining the activation energies based on fitting the experimental data into a computational model of the reaction. The fitting process can be practically run on a PC with a high-end graphics card. The method provided significantly more precise results than other methods and could achieve an almost perfect match with the data, allowing for a significantly more precise determination of the nature of bonds in thin films. A limitation of the method is that it cannot model cases where more reactions cause desorption of the same compound.

**Keywords:** Thermal desorption spectroscopy, computational model

## REGULAR SESSIONS

**Id-1353**

### **Transition Metal Oxide Materials with a Nonstoichiometry**

Albina Valeeva

Institute of Solid State Chemistry of the Ural Branch of the Russian Academy of Sciences, 620990 Ekaterinburg,  
Pervomaiskaya 91, Russia, Fax: +7 343 374 4495

Corresponding author: anibla\_v@mail.ru

**Abstract:** At present, the reason for the stabilization of the crystalline structure of nonstoichiometric transition metal oxides with high degree of atomic disorder depending on the nonstoichiometry and particle size is not known from thermodynamic and electronic structure points of view. Therefore, the aim of present work is obtaining stable nanoparticles and establishing the relation between the nonstoichiometry of nanoparticles and their size, crystalline and electronic structure, possible ordering and properties. The objects of the research are nonstoichiometric nanostructured niobium monoxides  $\text{NbO}_y$  with 25 at.% structural vacancies on both the sublattices simultaneously. The synthesis of nonstoichiometric  $\text{NbO}_y$  was carried out by physical methods, namely by vacuum solid-phase sintering from a mixture of niobium metal Nb and niobium oxide  $\text{Nb}_2\text{O}_5$  powders followed by high-energy ball milling. The crystal structure and properties were studied by using X-ray diffraction, electron microscopy, specific surface measurements, positron annihilation lifetime spectroscopy and first-principal quantum mechanical calculations. It was established that nonstoichiometry and particle size of nanocrystals effect strongly on their crystal and electronic structure, possible ordering and functional properties.

**Keywords:** Transition metal oxide, nanocrystal, nonstoichiometry, size effect, crystal structure, properties

**Acknowledgements:** This work is supported by the Russian Science Foundation (project No. 19-73-20012) at the Institute of Solid State Chemistry, UB RAS.

## REGULAR SESSIONS

Id-1355

### Microstructure and Properties of Ti(C,N)-TiB<sub>2</sub>-FeCoCrNiAl High-Entropy Alloys Composite Cermets

Zhanjiang Li<sup>1</sup>, Pinqiang Dai<sup>1, 2, 3</sup>

<sup>1</sup>College of Materials Science and Engineering, Fujian University of Technology, Fuzhou, 350118, China

<sup>2</sup>Fujian Provincial Key Laboratory of New Material Preparation and Forming Technology, Fuzhou 350108, China

<sup>3</sup>School of Materials Science and Engineering, Fuzhou University, Fuzhou 350116, China

Corresponding author: l6z6j6@126.com

**Abstract:** The FeCoCrNiAl HEA was used as binder of the Ti(C, N)-TiB<sub>2</sub> composite cermets. The cermets were fabricated by mechanical alloying and vacuum hot-pressing sintering. For the FeCoCrNiAl HEA, a BCC structured solid solution with refined microstructure of 10-20 μm in grain size could be obtained after 30 h milling. For the cermets, apart from Ti(C, N) and TiB<sub>2</sub> phases, also a minority Fe<sub>2</sub>B were detected in the XRD patterns. TEM observation revealed that the structure of the HEA binder was a solid solution where the Ti(C, N) and TiB<sub>2</sub> were tightly bound. The cermets showed excellent mechanical properties with a fracture toughness of 9.6±0.2 MPa.m<sup>1/2</sup>, hardness of 1977.3±20 HV<sub>10</sub> and bending strength of 768.6±20MPa, respectively. The high-temperature hardness of the HEA cermets and traditional Ni/Co binder cermets was 993.7±30 HV<sub>20</sub> and 668.1±30 HV<sub>20</sub> at 1000 °C, respectively. And the HEA cermets possesses excellent oxidation and wear resistance. This is attributed to the formation of a continuous and dense external oxide scale and TiO<sub>2</sub> layer that effectively impede inward oxygen transport, which leads to a remarkable improvement in the oxidation resistance. At the lower temperatures, the abrasive wear mechanism was the dominant wear mechanism. When the temperature increased above 600 °C, the oxidative wear and adhesive wear were found to be the dominant wear mechanism for cermets. This study could provide a reference value for the selection of the binder phase of cermets.

**Keywords:** FeCoCrNiAl HEA, Ti(C, N)-TiB<sub>2</sub>-HEA composite cermets, microstructure, room-temperature and high-temperature properties

## REGULAR SESSIONS

Id-1361

### Self-Assembly of Colloidal Nanoparticles Ag<sub>2</sub>S in Water Solution

Svetlana Rempel<sup>1,2,\*</sup>, Yulia Kuznetsova<sup>1</sup>

<sup>1</sup>Institute of Solid State Chemistry, Ural Branch of the Russian Academy of Sciences, 620990 Ekaterinburg, Pervomaiskaya Str. 91, Russia

<sup>2</sup>Russia Ural Federal University, 620002 Ekaterinburg, Mira Str. 19

\*Corresponding author: svetlana\_rempel@ihim.uran.ru

**Abstract:** Silver sulfide (Ag<sub>2</sub>S) nanoparticles have attracted much attention due to their potential applications in photoconductors, solar cells, near-infrared photo-detectors, etc. [1]. In work [2] a simple one-step synthesis on Ag<sub>2</sub>S nanoparticles in an aqueous solution with (3-mercaptopropyl)trimethoxysilane (MPS) as the capping molecules was reported.

The aim of present study was to investigate the effects of different concentrations of MPS on the self-assembly of the colloidal nanoparticles. The solutions with different molar ratio of MPS:Ag<sub>2</sub>S were prepared. The self-organized nanoparticles was studied by optical, scanning electron microscopy (SEM), energy dispersive X-ray spectroscopy (EDX) and transmission electron microscopy (TEM).

The appearance of nano- and microtubes was detected. The tubes consist of both Ag<sub>2</sub>S and MPS. The geometrical parameters of these tubes such as length, diameter and thickness of walls have been determined. This parameters depend on molar ratio of MPS:Ag<sub>2</sub>S and stoichiometry of Ag<sub>2</sub>S nanoparticles.

**Keywords:** Silver sulfide, nanoparticles, self-assembly

**Acknowledgements:** This work is supported by the Russian Science Foundation (project No. 19-73-20012) at the Institute of Solid State Chemistry, UB RAS.

#### References

- [1]. C. Cui, X. Li, J. Liu, Y. Hou, Y. Zhao, G. Zhong, Synthesis and functions of Ag<sub>2</sub>S nanostructures, *Nanoscale Res. Lett.* 10 (431) (2015), <http://dx.doi.org/10.1186/s11671-015-1125-7>.
- [2]. Y.V. Kuznetsova, S.V. Rempel, I.D. Popov *et al*, Stabilization of Ag<sub>2</sub>S nanoparticles in aqueous solution by MPS, *Colloids and Surfaces A: Physicochem. Eng. Aspects*, <http://dx.doi.org/10.1016/j.colsurfa.2017.02.013>.

## REGULAR SESSIONS

Id-1363

**Electromagnetic Wave Propagation of Double Walled Wires**

Ayse Nihan Basmaci Filiz

Tekirdag Namik Kemal University, Corlu Vocational School, Tekirdag, Turkey

Corresponding author: anbasmaci@nku.edu.tr

**Abstract:** In this study, electromagnetic wave propagation behaviour of tubular double-walled wires carrying current is investigated. For his purpose, material property effects of internal and external parts of a double-walled wire are investigated in detail. Although the material properties of both the inner and outer parts of this double-walled wire differ from each other, they are isotropic. Thus, the Maxwell equations are solved to analyze electromagnetic wave dispersion and propagation characteristics of this double-walled wire. It should be noted that interaction between these inner and outer parts of this double-walled wire and its material property has an significant effect on electromagnetic wave dispersion and propagation.

**Keywords:** Electromagnetic wave propagation, Maxwell equations, double – walled wire, metamaterials; photonic structures.

**References**

- [1]. J. A. Kong, *Electromagnetic Wave Theory* (Chapter 1). New York: Wiley Interscience, 1990.
- [2]. D. M. Pozar, *Microwave Engineering* (4th ed.). London: John Wiley & Sons, 2012.
- [3]. A. Sommerfeld, *Electrodynamics* Academic Press, New York, 1964.
- [4]. L.D. Landau, E.M. Lifshitz, *Electrodynamics of Continuous Media* Pergamon, Oxford, 1984.
- [5]. J.D. Jackson, *Classical Electrodynamics* (third ed.), Wiley, 1999.
- [6]. Q. Liu, B. Cao, C. Feng, W. Zhang, S. Zhu, D. Zhang, High permittivity and microwave absorption of porous graphitic carbons encapsulating Fe nanoparticles. *Composite Science and Technology*, 72, 1632-1636, 2012.
- [7]. T. Zhao, X. Ji W. Jin, C. Xiong, W. Ma, C. Wang, S. Duan, A. Dang, H. Li, T. Li, S. Shang, Synthesis and electromagnetic wave absorption property of amorphous carbon nanotube networks on a 3D graphene aerogel/BaFe<sub>12</sub>O<sub>19</sub> nanocomposite. *Journal of Alloys and Compounds* 708, 115-122, 2007.
- [8]. C. Wang, V. Murugadoss, J. Kong, Z. He, X. Mai, Q. Shao, Y. Chen, L. Guo, C. Liu, S. Angaiah, Z. Guo, Overview of carbon nanostructures and nanocomposites for electromagnetic wave shielding. *Carbon*. 140, 696-733, 2018.
- [9]. H. Khosravi, A. Moradi, *Comment on:* Electromagnetic wave propagation in single-walled carbon nanotubes. *Physics Letters A*. 364, 515-516, 2007 and Wei, L., Wang, Y-N. "Electromagnetic wave propagation in single-walled carbon nanotubes." *Physics Letters A* 333, 303-309, 2004.

**REGULAR SESSIONS****Id-1364****Wave Propagation Behavior of Friction Welded Rods**Seckin Filiz<sup>1,\*</sup>, Munin Sahin<sup>2</sup><sup>1</sup>Tekirdag Namik Kemal University, Corlu Vocational School, Tekirdag, Turkey<sup>2</sup>Trakya University, Department of Mechanical Engineering, Edirne, Turkey

\*Corresponding author:sfiliz@nku.edu.tr

**Abstract:** In this article, wave propagation characteristics of a welded structure is investigated. The first part of this welded structure which is divided into three parts is material A, the second part is the Heat Affected Zone (HAZ) and the third part is material B. Changes in material properties are observed in the heat affected zone of this three-part welded structure due to temperature change. Since the length of the material is also effective in temperature change, the length of the three-part welded structure also has an effect on the change in material properties. Interactions such as reflections and transmissions between each parts of this three-part welded structure can occur, for instance, 100% transmission can also occur. All cases for reflections and transmissions are investigated by considering the wave propagation frequencies in this study. Furthermore, the phononic behavior of the linear elastic rods caused by welding temperature and length characteristics effects of these rods are investigated. By investigating the wave propagation characteristics of the three-part welded structure, the classical mechanical wave equations are solved for each of these three parts.

**Keywords:** Friction welding, phononic structures, wave propagation, temperature effect, mechanical failure

**References**

- [1]. S.D. Meshram T. Mohandas G. Madhusudhan Reddy, Friction welding of dissimilar pure metals. *Journal of Materials Processing Technology*, Volume 184, Issues 1–3 (2007), 330-337.
- [2]. B.-A. Behrens, A. Bouguecha, M. Vucetic, I. Peshekhodov, T. Matthias, N. Kolbasnikov, S. Sokolov, S. Ganin, Experimental investigations on the state of the friction-welded joint zone in steel hybrid components after process-relevant thermo-mechanical loadings, *AIP Conference Proceedings* 1769, 130013 (2016); <https://doi.org/10.1063/1.4963532>.
- [3]. A.G. Wahyu Wibowo, R. Ismail, J. Jamari, Microstructure analysis in friction welding of copper and aluminum,.
- [4]. Y. Wei, F. Sun, Microstructures and Mechanical Properties of Al/Fe and Cu/Fe Joints by Continuous Drive Friction Welding. *Advances in Materials Science and Engineering*, Volume 2018.
- [5]. S. Bati, M. Kılıç, İ. Kırık, Vol 6, Number 2, 2016, *European Journal of Technic EJT*, Friction welding of dissimilar AISI 304 and AISI 8640 steels.

- [6]. S. Celik, I. Ersozlu, Investigation of the mechanical properties and microstructure of friction welded joints between AISI 4140 and AISI 1050 steels, *Materials & Design*, Volume 30, Issue 4, April 2009, 970-976.
- [7]. J. Achenbach, *Wave Propagation in Elastic Solids*, Volume 16 1st Edition, 1st January 1984, North Holland, Paperback ISBN:9780720403251,
- [8]. E. Kim, J. Yang, Wave propagation in single column woodpile phononic crystals: Formation of tunable band gaps, *Journal of the Mechanics and Physics of Solids*, Volume 71, November 2014, 33-45.

## REGULAR SESSIONS

Id-1375

### The Influence of Twinning on the Tensile Properties of Nanocrystalline Light Weight Aluminum Alloys

Khaled Youssef\*, Sara I. Ahmed

Materials Science and Technology, Qatar University, Doha 2713, Qatar

\*Corresponding author: kyoussef@qu.edu.qa

**Abstract:** In this study, arti-fact free bulk nanocrystalline pure aluminum and aluminum-lithium alloys were prepared through mechanical milling under ultra-high purity argon and at both liquid nitrogen and room temperatures. The nanostructure evolution during milling was examined using X-ray diffraction and transmission electron microscope techniques. The in-situ consolidated samples after milling exhibited an average grain size of 30 nm. The tensile properties of this novel material are reported in comparison with coarse-grained aluminum alloys. The 0.2% offset yield strength of the nanocrystalline aluminum was found to be 340 MPa. This value is at least one order of magnitude higher than that of the coarse-grained aluminum alloy. In addition to this extraordinarily high strength, the nanocrystalline aluminum showed a significant tensile ductility, with 6% uniform elongation and 11% elongation-to-failure. The transmission electron microscope observations in this study provide evidence of deformation twinning in the plastically deformed nanocrystalline aluminum.

**Keywords:** Nanocrystalline, mechanical properties, aluminum, twinning

## REGULAR SESSIONS

Id-1397

### Modeling and Optimization of Experimental Parameters for the Removal of Heavy Metal and Production of Porous Adsorbents by RSM and ANN Techniques

Yunus Emre Şimşek

Bilecik Şeyh Edebali University, Chemical Engineering Department, Bilecik-TURKEY

Corresponding author: yunusemre.simsek@bilecik.edu.tr

**Abstract:** Alongside the swift development of a wide variety of industrial sectors, heavy metals containing wastewater is to pose a grave threat to the environment and human health. Heavy metals, unlike organic wastes and contaminants, are non-biodegradable and highly toxic even in a small amount. Various techniques have to date been proposed and employed to remove heavy metals from aqueous medium. One of these techniques, adsorption is the most preferred wastewater treatment because of its low-cost, high metal adsorption capacity and easy operation. To enhance the heavy metal removal efficiency of adsorbents used in adsorption processes the precursor is usually thermally carbonized. In this study, bovine animal waste was chemically activated and carbonized. The obtained highly porous adsorbents were utilized for the removal of lead heavy metal in an aqueous medium. Experimental parameters were optimized using Response Surface Method (RSM) and Artificial Neural Networks (ANN) for microwave irradiation power, impregnation ratios and carbonization temperatures. To check the accuracy of results, several statistics such as  $R^2$ , RMSE (root mean square error), mean squared error (MSE), mean absolute error (MAE) and Person's Chi-square measure were used. To determine input-output behavior in ANN algorithm hidden neuron numbers and tan-sigmoid, log-sigmoid and purelin transfer functions were also optimized. Prediction by both the RSM and ANN models was successfully evaluated and both of them showed a similar performance ( $R$ -value  $\approx 0.99$ ). Additionally, adsorption mechanism was enlightened by Brunauer-Emmett-Teller (BET), Scanning electron microscopy SEM-EDX, x-Ray diffraction (XRD), and Fourier transform infrared (FTIR) analysis. The adsorbents used in experiments were found to be mainly calcium, phosphorous and oxygen containing mesoporous materials with  $\approx 30 \text{ g/m}^2$  of surface area.

**Keywords:** Porous materials, heavy metal, optimization, RSM, ANN

## REGULAR SESSIONS

Id-1421

**Comparison of Nanoscale Adhesion Energies, Forces, Pull-Off Distances and Repulsion Energies Measured between Bacterial Cells and Silicon Nitride under Water by AFM**

Gamze Nur Aspar, Ayse Ordek, Fatma Pinar Gördesli Duatepe  
Faculty of Engineering, Izmir University of Economics, 35330 Izmir, Turkey  
Corresponding Author pinar.gordesli@ieu.edu.tr

**Abstract:** Exploring the mechanisms by which a bacterial cell attaches to a surface can improve our fundamental understanding of bacterial adhesion phenomenon, which is of great importance in many medical and environmental applications. Bacterial cell adhesion to a surface is mediated by a two-step process. The first step is dominated by nonspecific long-range interactions: as the bacterial cell approaches to a surface, the entire cell will be exposed to physiochemical forces and/or energies such as van der Waals and electrostatic interactions. The next step in the attachment process is the irreversible attachment of cells to the surface. Once a bacterial cell is in close proximity to a surface of interest, specific shortrange (<1nm) interactions come into play: as the bacterial cell locks onto the surface by the production of exopolysaccharides and/or specific ligands. Today, the precise mechanisms by which these interactions determine bacterial adhesion to surfaces are not yet fully understood. This is in part because most of the studies performed to investigate bacterial adhesion process were carried using macro-scale systems, which are limited in their resolution to disclose the mechanisms that govern the bacterial adhesion process. However, with the introduction of the atomic force microscope (AFM), it has become possible to identify and quantitatively evaluate the molecular characteristics of the bacterial adhesion process at the nanoscale.

In this study, the adhesion of Gram-positive *B. subtilis* and Gram-negative *E. coli* cells to silicon nitride AFM tips were measured under water using atomic force microscope (AFM). The nanoscale adhesion forces were measured as functions of the pull-off distances between silicon nitride AFM tips and the bacterial cells, and the characteristic adhesion (binding) forces during retraction events were determined. The areas under the retraction force–distance curves were calculated and assumed to represent the adhesion energies of the bacterial cells to silicon nitride. Similarly, the areas under the approach force–distance curves were calculated and assumed to represent the repulsion energies measured between silicon nitride and the bacterial surfaces. Our results indicated that mean values of adhesion forces, adhesion energies and lengths of bacterial surface biopolymers quantified for Gram-positive *B. subtilis* cells ( $0.895 \pm 0.02$  nN,  $313 \pm 33.5$  AJ, and  $0.640 \pm 0.01$   $\mu$ m, respectively) were higher than those quantified for Gram-negative *E. coli* cells ( $0.288 \pm 0.01$  nN,  $38.3 \pm 4.27$  AJ, and  $0.383 \pm 0.01$   $\mu$ m, respectively). However, the mean value of repulsion energies calculated between silicon nitride and *B. subtilis* cells ( $-1573 \pm 180$  AJ) was significantly lower compared to the mean repulsion energy value calculated for *E. coli* cells ( $-3798 \pm 295$  AJ).

The higher adhesion observed for *B. subtilis* was associated with longer bacterial surface biopolymers as quantified from measured pull-off distances, and significantly lower repulsion energy values as

calculated from the areas under the approach force–distance curves. To the best of our knowledge, this is the first study explaining the differences in adhesion capabilities of Gram-positive and Gram-negative cells by using measured adhesion and repulsion energies at the nanoscale.

**Keywords:** Bacterial adhesion, adhesion force, adhesion energy, repulsion energy, pull-off distance, bacterial surface biopolymers, atomic force microscope, AFM

## REGULAR SESSIONS

Id-1427

**Piezoelectric Nanogenerators Based on PVDF-HFP/ZnO-Mesoporous Silica Nanocomposites for Self-Powering Devices**

Noura AlSanari, Radwa Mohamed, Amal Daifallah, Ghidaa Abdullah, Jolly Bhadra, Asma Abdulkareem,  
Deepalekshmi Ponnamma, Noora Al-Thani  
Center for Advanced Materials, Qatar University, P O Box 2713, Doha, Qatar  
Corresponding author: Jollybhadra@qu.edu.qa

**Abstract:** Due to the rising global concern over energy catastrophe and environmental issues, attention has been diverted towards future energy. In recent times, rechargeable power and renewable energy sources have been considered as an attractive substitute for resolving the future environmental problems. Among them, mechanical energy is one of the most abundant energy sources, and easily transformable to other useful energy forms, such as electrical energy. For such purposes, piezoelectric materials with ability to convert the mechanical energy generated by various activities into electrical energy. In this research work, we have investigated the morphology, structure and piezoelectric performances of neat polyvinylidene fluoride hexafluoropropylene (PVDF-HFP), PVDF-HFP/ZnO, PVDF-HFP/Mesoporous silica, PVDF-HFP 1% and PVDF-HFP 3% ZnO-Mesoporous silica nanofibers, fabricated by electrospinning. Both SEM and TEM images of ZnO nanoparticles shows formation of uniform flake of about 5nm diameter and Mesoporous silica shows uniform spherical morphology with average diameter of 5  $\mu\text{m}$ . EDX plot justifies the presences of Zn, O and Si. An increase in the amount of crystalline  $\beta$ -phase of PVDF-HFP has been observed with the introduction of ZnO and mesoporous silica in the PVDF-HFP matrix are observed in FTIR spectra shown figure 1. All the XRD peaks observed in neat PVDF has the strongest intensity compared to rest of the other XRD peaks of polymer nanocomposite. The XRD spectra of all the nanocomposites have peaks at 17.8°, 18.6° correspond to  $\alpha$ - crystalline phase, the peaks observed at 19°, 20.1° correspond to the  $\gamma$ - crystalline phase, and the peak at 20.6° corresponds to the  $\beta$ - crystalline phase. The flexible nanogenerator manipulated from the polymer nanocomposite with 1% ZnO-Mesoporous silica exhibits an output voltage as high as 2 V compared with the neat PVDF-HFP sample (~120 mV). These results indicate that the investigated nanocomposite is appropriate for fabricating various flexible and wearable self-powered electrical devices and systems.

**Keywords:** Renewable energy, piezoelectric material, polymer, nanocomposite

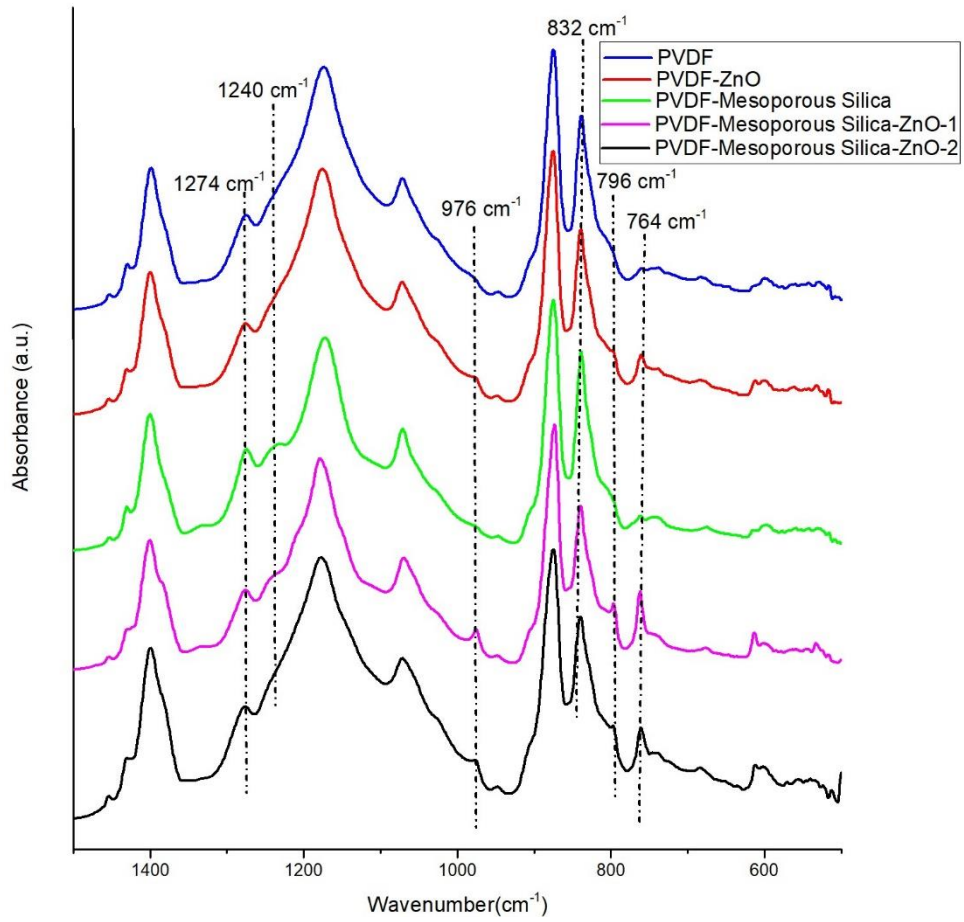


Fig 1: FTIR spectra of neat PVDF-HFP and the PVDF-HFP/nanocomposites.

## REGULAR SESSIONS

**Id-1439**

### **Neutron Diffraction Analysis of Cold Rotary Swaged Tungsten Heavy Alloys and Other Engineering Materials at CANAM Infrastructure**

Charles Hervoches<sup>1</sup>, Lenka Kunčická<sup>2</sup>, Radim Kocich<sup>2</sup>

<sup>1</sup>Nuclear Physics Institute ASCR, v.v.i., Dept. of Neutron Physics, 25068 Řež, Czech Republic, Tel.: +420 26617 2034,

<sup>2</sup>Regional Materials Science and Technology Centre, VSB – Technical University of Ostrava, 17. listopadu 15, 70833 Ostrava-Poruba, Czech Republic

Corresponding author: hervoches@ujf.cas.cz

**Abstract:** Tungsten heavy alloys (THAs) are widely used for applications such as kinetic energy penetrators, radiation shields, aircraft counter-balances, and gyroscope rotors. They typically contain 90–97 wt% of tungsten alloyed with other elements, such as Co, Ni, Fe, Mo, and Cu.

Severe plastic deformation by rotary swaging, which consists of reducing the diameters of the processed work-piece by the repeated action of rotating split dies, is an attractive way to modify conventionally manufactured metals to achieve ultrafine-grained or nanocrystalline structures. However, its effect on microstructure and related phenomena - such as residual stress or texture – has only rarely been studied.

This study presents the neutron diffraction results from the investigation of WNiCo alloy rotary swaged at room temperature. The method allows investigating the effect of rotary swaging on both texture and residual stresses within the bulk of the material.

A sintered rod of WNiCo alloy with the overall chemical composition of 92.6 wt% W, 5 wt% Ni and 2.40 wt% Co was subjected to one swaging pass at room temperature. The neutron diffraction measurements were carried out on the SPN-100 dedicated strain diffractometer at the LVR-15 research reactor, part of the CANAM infrastructure, located in Řež, Czech Republic.

The results of neutron diffraction analyses of residual stresses in the swaged-piece demonstrated the presence of residual stresses of variable values along the diameter. The stresses in the radial directions (x and y) differ from the stress distribution along the axial direction z, which features mostly compression character along the entire crosssection.

**Keywords:** Tungsten heavy alloys, rotary swaging, neutron diffraction, residual stresses

## REGULAR SESSIONS

Id-1446

**Optimizing the Migration Behavior of Vitreous Enamel Coatings**Nurullah Çöpoğlu<sup>1,2</sup>, Yasin Bozkurt Yılmaz<sup>1,2</sup>, Tamer Cengiz<sup>2</sup>, Buğra Çiçek<sup>1,3</sup><sup>1</sup> Yıldız Technical University, Department of Metallurgy and Materials Science Engineering, 34210

Esenler/Istanbul/Turkey

<sup>2</sup> Gizem Frit Research and Development Center, Enamel Solutions, Sakarya 2<sup>nd</sup> Organized Industrial Zone, 54300

Hendek/Sakarya/Turkey

<sup>3</sup> Koç University Akkim Boron Based Materials and High Technology Chemicals Research and Application Center,

Rumelifeneri Yolu, 34450 Sarıyer/Istanbul/Turkey

Corresponding author: nurullah.copoglu@gizemfrit.com

**Abstract:** A wide variety of cookware and utensils are continuously used throughout the world. Owing to the high mechanical and thermal properties, metallic surfaces such as cast iron, steel and aluminum are frequently used in this field. The development in cooking utensils are trending since their high strength and uniform heat distribution with heat retention properties are providing better cooking conditions. However, during cooking, metal atoms can enter the food from the metal surface due to the pH of the food, relatively high cooking temperature and contact time of the processed food. This condition is called migration and when the human body gets more metal than it needs to take daily or the harmful elements enter the body, it causes many diseases, notably cancer. It is therefore necessary to coat the cooking utensils. Enamel coating is an inorganic coating that has high heat capacity owing to the silicates in their chemical structure, high hardness and durability owing to their amorphous structure, chemical resistance and abrasion resistance. This coating can be used in different areas such as heaters, fire places, gas and electric cookers, BBQs, clock faces, cookware, hot water services etc. Hazardous compounds can be present in the enamel coatings which comes from the minor components used in production of frit compositions such as NiO and CoO to ensure chemical bonding in interface. These compounds can leach or migrate into food and from there into human body. Therefore, some regulations and standards have been developed to protect human health. ISO 4531:2018 standard states an ICP analysis for 30 minutes at 95 °C temperature, with limited release of 16 elements. However, some of these elements have a vital importance in the enamel coating technology hence it was aimed to replace the required oxides without causing a change in the enamel structure, according to Ellingham Diagram, for adhesion properties, and crystal structure of the raw materials. In this study, a typical borosilicate frit composition containing a high proportion of RO<sub>2</sub> groups and less fluorine, was used to provide heat resistance to the enamel structure and resistance to organic acids. Adhesion between metal – enamel substrate was achieved with minor components of other adhesion oxides such as MoO<sub>3</sub> since the two best adhesion providers, CoO and NiO, are subjected to the regulations. One coat-one fire technique was used with electrostatic deposition method at 840 °C for 4 minutes. The migration properties were investigated according to ISO 4531:2018 standard. It is stated that healthy and conforming to standards enamel compositions can be developed.

**Keywords:** Enamel coating, element release, ISO 4531:2018, food contact

## REGULAR SESSIONS

**Id-1447**

### **Investigation of Nickel Effects on Matt Cast Iron Enamel**

Yasin Bozkurt Yılmaz<sup>1,2</sup>, Nurullah Çöpoğlu<sup>1,2</sup>, Tamer Cengiz<sup>2</sup>, Buğra Çiçek<sup>1,3</sup>

<sup>1</sup>Department of Metallurgy and Materials Science Engineering, Yıldız Technical University, 34210 Istanbul/Turkey

<sup>2</sup>Gizem Frit Research and Development Center, Enamel Solutions, Sakarya 2nd Organized Industrial Zone,  
54300 Sakarya/Turkey

<sup>3</sup>Koç University Akkim Boron Based Materials and High Technology Chemicals Research and Application Center,  
Rumelifeneri Yolu, 34450 Istanbul/Turkey

Corresponding author: yasin.yilmaz@gizemfrit.com

**Abstract:** Cast iron is the general name for iron-carbon alloys containing more than 2% carbon content. It can melt at low temperatures compared to steels and has low cost. The surfaces of cast irons, which can be used in many areas from construction to kitchen equipment, are coated with enamel to prevent corrosion, increase wear resistance and easy to clean. Enamels of various oxides such as alumina (Al<sub>2</sub>O<sub>3</sub>), boron oxide (B<sub>2</sub>O<sub>3</sub>), zircon dioxide (ZrO<sub>2</sub>), nickel oxide (NiO), cobalt oxide (CoO), chromium (III) oxide (Cr<sub>2</sub>O<sub>3</sub>), calcium oxide (CaO) SiO<sub>2</sub> is obtained by the addition of vitreous coating materials. The raw materials used and the oxides formed during production have a direct effect on the end product properties of the enamel. Nickel oxide (NiO) and cobalt oxide (CoO) are the most important oxides affecting the bonding performance of the enamel to the metallic surface. Although nickel oxide (NiO) has little effect on glassy structures, it improves the adhesion performance of the enamel to the metal surface by providing the oxidation balance of iron oxide (FeO) which provides bonding at the enamel-metal interface. It is also effective on the aesthetic appearance of the enamel. Gives a dark color to the enamel and prevents fish scale error on its surface. However, with the latest regulations, the use of nickel in enamels has been restricted for health and environmental safety reasons. For this reason, studies have started to develop a new generation of nickel-free enamels suitable for regulations. In this study, the development of enamel that can be applied to cast iron surfaces having a matt appearance that does not contain nickel and the effect of nickel on enamel properties were investigated. In the existing frit compositions, new frit recipes were prepared which did not contain nickel and were applied to cast iron surfaces by wet application method by making improvements in the ratios of other adhesion agents. Particle size, thermal expansion coefficient, microstructure, viscosity and chemical characterization of the prepared frit were analyzed. The microstructure, chemical and mechanical abrasion resistance, color properties, refractoriness, surface properties, coating adhesion performance and the effect of nickel on these properties were investigated.

**Keywords:** Enamel, cast iron enamel, nickel free enamel, nickel effect,

## REGULAR SESSIONS

**Id-1527**

### **Measurement of Heat Transfer Coefficient in Interaction Zone of Multiple Liquid Jet Impingements**

Chaitanya Ghodake, Rajkumar Singh

Kalyani Centre for Technology & Innovation, Bharat Forge Ltd. India -411036

Corresponding author: chaitanya.ghodake@bharatforge.com

**Abstract:** The purpose of this study is to measure the local heat transfer coefficients for array of single phase round jets normally against a flat surface. The parameters investigated are jet Reynolds number (Re), nozzle-to-nozzle spacing (s), and nozzle- to-flat surface spacing (z). The jet spacing to jet diameter ratio s/d is maintained at 2, 4 and 6. Reynolds numbers equal to 15000, 25000, 35000 and 50000. The Nusselt number (Nu) plot increases with increase in Reynolds number monotonically. The local Nusselt number profile exhibits a sharp peak where the two round jets flow interact.

**Keywords:** Water jet impingement cooling, single phase liquid, Nusselt number distribution, Reynolds number

## POSTER SESSIONS

**Id-1129**

### **Production Productivity by Automation Application in Manufacturing Industry**

Sedat Firat<sup>1</sup>, Musaddin Kocaman<sup>1</sup>, Ali Serdar Vanli<sup>2,\*</sup>, Anil Akdogan<sup>2</sup>

<sup>1</sup>Mesan Plastik ve Metal San. A.Ş., Istanbul, Turkey

<sup>2</sup>Yildiz Technical University, Department of Mechanical Engineering, Istanbul, Turkey

Corresponding author: [svanli@yildiz.edu.tr](mailto:svanli@yildiz.edu.tr)

**Abstract:** One of the fundamental quality philosophies of ISO 9001 Quality Management System Standard certification is “improvement” approach. All organizations, aiming at quality products and quality systems, can expand their customer networks and ensure customer loyalty only as long as they constantly improve themselves. Improvement of quality leads to increase in productivity, it decreases in production costs and sales prices, thus increasing competitiveness in local and global markets could be reached. In this study, an increase in productivity with an automation cell installation is shown in a plastic and metal injection factory which produces accessories in furniture sector. This fully automated PLC controlled cell provides high quality assemble of shelf supports and fixing parts. In addition to labor and energy savings, it has contributed to the increase in productivity with shorter injection times achieved by reducing raw material quantities through part design modifications realized within this study.

**Keywords:** Production productivity; automation application; manufacturing industry

## POSTER SESSIONS

**Id-1138**

### **Investigating The Effects of Temperature on The Mechanical Properties of Austempered Ductile Iron Castings**

Kaya Ali Keçeli<sup>1,\*</sup>, Halil Gök<sup>1</sup>, Refik Kuyrukçu<sup>1</sup>, Barış Çetin<sup>2</sup>, Cengiz Baykasoğlu<sup>1,\*</sup>

<sup>1</sup> Hittite University, Department of Mechanical Engineering Çorum, Turkey,

<sup>2</sup> FNSS Defense Systems Co. Inc., Engineering and Research Department, Gölbaşı, Ankara, Turkey,

Corresponding author: cengizbaykasoglu@hitit.edu.tr

**Abstract:** Austempered Ductile Iron (ADI) castings have a wide range of application areas including defense, automotive, heavy-duty machinery industries due to its superior mechanical properties. ADI could provide excellent combination of high strength, toughness and wear resistance which is basically originated from its specific microstructure called “ausferrite”. Ausferrite microstructure has significant mechanical properties whereas it has an important disadvantage of metastability. Therefore, any possible heating which can be caused by the in-service conditions may degrade the final performance of component. This study investigated the effect of temperature on the metastable character of ADI. The experimental work conducted by means of tensile testing among the as-delivered and over-tempered ADI samples. The results revealed that up to 300°C, the change in the mechanical properties were in the negligible content. On the other hand, if ADI exposed to the environmental temperature higher than 300°C, the ductility of ADI has been lost up to 75%.

**Keywords:** Austempered ductile iron castings, ausferrite, mechanical properties

## POSTER SESSIONS

**Id-1142**

### **The effects of superstatistics on Nonthermal and suprathermic distributions**

Samia Dilmi<sup>1</sup>, Amal Lifa<sup>1</sup>, Abdelmalek Boumali<sup>2</sup>

<sup>1</sup>University of El Oued, Fa. Exact Sciences, <sup>2</sup>University Larbi Tébessi -Tébessa-, 12000,

W. Tébessa, Algeria

Corresponding author : samia-dilmi@univ-eloued.dz

**Abstract:** The statistics of all observed particles are covered by the two well-known realizations of quantum statistics: the Bose- Einstein (BE) statistics and the Fermi-Dirac (FD) statistics. Many complex systems exhibiting fluctuations can be described by decomposing their dynamics at different scales. Their statistical properties are then given by a mixture of statistics, i.e., superstatistics. Collisionally ionized plasmas are those formed by electron-impact ionization. Such plasmas are common in astrophysical sources, such as stars, supernova remnants, galaxies, and galaxy clusters. Modeling the emission from these objects requires knowing the charge state distribution within the plasma, which is set by the ionization rate. Electron-impact ionization (EII) can be important in dynamic systems where ions are suddenly exposed to higher electron temperatures. For this reason, EII may be important for studies of solar flares, nanoflare coronal heating, supernova remnants, and merging galaxy clusters. EII can also have a significant effect on the charge state distribution for plasmas with a non-thermal electron energy distribution. For such plasmas there is a substantial population of electrons in the high energy tail of the distribution that lie above the EII threshold. Thus, EII is relevant to the modeling of astrophysical systems where such non-thermal distributions are present.

**Keywords:** Superstatistics, fluctuation, steady-state plasmas, tsallis statistics

## POSTER SESSIONS

**Id-1151**

### **Valuation of Mill Scale as Anticorrosive Pigment**

Belgacem Bezzina<sup>1,2,\*</sup>, Mohamed Tayeb Abedghars<sup>1</sup>

<sup>1</sup>Research Centre in Industrial Technologies (CRTI), P.O.BOX 64, Cheraga 16014, Algiers, Algeria

<sup>2</sup>Laboratory of Computational Chemistry and nanostructures (LCCN), University of 08 May 45 Guelma - Algeria

\*Corresponding author: b.bezzina@crti.dz

**Abstract:** This work aims at conversion of iron waste (mill scale) generated by steel plants into valuable products in the field of anti-corrosive paints. Their properties were compared to an anti-corrosion paint trademark based totally on iron oxide. For this purpose varied techniques of mechanical and physical-chemical analysis were used; the grinding was applied to mill scale particles for obtained a fine powders (< 32  $\mu\text{m}$ ); to determine their particle size distribution, the milled scale was analyzed by Laser Granulometry (Hydro 2000MU); a primary electrochemical method used to evaluate the performance and scale vis-a-vis the phenomenon of corrosion behavior. The experimental outcomes showed that the anti-corrosion properties or rather inhibition efficiency increases with the mill scale concentration in the tested paints.

**Keywords:** Mill scale, corrosion inhibitor, electrochemical analysis.

## POSTER SESSIONS

**Id-1155**

### **The Influence of Dislocations on Crack Propagation in a Glass Material**

Hamid Hamli Benzahar<sup>1,\*</sup>, Mohamed Chabaat<sup>2</sup>

<sup>1</sup>Industrialist Fluid Measurement and Applications Laboratory, University Khemis miliana, Route de Theniet El-Had, 44225, Algeria,

<sup>2</sup>Built Environmental Research Lab., Civil Engineering Faculty U.S.T.H.B, BP32 El Alia, Bab Ezzouar, Algiers 16111, Algeria,

Corresponding author: h.hamli-zahar@univ-dbk.m.dz

**Abstract:** The present research studied the influence of dislocations on cracked in a glass material. The considered model is a glass material, having a Poisson ratio and a shear modulus. In this research, the proposed model is a glass material having a macro-crack at the end and a neighboring micro-crack, subjected to uniformly distributed loads according to the first mode of rupture (Mode I). The proposed model is treated by finite element method using ABAQUS. The variation of the micro-crack position with respect to the macro-fissure gives rise to constraints and deformations different from those found in the absence of the micro-crack. According to the constraints and strains found in two cases (macro-crack with/without micro-crack), the dislocation (micro-crack) can reduce and sometimes accelerate the propagation of the rupture. The results will be compared with those found by theoretically.

**Keywords:** Micro-crack, propagation, stress, finit element

## POSTER SESSIONS

**Id-1158**

### **Numerical Comparison Between Single and Twin Jets**

Rachid Sahnoun

University Mustapha Stambouli of Mascara. Algeria,

Corresponding author: r\_sahnoun@yahoo.fr.

**Abstract:** The present study is focused on the analysis of the dynamical field along the vertical central axis and horizontal ones. Comparison between single and twin-jets impingement against a flat and smooth surface without recirculation is improved to which is the best for increase the effectiveness of isolated compartment. The study is achieved using the Large Eddy Simulation (LES) approach with WALE model. The jet opening ratio is  $H/e = 10$  and the Reynolds Number is  $Re = 2000$ . The results are compared favorably to the experimental measurements data of the twin jets found in the literature.

**Keywords:** Corridor, air jet, LES

## POSTER SESSIONS

**Id-1162**

### **Synthesis of Uvarovite Garnet Using Different Synthesis Routes**

I. Balčiūnaitė<sup>1</sup>, R. Skaudžius<sup>2</sup>, E. Norkus<sup>1</sup>

<sup>1</sup> Department of Catalysis, Center for Physical Sciences and Technology, Saulėtekio av. 3, LT-10222, Vilnius, Lithuania

<sup>2</sup> Faculty of Chemistry and Geosciences, Vilnius University, Naugardukas str.24, LT-03225, Vilnius, Lithuania

Corresponding author: irena.balciunaite@ftmc.lt

**Abstract:** Uvarovite is the rarest of the common members of the garnet group. It is a unique garnet exhibiting consistently green colour. It only occurs in very small, lustrous and well-formed crystals. The size of crystals usually is rarely large enough for faceting. In the present work we present a simple sol-gel method based on metal chelates in aqueous solvents for the preparation of garnet crystal structure. The uvarovite with the formula  $\text{Ca}_3\text{Cr}_2(\text{SiO}_4)_3$  has been synthesised in different techniques: i) combustion route using urea as a fuel, ii) sol-gel using ethylene glycol as a complexing agent and, iii) sol-gel using with  $\text{Si}(\text{OC}_2\text{H}_5)_4$  (TEOS) as a source of silicon. The mixture of synthesis consists of  $\text{Ca}(\text{NO}_3)_2 \cdot 4\text{H}_2\text{O}$ ,  $\text{Cr}(\text{NO}_3)_3 \cdot 9\text{H}_2\text{O}$ ,  $\text{H}_2\text{NC}(\text{CH}_2\text{OH})_3$  and  $\text{SiO}_2$ . The dried synthesised gels or solid solutions were annealed at different temperature ranges (from 400 to 1000 °C) for 8-40 h. The phase purity, composition and microstructural features in the polycrystalline samples were studied by the X-ray powder diffraction analysis, the infrared spectroscopy and scanning electron microscopy. The phase formation of polycrystalline powders were observed starting 1000 °C temperature.

**Keywords:** Sol-gel method, uvarovite, garnet

## POSTER SESSIONS

**Id-1166**

### **Mechanical Properties of Austenitic Stainless Steel Welded by Laser and TIG**

Jae-Eun Paeng<sup>1,\*</sup>, Byung-Cheol Choi<sup>2</sup>, Sung-Min Jung<sup>2,3</sup>, In-Duck Park<sup>3</sup>, Ki-Woo Nam<sup>1,2</sup>

<sup>1</sup> Interdisciplinary Program of Marine Convergence Design, Pukyong Nat'l Univ., Busan, 48513, Korea

<sup>2</sup> Dept. of Materials Science and Engineering, Pukyong Nat'l Univ. Busan, 48513, Korea

<sup>3</sup> Korea Institute of Machinery and Material, Busan, 46744, Korea

Corresponding author: dms9564@naver.com

**Abstract:** Austenitic stainless steel is used in the nuclear industry as structural materials and coatings because it has excellent workability, weldability and high temperature characteristics. Nuclear power plant structures are mainly large structures manufactured using welding which is mainly arc welding. Arc welding is a welding method with relatively high heat input. However, austenitic stainless steel requires low heat input because it has high thermal expansion coefficient and lower thermal conductivity than that of carbon steels. Over heat input may cause various welding defects such as severe deformation and coarsening of the grain in the joint, which may result in deterioration of the mechanical properties. In recently, laser welding has been proposed to solve the problem of heat input. In this study, the thickness of 6 mm STS304L of austenitic phase was butt welded using laser and TIG and mechanical properties were compared and analyzed. Joints of laser welding show better tensile and impact properties than that of TIG. However, the bending properties were worse than that of TIG.

**Keywords:** High power laser, laser welding, austenitic stainless steel, mechanical properties, weibull analysis

## POSTER SESSIONS

**Id-1167**

### **Evaluation of Harmless Crack Size using a Uniformized Equation Considering the Nonlinear Region of the Crack Tip**

Min-Heon Kim<sup>1,\*</sup>, Jae-Yong Hyun<sup>2</sup>, And Ki-Woo Nam<sup>3\*</sup>

<sup>1</sup> Interdisciplinary Program of Marine Convergence Design, Pukyong Nat'l Univ., Busan, 48513, Korea

<sup>2</sup> UR Interdisciplinary Program of Mechanical Engineering, Pukyong Nat'l Univ., Busan, 48513, Korea

<sup>3</sup> Dept. of Materials Science and Engineering, Pukyong Nat'l Univ. Busan, 48513, Korea

Corresponding author: goheon0425@naver.com

**Abstract:** Haddad et al. have proposed the equation for crack length dependence of threshold stress intensity factor ( $\Delta K_{th}$ ), assuming  $l + l_0$  by adding micro crack length  $l_0$  to crack length  $l$ . Tange et al. have proposed the equation of more convenient threshold stress intensity factor ( $\Delta K_{th}$ ) by removing  $l$  from the equation of Haddad et al. On the other hand, Ando et al. have proposed the equation that can unify micro crack problems of various failure modes. The objective of the present study was to determine threshold stress intensity factor ( $\Delta K_{th(l)}^0$ ) of long cracks suitable for results of Nakagawa et al. and evaluate harmless crack lengths according to crack aspect ratios using the equation proposed by Ando et al. In this study, threshold stress intensity factors were obtained from relation to fatigue limit and crack depth. Evaluation results of fatigue limit using the determined threshold stress intensity factors were in good agreement with experimental results of the large crack. The harmless crack size could be predicted by using equation of Ando et al. with fatigue limit of Non-SP smooth specimen and compressive residual stress.

**Keywords:** Harmless crack size, threshold stress intensity factor, fatigue limit, ando's equation

## POSTER SESSIONS

**Id-1171**

### **Environmental-Friendly Composites Based on Natural Rubber and Plasticized Starch Obtained by Electron Beam Irradiation in the Presence of Polyfunctional Monomers**

Elena Manaila<sup>1</sup>, Gabriela Craciun<sup>\*1</sup>, Maria-Daniela Stelescu<sup>2</sup>, Daniel Ighigeanu<sup>1</sup>

<sup>1</sup>*National Institute for Laser, Plasma and Radiation Physics, Electron Accelerators Laboratory, #409 Atomistilor St., 077125 Magurele, Romania*

<sup>2</sup>*National R&D Institute for Textile and Leather – Leather and Footwear Research Institute, 93 Ion Minulescu St, Bucharest, Romania*

\*Correspondence to: gabriela.craciun@inflpr.ro

**Abstract:** Some environmental-friendly composites based on natural rubber and plasticized starch, were obtained by electron beam irradiation using the ALIN 10 of 6.23 MeV electron accelerator, in the presence of polyfunctional monomers. The influence of the irradiation dose (between 50 and 200 kGy), plasticized starch amount (between 2 and 20 phr) and polyfunctional monomer type (trimethylolpropane trimethacrylate – TMPT and triallylcyanurate – TAC) on the physical and mechanical properties has been investigated by different methods. The gel fraction and cross-link density were determined on the basis of equilibrium solvent-swelling measurements by applying the modified Flory-Rehner equation for tetra functional networks. The composites structural properties were evaluated by FTIR measurements. The results of Fourier Transform Infrared Spectroscopy and cross-link density measurements have demonstrated the starch binding to natural rubber and the positive effect of its presence respectively.

**Keywords:** natural rubber, plasticized starch, polyfunctional monomer, electron beam irradiation.

## POSTER SESSIONS

**Id-1172**

### **Flocculants for Water Treatment Obtained by Electron Beam Irradiation**

Gabriela Craciun, Elena Manaila<sup>\*</sup>, Daniel Ighigeanu

National Institute for Laser, Plasma and Radiation Physics, Electron Accelerators Laboratory,

409 Atomistilor St., 077125 Magurele, Romania

Correspondence to: elena.manaila@inflpr.ro

**Abstract:** Flocculants based on acrylamide, acrylic acid and sodium alginate (1 and 2%) were obtained by electron beam irradiation, characterized by different physical and chemical methods and tested under stirring conditions on kaolin suspension. For the flocculants obtaining, the ALIN 10 of 6.23 MeV electron accelerator in the dose range of 0.5 - 2 kGy was used. As a function of sodium alginate content and electron beam dose, the conversion coefficient, residual monomer content and intrinsic viscosity were determined and expressed. Fourier Transform Infrared Spectroscopy was done on dried samples in order to evaluate the binding of the basic monomers, acrylamide and acrylic acid, on the sodium alginate backbone. The results were correlated with the grafting ratio. The polymeric flocculant efficiencies in terms of transmittance against distilled water were investigated by flocculation studies made on blue kaolin suspension of 0.1 and 0.2 wt %. Even if the grafting ratio determined for the polymeric flocculants containing 1% sodium alginate was four times higher than for the polymeric flocculants containing 2% sodium alginate, the flocculation tests have demonstrated better efficiencies when the 2% sodium alginate content flocculant was used.

**Keywords:** Water treatment, flocculants, electron beam irradiation

## POSTER SESSIONS

**Id-1179**

### **Effects of Rotary Tubes on Aerodynamic Forces in Tube Bundles**

Ismail. Draï <sup>1</sup>, Tayeb. Yahiaoui <sup>2</sup>, Omar. Ladjedel <sup>2</sup>, Omar. Imine <sup>2</sup>, Rachid Sahnoun <sup>1</sup>

<sup>1</sup>University of Mustapha Stambouli MASCARA

<sup>2</sup>University of Sciences and Technology Mohamed Boudiaf Oran

Corresponding author: r\_sahnoun@yahoo.fr

**Abstract:** As fluid flow passes through the tubes; fluid energy is transmitted to the tubes. The forces brought into the tubes by the fluid are one of the most important issues in the tube bundle. This causes many problems in systems that include bundles of tubes. In the present work, first, for the solution method, an experimental study is made of the flow around nine horizontal cylinders of the in-line and tandem tube bundle. One cylinder rotates with a rotation speed of 1480 rpm, and the others are fixed. The purpose of this study is to know the effect of rotation of the rotating cylinder on the adjacent cylinders. This study is part of the physical analysis of the turbulent flow around obstacles, fixed or subject to a parietal rotation. The tube bundles were subjected to a series of subsonic wind tunnel experiments (Subsonic Wind Tunnel TE44). The test tube is equipped with a pressure tap placed on the center of the cylinder with a ratio between the tubes  $P / D = 1.44$  (in line),  $P / D = 2.24$  (zigzag) with a variation of the azimuth angle of  $0^\circ$ ,  $360^\circ$  with a pitch of  $15^\circ$ . The results obtained in this study showed that there is a large influence of rotational movement of the cylinder on the other adjacent cylinders, so there are different excitation forces on the tube for the different positions within the beam as well as deformation of the tube due to the pressure forces exerted on the latter.

**Keywords:** Bundles, aerodynamic forces, CFD

## POSTER SESSIONS

**Id-1193**

### **Effect of Rubber Crumb on the Behavior of Concrete Sand**

Amar Mezidi <sup>1</sup>, Ratiba Kettab<sup>2</sup>

<sup>1</sup>Université Djilali Bounaama, Khemis, Miliana

<sup>2</sup>Civil Engineering Department, National Polytechnic school of Algiers, 10 BP

182 Avenue Hassen Badi El Harrach 16200, Algeria

Corresponding author: aomez2009@gmail.com

**Abstract:** This study has highlighted the possibility of valorization of sand dunes which represents 70% of south local materials Algerian and a waste product resulting from used tires in large amounts non-recoverable. We are interested in incorporating an acrylonitrile butadiene rubber (NBR) as rubber crumb in a by dunes of sand concrete, rather than the sake of improving the mechanical performance, but in order to compare their characteristics and behavior in relation to control concrete. This polymer which is not biodegradable is an industrial waste. It has been proposed to us by the elastomer Algerian society (SAEL) to find eventual use in buildings. This article is a contribution to the promotion of local materials and the use of industrial waste. He substituted intended to rubber crumb by sand dunes and see the features and behavior of sand dunes concrete modified with rubber crumb weight contents of this latter from 1 to 5 % (in steps of 1). The optimal percentage of incorporation of the rubber crumb is 3%. Moreover, the results obtained showed that the elastic modulus of the modified sand dunes concrete is lower, consequently it cannot use for structural elements but against it can be used for other elements such as curbs, foundation layer and burying of weakly radioactive materials, decorative elements and in the separation lanes for motorways.

**Keywords:** Concrete of sand, rubber crumb, elastic modulus, elastomeric, polymer.

## POSTER SESSIONS

**Id-1194**

### **Unraveling the Acoustic Exciton-Phonons Interaction in a Single GaN/Aln Quantum Dot**

Mouna Triki, S. Jaziri

University of Tunis El Manar, Tunisia

Corresponding author: mounasellami@yahoo.fr

**Abstract:** Coupling of acoustic phonons to an exciton in a single GaN/AlN quantum dots is investigated. Contributions of piezoelectric and deformation potential couplings are analyzed separately. It is found that, unlike nonpolar semiconductor based QDs, piezoelectric coupling influences significantly the QD's spectral line shape. Calculations show that deformation-potential and piezoelectric coupling mechanisms have comparative order of magnitude but with different behaviors. While the first mechanism involves all phonon modes the second involves only less energetic phonons. In accordance with experimental spectra, calculation shows also, that, increasing temperature leads to the quenching of the ZPL with the increase of the phonon wings.

**Keywords:** Acoustic phonons, piezoelectric coupling, deformation potential coupling, excitonic line shape

## POSTER SESSIONS

**Id-1199**

### **Excitonic Properties in the Vertical Heterobilayer Semiconducting Transition Metal Dichalcogenides $\text{MoS}_2\text{-WSe}_2$ Within Wannier Mott Model**

EMNA BEN SALEM<sup>1,2,\*</sup> & SIHEM JAZIRI<sup>3</sup>

<sup>1</sup>Institut Préparatoire aux Etudes d'Ingénieurs de Tunis, 2, Rue Jawaher LeI Nahrou - Monfleury - 1089 Tunis, Université de Tunis. Tunisie.

<sup>2</sup>Laboratoire de Physique de la Matière Condensée, Département de Physique, Faculté des Sciences de Tunis, Campus Universitaire 2092, Université Tunis El Manar, Tunisie.

<sup>3</sup>Laboratoire de Physique des Matériaux, Faculté des Sciences de Bizerte 7021 Jarzouna, Université de Carthage, Tunisia.

Corresponding athor: emna.bensalem@fst.rnu.tn

**Abstract:** Recently, layered Transition metal dichalcogenides (TMDCs) seems to be very promising for electronic, optoelectronic devices and future research because they offer tunability of several properties such as band gap and band offset. Vertical hetero-bilayer  $\text{MoS}_2\text{-WSe}_2$ , form a type II (staggered) hetero-structure where the top of the valence band is located on one layer while the bottom of the conduction band belongs to the second layer. In this case a transition appears at the interface, corresponding to the recombination between an electron and a hole separated between the two different layers which constitute the bilayer heterostructure. In this work we report a theoretical study on the excitonic properties of bilayer  $\text{MoS}_2\text{-WSe}_2$  type II bilayer heterostructure based on a 2D effective mass Wannier-Mott approximation Hamiltonian, with a nonlocally-screened carrier's interaction. Effects of the environmental relative dielectric constant and the spin orbit on the neutral and charged exciton's properties are studied.

**Keywords:** Hetero-bilayer tmcdc, type ii band structure alignment, exciton and trion.

## POSTER SESSIONS

**Id-1200**

### **Magneto Transport in Metal Nanoparticles Embedded Conducting Polymer Nano Fibres**

Tebogomahule<sup>1,\*</sup>, Vijaya Srinivasu Vallabhapurapu<sup>1</sup>, Madhumita Bhaumik<sup>1</sup> And Arjun Maity<sup>2</sup>

<sup>1</sup>Department of Physics, University of South Africa, Johannesburg 1710, South Africa.

<sup>2</sup> National Centre for Nanostructured Material, Council for Scientific and Industrial Research (CSIR), Pretoria, South Africa

Corresponding author: mahults@unisa.ac.za

**Abstract:** Temperature dependent magnetic and transport properties are studied in the one dimensional (1D) PANI-CI-Fe composite nanofibers (CNFs). Our measurements revealed ferromagnetic nature of this system. Depending on the Fe nanoparticles loading, the PANI-CI-Fe CNFs showed both metallic and semiconducting behaviour. The temperature dependent charge transport of semiconducting PANI-CI-Fe CNFs follows two different mechanisms at low and high temperature regimes. Efros-Shklovskii-variable range hopping (ES-VRH) dominates at low temperature and Mott-three dimensional-variable range hopping (Mott-3D-VRH) at high temperature regimes. Magnetoresistance (MR) studies were carried at different temperatures and magnetic fields for the pellets of PANI-CI-Fe CNFs in semiconducting form. At room temperature (300K) negative MR values were established in both low and high magnetic field regions. MR increases significantly with decrease in temperature from 300 K to 5K. Forward interference model can successfully explain the observed low field negative MR behaviour of PANI-CI-Fe CNFs. PANI-CI-Fe CNFs has a potential for magnetic field sensor devices.

**Keywords:** Conducting polymer, polyaniline, iron nanoparticles, electrical transport, magnetoresistance

## POSTER SESSIONS

**Id-1211**

### **The Boriding Treatment of XC38 Steel: Characterization and Optimization of the Paste Composition for Wear Resistance**

Abdelhalim. Brahim<sup>1</sup>, Mohamed. Sidi Moussa<sup>2</sup>

<sup>1</sup>LTSM, Université de Blida 1. Université SAAD DAHLAB de BLIDA route de SOUMÂA BP 270 BLIDA (09000) ALGERIE,

<sup>2</sup>LTSM, Université de Blida 1, Algérie.

Corresponding author : brahimi1963@yahoo.fr,

**Abstract:** In this study, the paste boriding treatment was carried out at 900 °C for 4 h on the surface of XC38 steel. The composition of the applied paste consisting of B<sub>4</sub>C, Al and SiC was taken as variable parameter. The generated boride layers were characterized by hardness measurements, optical microscopy examinations and XRD analysis. It is shown that the interface morphology of the borided layers and their properties such as wear resistance depend strongly on the paste composition. Furthermore, an optimization method was applied on the basis of experimental results to find an optimal value of the resistance against wear as a function of the paste composition.

**Keywords:** Boriding, multi–element paste, diffusion, wear resistance, optimization.

## POSTER SESSIONS

**Id-1212**

### **Mechanical Behavior and Microstructure of Gas Pipelines Welded Joints Achieved with Hybrid Welding Process**

Abderrahmane Abderrahmane<sup>1</sup>, Mohamed. Gaceb<sup>2</sup>, Khireddine Bettahar<sup>3</sup>

<sup>1</sup>LTSM, Université de Blida 1. Université SAAD DAHLAB de BLIDA route de SOUMÂA BP 270 BLIDA  
(09000) ALGERIE.

<sup>2</sup>LFEPM, Université M'hamed Bougara de Boumerdès. Université de BOUMERDES, Avenue de  
l'indépendance, BOUMERDES (35000) ALGERIE.

<sup>3</sup>Centre de Recherche en Technologies Industrielles (CRTI), BP 64, Route de Dely Brahim, CHERAGA  
16014 ALGER - ALGERIE.

Corresponding author : abderrahmane\_abd@yahoo.fr

**Abstract:** This work deals with the study of the quality of welded joints of gas pipelines carried out using a mixed welding process TIG / SMAW. For this purpose, we have proceeded to the welding of a 254 mm diameter and 19.1 mm thickness high strength steel tube. The quality of welded joints has been assessed by means of welding process certification tests, namely non-destructive tests (NDT) as well as mechanical testing. The results of NDT tests and optical macrography clearly showed a regular weld bead, defect-free with a thermal affected zone almost uniform of a width of 5 to 7 mm approximately. The behavior of the welded joints during tensile, nick-break and bend tests has proved a good ductility with very acceptable mechanical characteristics and within the tolerances allowed by the API 5L standard for the same grade steel. As a result, the resistance of the welded joints in service is equivalent to that of the base metal and no risks of crack initiation, brittle fracture or failing are to be feared during the operation of these assemblies. This qualification proves that filler metals and welding techniques used in the assembly of API 5L X60 steel are greatly appropriate for raw natural gas transport pipelines construction and largely meet the service requirements.

**Keywords:** TIG welding; HSLA steel; NDT; Mechanical properties

## POSTER SESSIONS

**Id-1222**

### **About Rock Strength Certificate**

Rychkov Boris Aleksandrovich\*, Komartsov Nikita Mihailovich, Kulagina Margarita Alekseevna,  
Kyrgyzstan, Bishkek, Kievskaya street, 44,  
Kyrgyz-Russian Slavic University,  
Corresponding author: rychkovba@mail.ru

**Abstract:** The stress state of rocks in the massif is modeled by testing standard cylindrical specimens on equipment according to the Karman's scheme, when the ratio between the axial compressive stress  $\sigma_1$  and the principal stresses  $\sigma_2$  and  $\sigma_3$  from uniform lateral pressure is:  $\sigma_1 > \sigma_2 = \sigma_3$ . In this case their ratio at the time of destruction indicates the strength of rocks. Stresses  $\sigma_1$  and  $\sigma_3$  can take many values, and it is impossible to carry out the whole complex of experiments with different ratios of these components. Therefore, various methods of calculation are being developed, which can be used to estimate the degree of danger of the stress state by the postulated dependencies between the main stresses, i.e. to predict the strength properties of materials at the moment of destruction. The envelope of limit stress circles on the Mohr's diagram in the coordinates "normal stress - shear stress" is considered as the rock strength certificate. To construct the envelope was used the relationship between the maximum and minimum principal stresses, presented in the form of two different strength criteria. One of them is the well-known criterion of Hoek-Brown, the other is proposed recently by T.B. Duyshenaliev and K. T. Koichumanov. The applicability of these criteria was checked on A.N. Stavrogin's and K. Mogi's experimental data, which were received by testing cylindrical specimens of various rocks under triaxial compression, as well as in the case of uniaxial tension.

**Keywords:** Rock strength, envelope of limit stress circles, strength criterion, principal stresses, Mohr diagram

## POSTER SESSIONS

Id-1225

### Crystallization and Properties Degradation in Ultrathin Amorphous HfO<sub>2</sub> Films Induced by Swift Heavy Ions

Jie Liu<sup>1,\*</sup>, Zongzhen Li<sup>1,2</sup>, Pengfei Zhai<sup>1</sup>, Tianqi Liu<sup>1,2</sup>, Shengxia Zhang<sup>1</sup>, Peipei Hu<sup>1,2</sup>, Lijun Xu<sup>1,2</sup>,  
Jian Zeng<sup>1</sup>, Youmei Sun<sup>1</sup>

<sup>1</sup> Institute of Modern Physics, Chinese Academy of Sciences (CAS), Lanzhou 730000, China

<sup>2</sup> School of Nuclear Science and Technology, University of Chinese Academy of Sciences,  
Beijing 100049, China

Corresponding author: j.liu@impcas.ac.cn

**Abstract:** Amorphous HfO<sub>2</sub> is the most used high-k gate dielectric materials in nano-electronic devices for reducing the tunneling leakage current and improving the reliability to overcome the physical limitation of SiO<sub>2</sub>. However, the heavy ions can result in amorphous-to-crystalline phase transition when the electronic energy loss  $((dE/dx)_e)$  exceeds a threshold value, thereby affecting the device performance in the space radiation environment. In this study, HfO<sub>2</sub>-based MOS capacitors were irradiated with 25 MeV/u <sup>86</sup>Kr and 12.5 MeV/u <sup>181</sup>Ta ions supplied by Heavy Ion Research Facility in Lanzhou (HIRFL) with  $(dE/dx)_e$  from 12.6 to 44.8 keV/nm and fluences up to  $1 \times 10^{12}$  ions/cm<sup>2</sup> without electrical bias. The amorphous HfO<sub>2</sub> films transformed to a monoclinic crystal structure induced by swift heavy ions (SHIs) was observed directly. The dielectric properties of HfO<sub>2</sub> thin films were deteriorated with increasing ion fluences and electronic energy loss  $(dE/dx)_e$  due to crystallization. Furthermore, the threshold of the  $(dE/dx)_e$  for crystallization is about 10 keV/nm deduced by fitting the relationship between the area of latent track changing as function of  $(dE/dx)_e$ . The quantitative relationship between microstructures and dielectric properties allows for prediction of device sensitivity to heavy ion irradiation and provides a new method to estimate the threshold of the  $(dE/dx)_e$  for crystallization.

**Keywords:** Radiation effect, high-k gate dielectric materials, latent track, crystallization

## POSTER SESSIONS

Id-1227

**Irradiated Effects in Few- and Mono-Layer MoS<sub>2</sub> Induced by Heavy Ions**

Youmei Sun\*, Hang Guo, Jie Liu, Pengfei Zhai, Jian Zeng, Shengxia Zhang, Huijun Yao  
Institute of Modern Physics, Chinese Academy of Sciences (CAS), Lanzhou 730000, China

Corresponding author: ymsun@impcas.ac.cn

**Abstract:** Molybdenum disulphide (MoS<sub>2</sub>) in two-dimensional form has attracted much attention for its potential applications in future electronic and optoelectronic devices. The latent tracks in mono- and few-layer MoS<sub>2</sub> induced by <sup>209</sup>Bi ions with energies of 0.45–1.23 GeV were characterized by atomic force microscopy (AFM). The hillock-like latent tracks were observed on the surface of irradiated monolayer MoS<sub>2</sub>. The diameter of the hillock after deconvolution procedure is  $15.8 \pm 1.7$  nm and the height is  $1.0 \pm 0.3$  nm. Hillock-like tracks are induced by energy transfer from energetic <sup>209</sup>Bi ions to electron system of MoS<sub>2</sub>, resulting in the ionization and excitation and then the displacement of target atoms. Since Raman spectroscopy is sensitive to damages induced by swift-heavy ion irradiation, the in-plane  $E_{2g}^1$  mode ( $\sim 385$  cm<sup>-1</sup>) and the out-of-plane  $A_{1g}$  mode ( $\sim 408$  cm<sup>-1</sup>) of MoS<sub>2</sub> were investigated. With increasing ion fluence, the  $A_{1g}$  peak shifts to higher frequencies, and the intensity ratio between  $A_{1g}$  and  $E_{2g}^1$  peak increases. The evolution of the structural and vibrational properties of MoS<sub>2</sub> with fluence is discussed. It can be concluded that the blue shift and narrowing of  $A_{1g}$  peak in irradiated MoS<sub>2</sub> is due to the adsorption of oxygen molecules at latent tracks. With decreasing thickness of MoS<sub>2</sub>, the irradiation resistance decreases.

**Keywords:** Latent track, MoS<sub>2</sub>, heavy ion, irradiation

## POSTER SESSIONS

**Id-1245**

### **Deformation Effect on The Structural and Energy Characteristics of Intermetallic NiAl and Ni<sub>2</sub>AlNb**

Aleksandra Chaplygina\*, Mikhail Starostenkov, Pavel Chaplygin  
Polzunov Altai State Technical University  
656038 – 46 Lenina st., Barnaul, Altai, Russia  
Corresponding author: alesya\_ch@mail.ru

**Abstract:** Bi-component alloys, depending on the concentration of the components upon transition from a disordered state on the basis of fcc lattice, can be converted into a large set of superstructures based on fcc, hcp, bcc, rhombic crystal lattices and others. In each case, similar phase transformations are accompanied by changes in the crystal structure symmetry, the anisotropy manifestation physical and mechanical properties of the materials. Such a property may be considered at the nanoscale as an element of shape-memory, or physical properties memory. We used Monte Carlo method for research structural and phase transformations, as in previous studies [1-2]. We took ordered alloys with different superstructures (B2 for NiAl and L<sub>2</sub>1 for Ni<sub>2</sub>AlNb) and made all-round deformation tension and compression. The hysteresis loop width increases with increasing percent strain during tensile strain. The hysteresis loop width decreases with increasing percent strain during compressive strain. The deformation leads to an increase in the average configurational energy, no noticeable changes in the structural characteristics occur, which does not indicate the presence of possible superstructural rearrangements for the NiAl and Ni<sub>2</sub>AlNb. All types tension and compression deformation for examined alloys leads to higher values of energy. These results are in good agreement with experimental data.

**Keywords:** Alloy, superstructure, deformation, NiAl, Ni<sub>2</sub>AlNb

**Acknowledgements:** Work supported by the grant MK-5094.2018.2

#### **References**

- [1]. Starostenkov M., Chaplygina A., Romanenko V., Details of the formation of superstructures in the process of ordering in Cu-Pt alloys / Key Engineering Materials, 2014, v.592-593, p.321-324.
- [2]. Potekaev A.I., Grinkevich L.S., Kulagina V.V., Chaplygina A.A., Chaplygin P.A., Starostenkov M.D. Structural-phase transformations of CuZn alloy under thermal-impact cycling / Russian Physics Journal, 2017, v.59. №10, p.1532-1542.

## POSTER SESSIONS

**Id-1247**

### **Radionuclide Characterization of Tritiated Water Using NMR Spectrometry**

Catalin Stelian Tuta\*, Viorel Fugaru, Cristian Postolache, George Bubueanu, Mihail-Razvan Ioan  
Horia Hulubei National Institute for Physics and Nuclear Engineering, 30, Reactorului St., Magurele, Ilfov,  
Romania, Corresponding author: catalin.tuta@nipne.ro

**Abstract:** This paper presents the preliminary results on determination of nuclidic purity and radioactive concentration of tritiated water (HTO and DTO) using NMR spectrometry. The tritiated water and heavy water samples were obtained by heterogeneous isotopic exchange technique using recovery tritium from expired sources. The obtained samples were characterized in point of view of radioactive concentration: using a TRICARB TR 2800 LSC type (dilution factor of the samples between 400.000 and 800.000).

The H and T nuclides in the samples were analysed using FT NMR Spectrometer AVANCE 400 MHz Micro-bay Bruker Biospin type. The H-NMR and T-NMR spectra of HTO/DTO were accumulated and chemical shift were determined ( $^1\text{H}$ : 4.703 ppm;  $^3\text{H}$ : 4.718 ppm). The ratio between the T-NMR amplitude signal and the radioactive concentration of HTO/DTO is linear on the analysed range of the radioactive concentrations. Also, the ratio between signals amplitude of the T signal and nuclide content of samples is linear. In conclusion, the preliminary obtained results sustain the possibility of the use of NMR spectrometry in determination of nuclide composition and radioactive concentration for high activity tritiated water samples.

**Keywords:** Tritium, NMR spectrometry, radioactive concentration

## POSTER SESSIONS

**Id-1248**

### **Determination of Tritium Contents in Stainless Steel Samples Using Full Combustion Method**

George Bubueanu\*, Viorel Fugaru, Cristian Postolache, Catalin Stelian Tuta, Mihail-Razvan Ioan  
Horia Hulubei National Institute for Physics and Nuclear Engineering, 30, Reactorului St., Magurele, Ilfov,  
Romania, Corresponding author: gbubueanu@nipne.ro

**Abstract:** An apparatus based on Total Degassing/Full Combustion method was designed and built for determination of tritium content in metallic samples. Equipment used in experiment is constituted from:

- Oxygen supply with pressure regulator and flow control meter
- 2 tube furnaces with temperature controller, one for Total Degassing (at 1100<sup>o</sup> C temperatures) and secondary for catalytic oxidation of resulted gases at water and carbon dioxide (800<sup>o</sup> C in presence of CuO wires)
- HTO collector

The protocol consists of calcination of samples followed by catalytic oxidation in oxygen atmosphere of emitted hydrogen, obtained HTO kept and determined of T activities at Liquid Scintillation Counting. The overall yield of the Full Combustion facility was determined using as standard sintered composite materials made from virgin stainless steel and Titanium tritide powders. The determined yield (94.3 ± 3.2%) was used for correction of the obtained experimental values. The new equipment was used in the radiological characterization of stainless steel samples from JET Culham UK and the decommissioned materials within TRITIULAB NIPNE Romania.

**Keywords:** Full Combustion, Tritium, Radioactive waste

## POSTER SESSIONS

**Id-1249**

### **Gamma-Rays Shielding Properties of Heavy Concrete with Barite and Tungsten Aggregate**

Viorel Fugaru<sup>1,\*</sup>, Cristian Postolache<sup>1</sup>, George Bubueanu<sup>1</sup>, Adriana Moanta<sup>2</sup>

<sup>1</sup>Horia Hulubei National Institute for Physics and Nuclear Engineering, 30 Reactorului St., Bucharest-Magurele, RO-077125, ROMANIA

<sup>2</sup>CEPROCIM S.A. - 6 Blvd. Preciziei, Bucharest, code 062203, ROMANIA

Corresponding author: vfugaru@nipne.ro

**Abstract:** For the adequate shielding of the radiological equipment using X and gamma rays special materials with high attenuation properties are needed. This objective may be achieved by the use of concrete, which is by far the most widely used material. In recent years, there have been many attempts to increase the capability of concrete for the shielding of gamma rays, with heavy aggregates as supplementary materials in concrete. Radiation shielding concrete effectiveness varies with the composition of the concrete (which contains water and inert aggregate held together by hardened cement paste). The heavy aggregate of concrete plays an essential role in modifying the physical and mechanical properties of the concrete and affects significantly on its shielding properties. In this work concrete with different heavy aggregates was used to study gamma ray shielding properties. Ordinary Portland cement concrete and 2 types of heavy aggregates concrete (barite and tungsten in different ratio) were poured in parallelepiped molds with the dimensions of 210 x 300 mm and different thicknesses (2- 10 cm). The experimental set-up and the results of the experiments concerning the shielding properties of the heavy concrete are given in the paper. In this study, linear attenuation coefficient of gamma rays of conventional concrete and heavy concrete (barite and tungsten) at energies of 1.25 MeV, 0.662 MeV and mass attenuation coefficients of each sample have been determined.

**Keywords:** Concrete, tungsten, radiation, shield

## POSTER SESSIONS

**Id-1253**

### **Electrodeposition of Vanadium Oxides Films, for Lithium-Ion Insertion**

Katia Ayouz-Chebout<sup>1</sup>, Malika Berouaken<sup>1</sup>, Maha Ayat<sup>1</sup>, Noureddine Gabouze<sup>1</sup>

<sup>1</sup>02, BD FRANTZ FANON ALGER, B.P. 140 ALGER – 7 MERVEILLES, TÉL. & FAX. : 2130(0)21 43.35.11.

Corresponding author: ay\_kat78@yahoo.fr

**Abstract:** Mesoporous vanadium pentoxide ( $V_2O_5$ ) thin films were deposited electrochemically onto indium tin oxide-coated glass substrates, and porous silicon, from an aqueous solution of vanadyl sulfate.

The results samples, electrodeposited films, or the crystallinity of the  $V_2O_5$  thin films were confirmed by X-ray diffraction, FTIR, MEB and UV characterizations. Cyclic voltometry and chrono-amperometry were used to measure the electrochemical properties of the synthesized films. The prepared  $V_2O_5$  films had high lithium-ion capacity and diffusion [1].

**Keywords:** Electrodeposition of  $V_2O_5$ , lithium-ion capacity

#### **References**

- [1]. Jin-Kyu Lee and All, "Electrodeposition of mesoporous  $V_2O_5$  with enhanced lithium-ion intercalation property", *Electrochemistry Communications* 11,1571–1574 (2009).

## POSTER SESSIONS

**Id-1254**

### **Morphological and Optical Parameters of Monolayers and Multilayers Porous Silicon Studied by Spectroscopic Ellipsometry**

**Hadj Yahia Seba<sup>1,2,\*</sup>, Nacéra Zebbar<sup>2</sup>, Mohamed Kechouane<sup>2</sup>**

<sup>1</sup>Laboratoire de Matériaux, Technologie de systèmes énergétiques et environnement, Université de Ghardaïa. Noumirat BP 455, route de Ouargla Ghardaïa 47000, Algeria

<sup>2</sup>Laboratoire de Physique des Matériaux équipe "Couches Minces et Semi-conducteurs", Faculté de physique USTHB, BP. 32 EL ALIA, 16111 Bab Ezzouar, Algiers, Algeria

Corresponding author: seba.hadjyahia@univ-ghardaia.dz

**Abstract:** In this communication, the evaluation of the optical and morphological parameters of porous silicon (Psi) monolayers and multilayers are studied by spectroscopic ellipsometry (SE). The Psi monolayers and multilayers were prepared by electrochemical etching of monocrystalline silicon wafers in a hydrofluoric acid electrolyte. We started by optimizing and controlling the process of formation of the porous silicon into monolayers and multilayers. This has allowed us to produce photonic crystals as Bragg mirrors and microcavities. In order to measure the degree of validity of the values of porosities, thicknesses and optical refractive indices obtained by SE, we compared these values with their corresponding values determined directly by gravimetry and optical reflectivity. For porous monolayers, we have obtained a good agreement between the porosity and thickness values obtained by both gravimetry and ellipsometry. As a result, the characteristics of PSi (porosity, thickness and refractive index) can be estimated using two non-destructive optical techniques: spectroscopic ellipsometry and optical reflectivity. For multilayers, we can use spectroscopic ellipsometry only to determine accurately the porosity of the two layers that constitute the structure.

**Keywords:** Multilayered porous silicon, electrochemical etching, spectroscopic ellipsometry analysis.

## POSTER SESSIONS

**Id-1255**

### **Determination of Radioactive Concentration of Tritiated Water Using EPR Spectrometry**

Cristian Postolache\*, Constantin Daniel Negut, Catalin Stelian Tuta, Viorel Fugaru, Mihail-Razvan Ioan, George Bubueanu

Horia Hulubei National Institute for Physics and Nuclear Engineering, 30, Reactorului St., Magurele, Ilfov, Romania, Corresponding author: cristip@nipne.ro

**Abstract:** Usually, the radioactive concentration of tritiated liquids is determined by Liquid Scintillation Spectrometry (LSC). The measurement of radioactivity for tritiated water with high specific activities using LSC implies multiple isotopic dilutions leading to liquid radioactive wastes with medium activities. In the present study, a novel method for determination of radioactive concentration in samples of tritiated water (HTO) and heavy water (DTO) was proposed. The method relies on the accumulation and detection of free radicals' radio-induced by self-radiolysis in frozen samples. The EPR analysis of the samples stored in liquid nitrogen confirmed the accumulation of HO• (asymmetric doublet with  $g_1 = 2.048$ ,  $g_2 = 2.026$  and  $g_3 = 1.996$ ) and respectively DO• (triplet with  $g = 2.013$  and  $a = 0.69$  mT) radicals. Because is not stable at the  $-196^\circ$  C temperature, the H• and D•, the secondary radical generated in self-radiolytically processes of the HTO/DTO was not identified. The linear dependence between EPR signal of the HO•/DO• radicals and storage time at  $-196^\circ$  C temperature suggests a constant accumulation of HO•/DO• radicals. But a recombination tendency of the formed radicals at high accumulation time has been identified. The ratio between the EPR amplitude signal and the radioactive concentration is linear on the analysed range of the radioactive concentrations. The preliminary obtained results sustain the possibility of the use of EPR spectrometry in determination of radioactive concentration for high activity samples.

**Keywords:** Tritiated water, self-radiolysis, EPR, radioactive concentration

## POSTER SESSIONS

**Id-1257**

### **Simulation of Hole Transient Photocurrents**

Serdouk Fadila, Benkhedir Mouhamed Loutfi

Laboratory of LPAT, University of Larbi-Tebessi-Tebessa, Algeria

Corresponding author: iserdouk@yahoo.fr

**Abstract:** Amorphous selenium is one of the leading candidates to be used as X-Ray Photo-conductor. The electronic properties of amorphous materials are greatly affected by the density of localized states. The exact shape of the density above the valance band edge in amorphous selenium is still unresolved despite decades of researchs. The density of localized states studied in detail by Serdouk and Benkhedir using the high resolution Laplace transform has distinct features. The calculated TPC transient photocurrents were compared to the measured one. A good agreement was found Later Serdouk and Benkhedir confirmed this result by the calculation of the hole lifetime. In this paper, we survey the electronic properties of stabilized amorphous selenium by the simulation of TOF transient photocurrents at different electric field. The calculations were done by using the inverse Laplace transform our results are compared with the experimental data of Kasap. The calculation of the lifetime from the simulated TOF transient photocurrents support our density of states model above the valance band edge.

**Keywords:** Density of localized states, transient photocurrents (TPC), Time of flight otocurrents (TOF); High resolution Laplace transform, Inverse Laplace transform; stabilized amorphous selenium

## POSTER SESSIONS

**Id-1260**

### **Elaboration and Characterization of Porous Hydroxyapatite Materials via the Reaction-Sintering of Phosphate and Aluminium Powder**

Hocine Belhouchet <sup>\*</sup>, Afaf Mokhtari

<sup>\*</sup>Physics Department, Faculty of Sciences, University Mohamed Boudiaf of M'sila, M'sila, 28000, Algeria.

Corresponding author: h.belhouchet@gmail.com

**Abstract:** In this work, the effects of mechanical activation on the reaction-sintering of hydroxyapatite/aluminum powder were investigated. Hydroxyapatite (HAp) biomaterials have been widely applied as bone substitutes because of its excellent bioactive properties. However, the low mechanical properties of this ceramic have been the main problem of the extensive use of this material. The addition of alumina, resulting from the oxidation of aluminum, to the hydroxyapatite has been carried out to improve the mechanical properties of sintered HAp. All samples were heated at different temperatures (1200, 1250, 1300, 1350, 1400 and 1450°C) for 2 h and characterized by apparent density, open porosity measurements, XRD, Raman spectroscopy, micro-hardness and SEM analysis. All mixture powders milled for different time showed the formation of a new phase of yeelimite (calcium sulfoaluminate,  $\text{Ca}_4(\text{AlO}_2)_6\text{SO}_3$ ) through heat treatment. The mechanical treatment enhances the reaction-sintering of the hydroxyapatite-aluminum powder. The mixture of hydroxyapatite and aluminum show the partial decomposition of hydroxyapatite at high temperature.

**Keywords:** Hydroxyapatite, bioceramics, mechanical activation, aluminum oxidation, calcium sulfoaluminate.

## POSTER SESSIONS

**Id-1262**

### **X-Ray Exposure Configuration and Dose Measurements at Different Thicknesses of Water Layer Using Individual Dosimeter**

Felicia Mihai\*, Constantin Cenusă, Ana Stochioiu

Horia Hulubei, National Institute for R&D in Physics and Nuclear Engineering,  
30 Reactorului Str., Magurele, jud Ilfov, P.O.B. MG-6, RO-077125, Romania,

Corresponding author: fmihai@nipne.ro

**Abstract:** In this paper are presented the doses recorded behind of water layers using the halide film dosimeter. The radiation exposure was performed with x- strahl medical x-ray generator at the 40 kV and 150 kV voltages and doses from 0.1 mSv to 100 mSv. From the experimental data a significant attenuation of the doses was recorded by the dosimeters placed behind of 15 cm water layer. At 40 kV at the conventional true values of 10 mSv and 30 mSv the dosimeters from the behind of the container record doses of  $0,1 \pm 0.01$  mSv and  $0.32 \pm 0.01$  mSv, respectively. At 150 kV the saturation threshold is reached at 50 mSv on the D2 films of the front dosimeters and at 15 mSv on the D10 film of the behind dosimeter. The optical density measured on D2 films of the behind dosimeters is under 1 optical density unit. At 150 kV at the conventional true values of 10 mSv and 30 mSv the dosimeters from the behind of the container record doses of  $1,12 \pm 0.01$  mSv and  $3.41 \pm 0.01$  mSv, respectively. The study was performed with the purpose to establish the doses recorded in special radiation conditions at a certain thickness of an aqueous material. In radiology medical procedures the patients may be exposed more or less that it is necessary for diagnostic or treatment.

**Keywords:** Dose, x-ray, dosimetry

## POSTER SESSIONS

**Id-1263**

### **Enhanced Sensitivity of H<sub>2</sub> Gas Sensor Based on Nanostructured Amorphous Methylated Silicon Films**

Lamia Talbi<sup>1</sup>, Sabrina Belaid<sup>1</sup>, Amar Manseri<sup>1</sup>, Hamid Menari<sup>1</sup>, Samira Kaci<sup>1</sup>, Aissa Keffous<sup>1</sup>, Mohamed Trari<sup>2</sup>

<sup>1</sup>Centre de Recherche en Technologie des Semi-conducteurs pour l'Energétique (C.R.T.S.E), Division Couches Minces Surfaces et Interfaces (C.M.S.I), 02 Bd., Frantz FANON, B.P. 140, Algiers, Algeria

<sup>2</sup>Houari Boumediene University (U.S.T.H.B), Chemical Faculty, Algiers, Algeria

*Corresponding author: lamias19@yahoo.fr*

**Abstract:** Silicon carbide nanostructures, including silicon carbide nanohole, silicon carbide nanowire, and silicon carbide nanopillar, have attracted great attention due to their potential in various fields of application, such as solar cells, insulator transistors, lithium batteries, energy storage, chemical and bio-sensing, thermoelectric modules and detection of the gas molecules. The formation of hydrogenated amorphous silicon-carbon alloy ( $a\text{-Si}_{1-x}(\text{CH}_3)_x\text{:H}$ ) nanowires were elaborated, using Ag-assisted electroless etching of the thin  $a\text{-Si}_{1-x}\text{C}_x\text{:H}$  films deposited by plasma-enhanced chemical vapour deposition from silane/methane gas mixtures, for a gas sensing application. The structure of SiCNWs was characterized by scanning electron Microscope (SEM) and photoluminescence measurements (PL). The nanowires morphologies strongly depend on the etching time and reveal the presence of the main emission bands located in the blue region. The answer of the obtained structure via Hydrogen gas was achieved. The results show that the fabricated structure can be used as an H<sub>2</sub> sensor at room temperature with a good sensitive and a good response time as 9 s and 2 s as recovery time for a low H<sub>2</sub> concentration.

**Keywords:** Porous amorphous hydrogenated materials; chemical etching; thin films, PECVD, gas

## POSTER SESSIONS

Id-1290

### Optical Properties of Hybrid Structures Based on Amorphous Hydrogenated Carbon and Silver Nanogranulated Films

Dmitrii Shcherbinin\*, Elena Konshina, Mohamed Abboud

ITMO University, 49 Kronverksky Pr., St. Petersburg, 197101, Russia

Corresponding author:dmitrij@gmail.com

**Abstract:** In the present study, the optical properties of thin-solids hybrid structures consisted of the silver nanogranulated film deposited on amorphous hydrogenated carbon have been investigated. The gravimetric thickness of silver film varied as 2, 4 and 10 nm. Amorphous hydrogenated carbon films with narrow (0.4 eV) and wide (2.7 eV) optical gap were used. The blue shift of plasmonic peak has been observed in the hybrid structures with the enhancement of a-C:H optical gap regardless of the gravimetric thickness of silver films. The maximum value of a blue shift (150 nm) compared to the carbonless samples was observed in the hybrid structures with wide-gap carbon. In the hybrid structures with 4 and 10 nm silver gravimetric thickness, weak short wave peak was excited in addition to the main peak. The effect of silver film morphology on a-C:H photoluminescence intensity in hybrid structures have been investigated. PL quenching has been observed in the hybrid structures consisted of wide-gap carbon and 2 and 4 nm silver film. In the same time two-fold enhancement of wide-gap a-C:H PL have been achieved in hybrid structures with 10 nm silver thickness. The same silver film led to 19 times PL enhancement of narrow gap a-C:H. It has been shown, that the efficiency of interaction between a-C:H  $\pi$ -electrons and silver NP localized surface plasmons depend on both - silver film morphology and structures features of a-CH.

**Keywords:** Plasmonic nanostructures, silver nanogranulated film, amorphous carbon, photoluminescence

## POSTER SESSIONS

**Id-1295**

### **Growth and Characterization of Cu<sub>2</sub>SnS<sub>3</sub> Single Crystal by the Melting Method for Thin Film Solar Cells**

Rania Mahdadi <sup>1,2</sup>, Abdesselam Bouloufa <sup>1,2,\*</sup>

<sup>1</sup> Electronics Department, Faculty of Technology, Ferhat Abbas Sétif-1 University

<sup>2</sup> Electrochemical and Materials Laboratory, Ferhat Abbas Sétif-1 University

Maabouda Street Sétif, 19000, Algeria

Corresponding author: abdeslam\_bouloufa@yahoo.fr

**Abstract:** Cu<sub>2</sub>SnS<sub>3</sub> (CTS) polycrystalline single crystal was grown by a melt growth method. Stoichiometric ratios of Cu (5N), Zn (6N), Sn (6N), S (6N), and Se (5N) were charged into a quartz ampoule. The ampoule, charged with the elements, was sealed off after evacuation to a pressure about 10<sup>-6</sup>Torr. The ampoule was inserted into a vertical furnace, heated up to 1100 °C in three steps with different rates, and kept at this temperature for 24 h. After, the ampoule was cooled to 300 °C with different rates and in the last phase in the atmosphere. The XRD patterns of CTS powder exhibit major peaks corresponding to diffraction lines of the monoclinic structure of CTS and no distinct peaks of secondary phases were observed in the XRD pattern. This result is confirmed by Raman measurements. Electrical parameters were carried out by Hall effect measurements. The p-type material was observed. The carrier concentration, the resistivity and the mobility were 4.76x10<sup>15</sup> cm<sup>-3</sup>, 2.8 Ωcm and 19.3 cm<sup>2</sup>V<sup>-1</sup>s<sup>-1</sup>, respectively. Measurements at low and high temperatures (from 80 K to 350 K), the Cu on Sn antisite defect (Cu<sub>Sn</sub>) and the Cu vacancy (V<sub>Cu</sub>) were detected and are the dominant acceptor defects in CTS, which leads to p-type conductivity. The activation energies of 33 and 75 meV at low and high temperatures were determined, respectively from Arrhenius plot of ln(σ) versus 1/T. The study of variation of mobility with temperature result in the acoustic and impurity scattering mechanisms at high and low temperatures, respectively.

**Keywords:** Cu<sub>2</sub>SnSe<sub>3</sub>, solar cell, single crystal, electrical parameters

## POSTER SESSIONS

**Id-1301**

### **Preparation of Synthetic Copper-Oxidases Mimics by Molecular Imprinting within Suspension and Precipitation Polymers**

Anna Jakubiak-Marcinkowska\*, Kinga Grodzka

Faculty of Chemistry, Wrocław University of Science and Technology,

Wyb. Wyspińskiego 27, 50-370 Wrocław, Poland

Corresponding author: anna.jakubiak@pwr.edu.pl

**Abstract:** In recent years, molecular imprinting technique (MIT) has become one of the most interesting method for preparation of synthetic enzymes analogues useful in organic and pharmaceutical chemistry, environment protection or food and agrochemical industry. Possibility of formation catalytically active centres similar in structure and functions to natural catalysts in synthetic materials, helps to overcome the limitations defined for enzymes such as low stability, sensitivity to external conditions, complicated isolation etc. Our studies focus on the creation of copper enzyme-like catalysts that mimics common oxidases by imprinting the Cu(II) ions in polymer beads prepared by two different techniques – suspension and precipitation polymerization. The assemblies of a crosslinked polymer matrix around templating metal-complex moieties are then formed giving binding cavities complementary in functionality and shape to the original analyte. Obtained catalysts were characterized by physicochemical analysis with BET measurements, SEM, FTIR, and EPR methods. The catalytic activity of various MIP mimics, as well as non-imprinted samples with metal ions, was compared in model reaction of *o*-aminophenol oxidation using hydrogen peroxide. All obtained catalysts were found active. Their activity depended on polymerization method, copolymer composition, polymer morphology, presence of cavities with Cu(II) ions inside, Cu(II) loading and structure of the active complex between copper ions and imidazole ligands. Imprinting process led to the formation of more active enzyme-like Cu(II) catalysts. Among all samples, the best were MIP microspheres obtained in precipitation polymerization (according to the reaction temperature, time and yield – up to the 80% after 40 min in 25°C).

**Keywords:** Molecular imprinting, enzyme mimics, suspension polymerization, precipitation polymerization, copper(II) catalysts

## POSTER SESSIONS

**Id-1308**

### **Porous Lime Pastes with Improved Mechanical Properties after Addition of Synthetic Aragonite**

Radek Ševčík<sup>1,\*</sup>, Lucie Zárybnická<sup>1</sup>, Petra Mácová<sup>1</sup>, Shota Urushadze<sup>1</sup>

<sup>1</sup> Institute of Theoretical and Applied Mechanics of the Czech Academy of Sciences, Prosecká 76, 19000 Praha 9, Czech Republic

Corresponding author: sevcik@itam.cas.cz

**Abstract:** Lime-based materials are still one of the key materials applied in the building industry. For example, they are used as binders in mortars. The hardening process, reaction between atmospheric CO<sub>2</sub> and Ca(OH)<sub>2</sub> in aqueous medium, results into formation of calcium carbonate (CaCO<sub>3</sub>). This reaction, so-called carbonation, is a multistep process and different polymorphs of CaCO<sub>3</sub> may be formed. Lime (Ca(OH)<sub>2</sub>) has been used for hundreds years, but, still many efforts are dedicated to improve its properties. This contribution is focused on the investigation of addition of aragonite, one of the metastable polymorphs of CaCO<sub>3</sub>, into pastes specimens prepared from aged lime putty. During carbonation reaction, the phase composition was analyzed using X-ray powder diffraction. Selected samples were observed under scanning electron microscope. The mechanical properties, compressive and flexural strength, were determined using load frame machine. The obtained results showed that addition of synthetic aragonite into lime putty influenced the carbonation reaction, modified the morphology of lime putty specimens, increased the compressive and flexural strength and increased the specimens` s porosity in comparison with reference specimens. The improvement of described properties was carry out with the preserving of the chemical composition because only CaCO<sub>3</sub> is present in all specimens after the full carbonation is achieved. Thus, the compatibility, important factor in case of restoration of cultural heritage objects, with lime-based materials, is preserved. The obtained results may help in engineering and designing new lime - based materials with improved properties for applications.

**Keywords:** Aragonite, CaCO<sub>3</sub>, lime, carbonation, mechanical testing.

**Acknowledgements:** Authors acknowledge support from GA ČR grant 17-05030S.

## POSTER SESSIONS

**Id-1322**

### **Modal Analysis and Natural Frequencies for Helicopter Rotor Blade**

Merouane Salhi\*, Abdelkader Kirad

Mechanical Engineering Department, Faculty of Technology,  
University of Blida 1, BP 270 Blida 09000 Algeria.

Corresponding author: [msalhi-aerospatiale@univ-blida.dz](mailto:msalhi-aerospatiale@univ-blida.dz)

**Abstract:** This aim of this paper is the static and dynamic analysis with simulations of a helicopter blade behavior by finite elements analysis FEM. A modal analysis was made to determine eight modes with their frequencies and deformation shapes applied on the helicopter blade by numerical simulation. The analysis of the reactions acting on the blade has been made. A simple model has been defined to study the vibration phenomena. To deal with real systems, a finite element model has been developed. This model makes it possible to extract the natural frequencies and the modal deformations of the blade, and to calculate the stresses and displacements acting on the structure for the different mode shapes.

**Keywords:** Rotor blade, Static and dynamic analysis, Finite elements method, Vibrations, Deformation, Stress.

## POSTER SESSIONS

**Id-1323**

### **Determination of the Natural Frequencies for a Light Aircraft Engine Suspension**

Abdelkader Kirad\*, Merouane Salhi

*Mechanical Engineering Department, Faculty of Technology,*

University of Blida 1, BP 270 Blida 09000 Algeria.

Corresponding author: abdelkader\_kirad62@yahoo.com

**Abstract:** The choice of an effective suspension, increases the efficiency of a device, ensures a longer life, and improves comfort. This work aims to study and set up a suspension of a powertrain suspension in a light aircraft, which usually comes down to knowing the different parameters, static and dynamic powertrain and choose the type material (media characteristics). The work presented is to develop a numerical calculation program, to position and choose suspension watch. The elastic suspension allows a better balanced distribution of static charges. The elastic supports absorb without difficulty small inter-axis differences or conformation, with negligible efforts, allow wider tolerances and dangerous stress, small relative movements of the machine relative to its fixed support, resulting in example of the efforts of the thermal expansion or deformations of the chassis. The essential role of elastic suspensions, in particular what interests us is the case of the vibrations which will be specially studied. An elastically suspended machine is subjected to a vibration when it undergoes alternating periodic Solicitation which results in more or less important oscillations. The purpose of the elastic suspension is to attenuate the transmission of vibrations and not to prevent the machine from vibrations.

**Keywords:** Transmissibility, natural frequency, kinetic moment, dynamic moment, coupling.

## POSTER SESSIONS

Id-1336

### Ageing Effect of DBD Activated Ceramic Powders: The Impact of Storage Humidity on the Electrophoretic Deposition Rate

Martina Ilčíková, Jozef Ráhel, Lubomír Prokeš\*,

CEPLANT - R&D Centre for Low-cost Plasma and Nanotechnology Surface Modifications, Masaryk University,  
Kotlářská 2, 611 37 Brno, Czech Republic

Corresponding author: luboprok@gmail.com

**Abstract:** Electrophoretic deposition (EPD) of plasma pre-treated  $\text{Al}_2\text{O}_3$  powders results in ceramic layers of substantially improved deposit homogeneity [1]. To evaluate the practical applicability of this phenomenon, we report on the magnitude and dynamics of undesired gradual deterioration on plasma treatment – the ageing effect. Powder samples were treated by diffuse coplanar dielectric barrier discharge (DBD) and sequentially evaluated for their EPD performance for the time span of 30 days. Two sets of powder samples were evaluated. The first was stored in arid environment of 23% RH, the second one in a humid air of 86% RH. The storage in the arid environment resulted in a slow but gradual decline of deposition rate (Fig. 1 left). However, the uniformity of deposited layers remained unaffected. The samples stored in the humid environment exhibited a substantially more complex behavior (Fig. 1 right). Already after one week the effect of plasma treatment had disappeared, and the deposition polarity had to be changed from anodic to cathodic. Afterwards gradual increase of deposition rate was observed until the final recurrent decline at fourth week. The results point out the importance of water molecules controlled secondary processes on the treated powder surface.

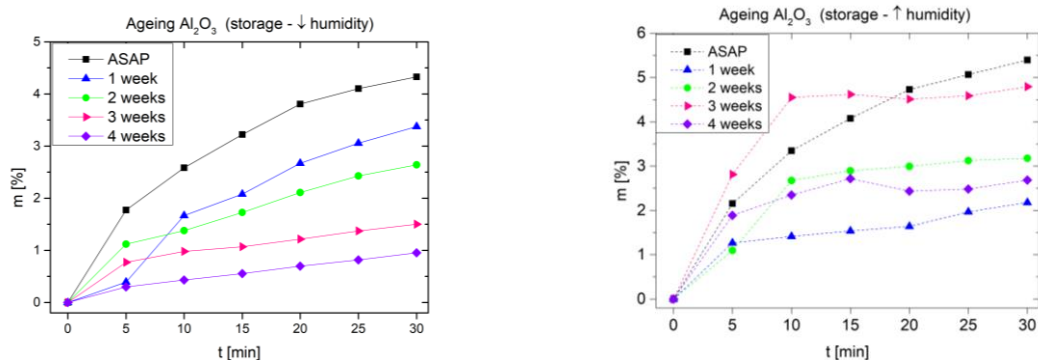


**Fig. 1.** EPD deposition rate for DBD plasma activated  $\text{Al}_2\text{O}_3$  powders stored in air of low (left) and high (right) relative humidity level.

**Keywords:** Ceramic, plasma,  $\text{Al}_2\text{O}_3$

**Acknowledgements:** The work was financially supported by the Czech Science Foundation, contract No. GA17-05620S, project CZ.1.05/2.1.00/03.0086 funded by European Regional Development Fund and project LO1411 (NPU I) funded by Ministry of Education, Youth and Sports of Czech Republic.

#### References

- [1]. Drdlik D, Moravek T, Rahel J *et al.* (2018) *Ceramics International*, 44 (8) 9787.

## POSTER SESSIONS

**Id-1337**

### **Thermal Desorption Spectroscopy Investigation of DBD Plasma Modified Aluminium Oxide Submicron Powders**

Ján Dugáček, Lubomír Prokeš, Pavel Šťáhel\*, Jozef Ráhel, Martina Ilčíková

CEPLANT - R&D Centre For Low-cost Plasma and Nanotechnology Surface Modifications, Masaryk University,  
Kotlářská 2, 611 37 Brno, Czech Republic,

Corresponding author: pstahel@physics.muni.cz

**Abstract:** Our recent work on the activation of fine Al<sub>2</sub>O<sub>3</sub> ceramic powders by atmospheric pressure coplanar DBD (dielectric barrier discharge) revealed several benefits which such activation may have for advanced ceramic engineering. The need of dispersant additives for preparing stable water-based ceramic suspensions can be reduced or even completely removed [1]. Slip casted Al<sub>2</sub>O<sub>3</sub> samples from DBD activated powders exhibited finer pore size distribution and higher sinterability. Final microstructure of sintered samples had the grain size reduced by a factor of 1.7 [2]. The performance of electrophoretic deposition (EPD) reduced significantly the deposited layer surface roughness, due to the reduced deposition rate and reversed deposition polarity from cathodic to anodic [3]. To address the nature of underlying physico-chemical processes, DBD plasma activated Al<sub>2</sub>O<sub>3</sub> as well as yttria stabilized ZrO<sub>2</sub> powders were thoroughly investigated by means of thermal desorption spectroscopy. We have found that plasma treated powders contains additional oxygen, nitrogen monoxide, nitrogen dioxide and carbon dioxide functional groups. Performed experiments pointed out top the important role of plasma originated molecular gasses physisorbed on the ceramic particles surface.

**Keywords:** Ceramic, plasma, Al<sub>2</sub>O<sub>3</sub>

**Acknowledgements:** The work was financially supported by the Czech Science Foundation, contract No. GA17-05620S, project CZ.1.05/2.1.00/03.0086 funded by European Regional Development Fund and project LO1411 (NPU I) funded by Ministry of Education, Youth and Sports of Czech Republic.

#### **References**

- [1]. Szalay Zs, Bodišová K, Pálková H *et al.* (2014) *Ceramics International*, 40 (8B) 12737.
- [2]. Pouchlý V, Ráhel J, Spusta T *et al.* (2019) *J. Eur. Ceram. Soc.* 39(4), pp. 1297-1303
- [3]. Drdlik D, Moravek T, Ráhel J *et al.* (2018) *Ceramics International*, 44 (8) 9787.

## POSTER SESSIONS

**Id-1338**

### **A Comparative Electrochemical Study on Corrosion Inhibition by Méthoxy Carbonyl Triphenyl Phosphonium Bromide in Acid Media HCl 1M**

Khaled Mansouri<sup>1\*</sup>, Ahmed Tabchouche<sup>2</sup>, Oussama Bacha<sup>2</sup>

Oumelkheir Rahim<sup>3</sup>

<sup>1</sup> Lab. Mathematics and Applied Science, Ghardaia University BP 455 Ghardaia, Algeria

<sup>2</sup> Lab. Dynamic Interactions and Reactivity of Systems, Process Engineering Department, Faculty of Applied Sciences, University Kasdi Merbah, Ouargla 30000, Algeria.

<sup>3</sup> Electrochemical Laboratory, Chemistry Department, Faculty of mathematics and Matter Sciences, University Kasdi Merbah, Ouargla 30000, Algeria.

Corresponding author: khaledmansouri31@yahoo.fr

**Abstract:** In this work, we study the inhibitory efficacy of new organ metallic compounds (phosphonium salts) used as a inhibitor on the corrosion of carbon steel X70. The compound is Méthoxy carbonyl Triphenyl Phosphonium bromide The study was performed in a 0.5M H<sub>2</sub>SO<sub>4</sub> middle. The measurements were performed by two electrochemical methods (electrochemical impedance spectroscopy and potentiometre).

The results have allowed us to deduce the steel corrosion rate as well as other electrochemical parameters. The overall results show that the compounds (MCTP Br) was chemically adsorbed on the steel surface. and adsorption of these consisted to the metal surface is according to the model of adsorption of the Langmuir isotherm. In 1M HCl solution. And The best concentration that decreasing the corrosion rate and gives good inhibition is 80ppm (44.49%).

**Keywords:** Corrosion; Electrochemical; Inhibitory; Phosphonium; Impedance

## POSTER SESSIONS

**Id-1346**

### **Dynamic Analysis of the Effect of a Wall on the Wake Behaviour in the Fluid Flow Behind Cylindrical Obstacle.**

Sidali Bensedira<sup>1,\*</sup>, Abdellah Abdellah El-Hadj<sup>2</sup>, Djaffar Semmar<sup>1</sup>, Samir Danouni<sup>3</sup>

<sup>1</sup>Faculty of Technology, University of Blida1, 09000 Blida 1, Algeria

<sup>2</sup>Laboratory LMP2M, Medea University, 26000 Ain D'heb Medea, Algeria

<sup>3</sup>University of Tipaza, Tipaza 42000, Algeria

Corresponding author : bensedirasidali@gmail.com

**Abstract:** The purpose of this work is studied numerically the dynamic behavior of flow around circular cylinders placed near a solid wall. The ANSYS CFX code is used to solve the flow problem in laminar flow for an incompressible fluid. The flow equations are solved by finite element method. First, we compared our results with other numerical results for a flow around a free cylinder (without wall), then we placed a wall near a cylinder and we varied the distance between the wall and the cylinder ( $G/D$ ). It has been found that a great effect of the wall on the mean hydrodynamic coefficient. The values of  $CL$  tend to zero when the distance ( $G/D$ ) is very close compared to those of without wall. The pressure and velocity contours are also presented. Finally, it is also found that Strouhal number values of the cylinder near the wall vary between 0.21 and 0.23, therefore the effect of the wall on the hydrodynamic forces and on the structure of the flow behind the cylinder and the different parameters of the flow is very important.

**Keywords:** Cylinder, flow, flow, wake, wall, hydrodynamic force

## POSTER SESSIONS

**Id-1356**

### **Fault Diagnosis Based on Enhancement of Barkhausen Noise Using Hybrid Method Empirical Mode Decomposition-Savitzky-Golay Filter**

Rabah Abdelkader<sup>1,\*</sup>, Moahmmed Khorchef<sup>1</sup>, Mourad Zergoug<sup>1</sup>

<sup>1</sup>Research Center in Industrial Technologie, Algeria

Corresponding author: abderabeh\_8@yahoo.fr

**Abstract:** the barkhausen noise carries important information which can be used in early damage detection and fault diagnosis. The barkhausen noise is corrupted by interference signals from other sources during the measure and the information of fault can be lost. In this paper a new algorithm based on Empirical Mode Decomposition (EMD) and Savitzky-Golay is proposed to extract the information about the fault of materials from a measured barkhausen noise. Firstly, using EMD to decompose the barkhausen noise signal into elementary function called Intrinsic Mode Function (IMF). Secondly, we use the energy to select the relevant mode, these selected IMF is filtered by Savitzky-Golay filter and the reconstructed signal is obtained by the IMFs filtered. The envelope spectra are used to test the efficiency of the proposed method in enhancement the quality of barkhausen noise signal. The proposed method is validated using the measuring chain of barkhausen noise (Fig (3-8)) and the obtained results shows the effectiveness of the proposed method in fault detection.

**Keywords:** Barkhausen noise; emd; savisky golay filter; enrgy, envlope spectra

## POSTER SESSIONS

**Id-1357**

### **Dielectric and Thermal Analysis of a Leaf of Vegetation for the Modeling of Forest Fires**

Khadija Khelloufi <sup>1,2,3\*</sup>, Cláudia Pinto <sup>3</sup>, Domingos Xavier Viegas <sup>3,4</sup>

<sup>1</sup>University of Sciences and Technology Oran Mohamed Boudiaf USTOMB, Physics Department, LEPM, BP 1505  
El Mnaouer, Oran, Algeria

<sup>2</sup>Superior School in Electrical Engineering and Energy ORAN ESG2E BP 64 ch2 Achaba Hanifi-USTO- Oran,  
Algeria

<sup>3</sup> Forest Fire Research Centre (CEIF / ADAI), University of Coimbra, Rua Pedro Hispano, 12, 3031-601, Coimbra,  
Portugal

<sup>4</sup> Dept. of Mechanical Engineering, University of Coimbra, Pinhal de Marrocos 3030-788, Coimbra, Portugal

Corresponding author: ph\_khadij@hotmail.fr

**Abstract:** Most Mediterranean regions face a high risk to forest fires, estimation and anticipation of his risk modeled as a stochastic propagation process reproduces well some fire properties. Our model needs information on different types of vegetation including their bio-physical properties behavior associated to combustion. In this work, an experimental study to analyze the structure of a leaf of Laurel shrub at different biological stages is presented; it allows following the structural exchanges induced on the leaf by the effect of increasing temperature. For this purpose, we performed both dielectric and TG/DT Analysis for a better understanding of the pyrolysis phenomenon and to determine accurately the chemical parameters such as activation energy and time associated to each reaction caused by temperature increase. The results obtained provide information on the process of thermal degradation caused by fire. The evolution of the leaf impedance as a function of the applied frequency characterizes the moisture loss in plant species during pyrolysis. The dielectric response confirms our proposition to the equivalent circuit of the leaf of vegetation as a composite of liquid and solid parts. The TGA / DTA results detected the behavior of the solid parts in the fire under a constant heating rate, and were able to show all the transformation subjected by the Laurel leaf until ignition and all the gases released during it.

**Keywords:** Impedance spectroscopy, TGA/DTA Analysis, Pyrolysis, Modeling, forest fire

## POSTER SESSIONS

Id-1366

### Polymeric Micelles Based on Pluronics as Flavonoids' Nanocarriers

Sylwia Ronka<sup>1,\*</sup>, Aleksandra Peszczyńska<sup>1</sup>, Anna Żołnierczyk<sup>2</sup>, Dagmara Baczyńska<sup>3</sup>

<sup>1</sup>Department of Polymer Engineering and Technology, Faculty of Chemistry, Wrocław University of Science and Technology, Wybrzeże Wyspiańskiego 27, 50-370 Wrocław, Poland

<sup>2</sup>Department of Chemistry, Faculty of Biotechnology and Food Science, Wrocław University of Environmental and Life Sciences, Norwida 25, 50-375 Wrocław, Poland

<sup>3</sup>Department of Molecular and Cellular Biology, Faculty of Pharmacy with Division of Laboratory Diagnostics, Wrocław Medical University, Borowska 211A, 50-556 Wrocław, Poland,

Corresponding author: sylwia.ronka@pwr.edu.pl

**Abstract:** Polymeric micelles are formed by amphiphilic copolymer molecules, which are able to self-assemble in an aqueous environment when their concentration exceeds a particular value called critical micellization concentrations – CMC [1]. These nanocarriers have core-shell structures. The inner core of polymeric micelle, built from hydrophobic parts of amphiphilic polymer molecules, is capable of entrapment of poorly water-soluble active substances, whereas external hydrophilic shell provides micelle stabilization in aqueous solutions, an ability to interact with the cells and isolation of a drug from adverse environmental conditions such as acidic pH [2]. Polymeric micelles have been found as more stable than micelles made from conventional surfactants and phospholipids. If the structures which form the core of micelles are finely designed, they may exhibit a good thermodynamic and kinetic stability. Thanks to their low CMC values polymeric micelles are able to retain drug molecules for a longer period of time, even upon dilution in systemic fluids. They exhibit suitable micelle sizes, high encapsulation capacities, ease of preparation, and a large possibility in system modifications [3]. Among various polymers approved to medical applications, significant attention has been drawn to Pluronics - amphiphilic PEO-PPO-PEO copolymers. They are not only pharmacokinetic but also biological response modifiers, which means that they are able to sensitize even multidrug resistance in cancer cells.

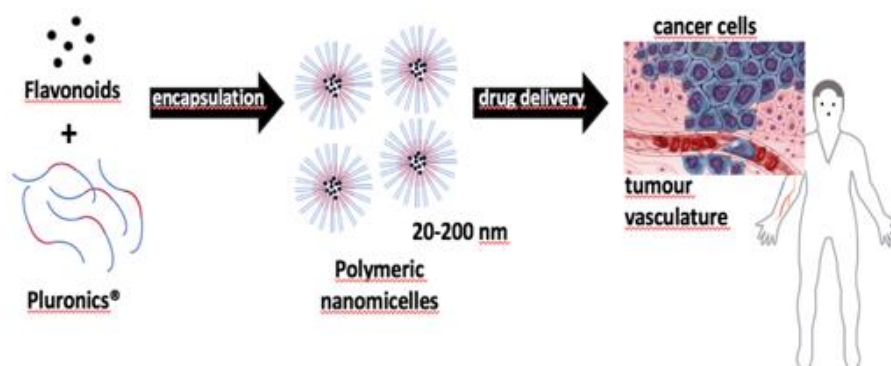


Figure 1. Research scheme.

Encapsulation of two flavonoids – naringenin and xanthohumol (isolated from spent hop) in polymeric micelles based on Pluronic P123, F127 and mixture of them by thin-film formation method was investigated. The results of the research including evaluation of the size of the formed micelles and their stability upon dilution in order to assess their potential of tumour cells targeting and also the investigation of the drug release profile of encapsulated flavonoids and their in vitro cytotoxicity against human colon cancer cells will be presented.

**Keywords:** Polymeric micelles, Pluronic, drug delivery system, flavonoids

**Acknowledgement:** The work was financed by a statutory activity subsidy from the Polish Ministry of Science and Higher Education for the Faculty of Chemistry of Wrocław University of Science and Technology.

#### **References**

- [1]. X.B. Xiong, Z. Binkhathlan, O. Molavi, A. Lavasanifar, *Acta Biomater.*, 8 (2012) 2017.
- [2]. A.R. Bilia, B. Isacchi, C. Righeschi, C. Guccione, M.C. Bergonzi, *Food Nutr. Sci.*, 5 (2014) 1212.
- [3]. R.H. Prabhu, V.B. Patravale, M.D. Joshi, *Int. J. Nanomedicine*, 10 (2015) 1001.

## POSTER SESSIONS

**Id-1371**

### **Prediction and Modeling of the Mechanical Properties of the Laminate Hybrid Composite Material**

Djamel Zelmati<sup>1,2\*</sup>, Oualid Guelloudj<sup>1,2\*\*</sup>, Radouane Graine<sup>1</sup>, , Fahima Seheb<sup>1</sup>, Nadjet Seheb<sup>1</sup>, Mohamed Boulekraa<sup>1</sup>

<sup>1</sup> Research Center in Industrial Technologies (CRTI), P.O. Box 64, Cheraga 16014 Algiers, Algeria,

<sup>2</sup> LRTAPM: Research Laboratory of Advanced Technology in Mechanical Production, Department of Mechanical Engineering Faculty of Engineering Science, Badji Mokhtar University Annaba, BP 12, 23000 Annaba, Algeria

Corresponding author: d.zelmati@crti.dz

**Abstract:** In the present work, the behavior of the hybrid composite material is analyzed based on the first order laminate theory. A mechanical model is developed in order to predict the mechanical behavior of the hybrid composite material and estimate the mechanical properties. In the same time, a failure criterion is applied for the square geometrical configuration under a tensile load applied in the fiber direction in order to work within safe conditions. The assessment of the strain and the stress fields in all layers of the composite material is performed to assess and evaluate the security factor in all plies.

**Keywords:** Composite, Modeling, stress field, security factor, failure criterion

#### **References**

- [1]. Tsai, S.W. and Hahn, H.T., Introduction to Composite Materials, CRC Press, Boca Raton, FL, Table 1.7, p. 19 ; Table 7.1, p. 292 ; Table 8.3, p. 344.
- [2]. Mechanics of fibrous composites, Mahmood Husein Datoo, Elsevier, (1991)
- [3]. Wambua, Paul, Jan Ivens, and Ignaas Verpoest. Comp. Sci. Tech 63.9 (2003) 1259-1264
- [4]. Beukers A. In : Van Hinte, editor. Lightness, the inevitable renaissance of minimum energy structures. Rotterdam : 010 publishers ; 1999. p. 72 Mehmet Ali Akinlar, Aydin Secer, "Wavelet-Petrov-Galerkin Method for Numerical Solution of Boussinesq Equation", International Conference on Chemical, Mechanical and Materials Engineering, Melbourne, AUSTRALIA, (2013).

## POSTER SESSIONS

Id-1372

**Molecular Dynamics Simulations of Separation Membrane Based on Super Carbonaceous Materials for Small Gas Molecules**

Sebastian Muraru, Sorin Muraru, Mariana Ionita\*

Advanced Polymer Materials Group, University Politehnica of Bucharest, Gh Polizu 1-7, 011061, Bucharest, Romania

Corresponding author: mariana.ionita@polimi.it

**Abstract:** Super carbonaceous materials (SCMs) are hybrid super-structures based on intricate patterns of assembled fullerenes, graphene sheets and carbon nanotubes. By integrating synergistic features of their basic units, super carbonaceous materials are considered the supreme material which possesses the utmost potential to subdue insurmountable shortcomings of unadulterated graphene or carbon nanotubes and can become the ultimate membrane for challenging applications. Different Super carbonaceous structures were built computationally and their performance as separation membranes was tested through Molecular Dynamics (MD) for a range of small gas molecules (H<sub>2</sub>, CO<sub>2</sub>, CO and CH<sub>4</sub>). The MD simulations were performed using GROMACS software and the diffusion coefficients of H<sub>2</sub>, CO<sub>2</sub>, CO and CH<sub>4</sub> were assessed. The forcefield OPLS-AA was used, with some of its parameters modified according to existing literature to better suit the small gas molecules and the carbon structures. Given its layer-based layout leading to finer and finer filtering, the system presented in the Figure 1 was selected as a suitable separation membrane having achieved a selective separation for hydrogen (98% pure). The result is mainly due to the fit between the VdW radius of hydrogen molecules and the final pore present in the membrane and the preliminary sizing of the molecules attempting to cross the barrier, which aids in preventing pore blockages from taking place early on.

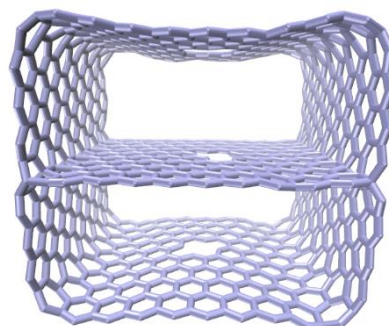


Figure1. Depiction graphene layer-based membranes with different pore size for selective gas separation

**Keywords:** Molecular dynamics, separation membrane, carbonaceous materials

**Acknowledgment:** This work was supported by a grant of the Executive Agency for Higher Education, Research, Development and innovation funding (UEFISCDI), project number PN-III-P1-1.1-TE-2016-24-2, contract TE 122/2018.

## POSTER SESSIONS

**Id-1374**

### **Micrographic and Chemical characterization of Timimoun quartz**

Sidali Medjahed<sup>1</sup>, Abdelkrim Kheloufi<sup>1</sup>, Ema Bobocioiu<sup>2</sup>, Fouad Kerkar<sup>1</sup>

<sup>1</sup>Centre de Recherche en technologie des Semi-conducteurs pour l'Energétique (CRTSE),

<sup>2</sup>Bd Frantz Fanon BP140, 7merveilles, Alger 16038, Algeria

Corresponding author : medjahesidali@crtse.dz

**Abstract :** Silica materials, in particular quartz, are characterized by specific properties (e.g., crystal shape, colour, trace element and isotopic composition, luminescence properties) —ranging from point defects to macroscopic appearance—which are dependent on the geological history and specific conditions of formation. The knowledge of the interrelation between genetic conditions and such properties can be used both for the reconstruction of geological processes and for specific technical applications [1]. The present work consists mainly in a chemical and micrographic study of the quartz samples from Timimoun deposit (central Sahara of Algeria). Chemical characterization comprises X-ray fluorescence (XRF), electron probe microanalysis (EPMA) and cathodo-luminescence (CL) analysis techniques in order to identify the major, minor and trace impurities contained in the samples. The micrographic observations were carried out by optical microscopy. Then, Raman spectroscopy is employed to define the nature of the mineral inclusions (fluids and solids) observed. Based on the specific characteristics of the quartz deposit, one or more processing stages will be required in order to liberate mineral impurities and fluid inclusions for further physical treatment:

**Keywords:** Quartz, impurities, mineral inclusions, characterization

#### **References**

- [1]. Götze J (2009) Chemistry, textures and physical properties of quartz—geological interpretation and technical application. *Mineral Mag* 73(4):645–671

## POSTER SESSIONS

### Id-1378

## Synthesis and Structural Characterization of Erbium Electrodepositing on Silicon nanowires

Afaf Brik<sup>1</sup>, S. B. Assiou<sup>2</sup>, T. Hadjersi<sup>3</sup>, B. Benyahia<sup>4</sup>, A. Manseri<sup>5</sup>

Centre de Recherche en Technologie des Semi-conducteurs pour l'Energétique (CRTSE)

2 Bd Frantz Fanon, B.P.140 Alger-7 Merveilles, Algiers (Algeria),

Corresponding author: brikafaf@yahoo.com

**Abstract:** In this work, we report the electrochemical deposition of Erbium on silicon nanowires array (SiNWs). The silicon nanowires were elaborated by metal assisted chemical etching and the Erbium was electrodeposited by two methods, Chronoamperometry and pulsed, then this was followed by a high temperature annealing step. We used several means of characterizations. We started, first, with the presentation of MEB, EDX, and DRX characterization. Figure 1 shows DRX spectrum, We found several peaks positioned at  $2\theta = 20.33^\circ$ ,  $41.60^\circ$ ,  $56.40^\circ$ ,  $60.64^\circ$  and  $80.71^\circ$  to cubic (space group Ia3) phase  $\text{Er}_2\text{O}_3$  according to the PDF 77-777, exhibit an intensity increase for doping pulzed during 40s. The results presented in this paper indicate that erbium doped silicon nanowires can be useful towards developing efficient and economical devices using these materials.

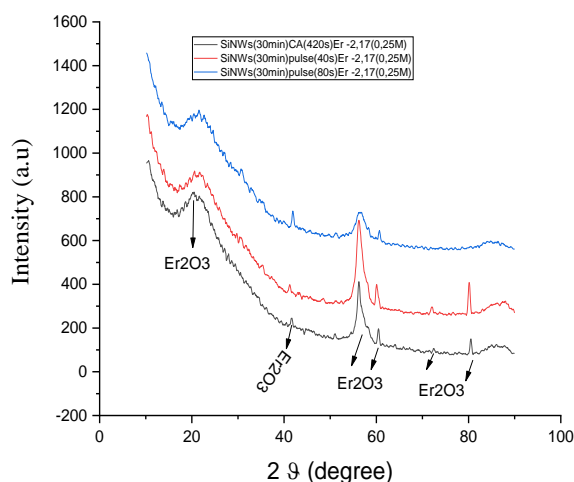


**Figure.1:** Diffractogram  $RX$  of a layer of silicon nanowires with electrodeposited erbium from 0.25M concentration solution (-2.17 potential)

**Keywords:** Erbium, silicon, silicon nanowires, electrochemistry.

## POSTER SESSIONS

**Id-1379**

### **Structural and Optical Properties of Silicon Carbide Nanoparticles Produced by Sol-Gel Method**

Karima Benfadel<sup>1,2\*</sup>, Samira Kaci<sup>1</sup>, Fahim Hamidouche<sup>2</sup>, Aissa Keffous<sup>1</sup>, Abdelbaki Benmounah<sup>2</sup>, H. Menari<sup>1</sup>, B. Mahmoudi<sup>1</sup>

<sup>1</sup>CMSI, Semiconductor Technology Research Center for Energetics, (CRTSE),

<sup>2</sup>UR-MPE: research unit materials, processes and environment M'hamed Bougara University.

Corresponding author: benfadelkarima@gmail.com

**Abstract:** The main objective of this work is the synthesis and characterization of silicon carbide nanoparticles. This material is particularly promising for numerous applications in the fields of high frequencies, high temperatures, etc. Silicon carbide exists in many crystalline or polytypes forms. The most studied are the hexagonal polytypes, 4H-SiC and 6H-SiC and the cubic 3C-SiC. In this study, silicon carbide nanopowders (SiC) were synthesized by the sol-gel method, in which sucrose and TEOS were used as precursors of carbon and silicon. The SOLs were prepared in the presence of water, solvent and catalysts. The Xerogel was stored in an Argon atmosphere furnace for carbothermal reduction. Other chemical and thermal treatments are carried out on the powder developed to eliminate excess silicon and carbon. The elaborated materials are characterized by FT-IR, Raman, SEM and XRD. The characterization of the samples by the FT-IR technique revealed the formation of silicon carbide "SiC" through the presence of the absorption peaks at the vibrations of the SiC bond. Raman spectroscopy characterization allowed us to identify SiC polytype. SEM micrographs of SiC powders revealed nanometric particles and the X-ray diffraction patterns of the powders indicated the presence of different SiC phases. The SiC nanoparticles excited with different wavelengths showed strong peak at 466nm, and intensity decreased by changing  $\lambda_{exc}$  from 290 nm to  $\lambda_{exc} = 310$  nm. EQE measurements whose showed a notably intensification of the peaks where the PV device have low optical response The sol-gel method is well recommended for the synthesis of SiC nanopowder provided that the carbothermic reduction is carried out.

**Keywords:** SiC nanoparticles, sol-gel, luminescent species; luminescent down-shifting layers.

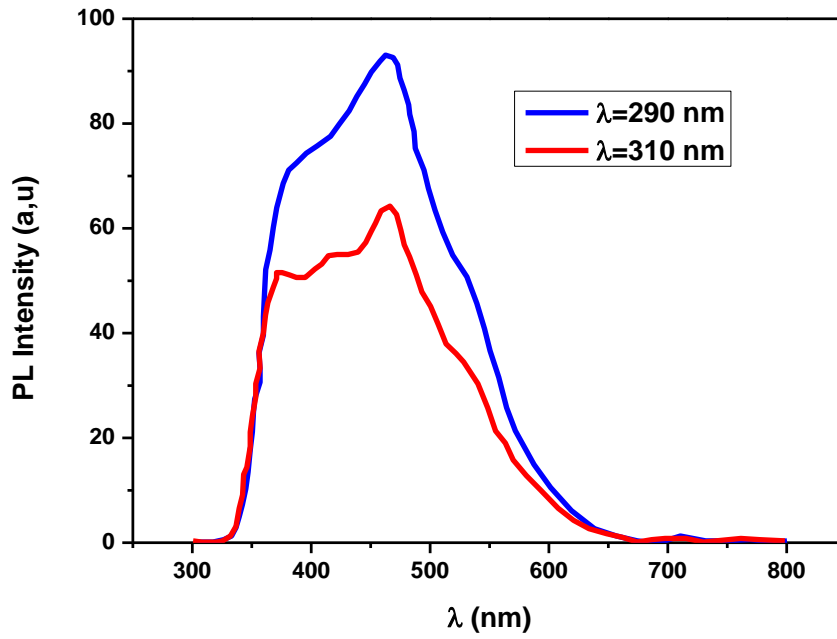


**Figure 01:** PL spectra of SiC nanoparticles excited with different wavelength



**Figure 02:** (a) Schematic of a solar cell with a luminescent down-shifting (LDS) layer on top; (b) Sketch of the photoluminescence process inside the LDS layer: the energy of a blue photon is absorbed by an electron and partly lost due to phonon emission. Subsequently, a lower-energy photon is emitted.

## POSTER SESSIONS

**Id-1380**

### **Mass Spectrum of Charmonium and Bottomonium Mesons Using an Energy-Dependent Potential and the Quantum Supersymmetry**

Elhadj Hocine<sup>1</sup>, Rabia Yekken<sup>2</sup>

Corresponding author: hocineelhadj@gmail.com

**Abstract:** Wave equations with energy-dependent potentials are well known in physics. They appear both in relativistic and non-relativistic quantum mechanics, also were used largely in particle, nuclear and atomic physics. More recently, a great interest has been brought to this type of potentials in non-relativistic quantum mechanics. Their presence in the Schrödinger wave equation generates a reformulation of the probability density to ensure the conservation of the continuity equation. Consequently, several implications related to the modification of the usual rules of quantum mechanics have been generated, in particular that of the scalar product.

In order to solve analytically the resulting wave equation, we use the Hamiltonian factorization method known by quantum supersymmetry (SUSYQM). It makes it possible not only to propose an exact solution to the problem in consideration, but also to reveal new analytically affordable potentials.

In the present work, we are interested in the study of the mass spectrum of Charmonium and Bottomonium mesons in the case of an energy-dependent interaction, using quantum supersymmetry method. We compare the obtained results with the available experimental data.

## POSTER SESSIONS

Id-1385

### Thermal, Physicochemical and Rheological Properties of Biobased Plasticizers Combinations used in Poly (Vinyl Chloride)

Boussaha Bouchoul<sup>1</sup>, Mohamed Tahar Benaniba<sup>2</sup>

<sup>1</sup>Research Center in Industrial Technologies CRTI, P.O. Box 64, Cheraga 16014, Algiers, Algeria.

<sup>2</sup>Laboratory of Multiphase Polymeric Materials (LMPMP), Process Engineering Department, Faculty of Technology, Université Ferhat Abbas-Setif1, 19000 Setif.

Corresponding author: b.bouchoul@crti.dz

**Abstract:** Fundamentally, Poly (vinyl chloride) (PVC) should be processed with various additives such as thermal stabilizers, plasticizers, lubricants, fillers ...etc. Plasticizers are mainly used to modify the polymer chain flexibility and the glass transition temperature (T<sub>g</sub>). Plasticizers based on phthalates as diethyl hexyl phthalate (DEHP) are most widely used in PVC. Unfortunately, these petroleum-based plasticizers reveal negative environmental and health effects. As an objective to substitute these dangerous products, the present study evaluates the performance of bio-based plasticizers combinations in polyvinylchloride (PVC). For this purpose, two natural secondary plasticizers were synthesized by the sunflower oil epoxidation reaction and the esterification of epoxidized sunflower oil to obtain epoxidized sunflower oil (ESO) and epoxidized sunflower oil methyl ester (ESOME) respectively. These new products were combined with two other primary bio-based plasticizers which are di-ester isosorbide (DEI) and acetyl tributyl citrate (ATBC). The formulations are prepared by mixing plasticizers combination and other additives with PVC resin. Then, blends are mixed and heated; films of plasticized PVC are obtained. Several techniques such as thermogravimetric analysis (TGA) in isothermal mode, internal mixer test and light transmission have been used to study the thermal, physicochemical and rheological properties in order to search for a synergism of properties between these combinations of plasticizers.

According to thermo gravimetric analysis, formulations which contain ESO or ESOME have minimal weight losses. Therefore, the incorporation of these secondary plasticizers into the plasticizer system improves the thermal stability of the PVC blends, better than the DEI or ATBC alone and even better than DEHP. The results of the internal mixer show that the thermal stability improves with the increase of the rate of ESO or ESOME. This confirms the results of TGA. The light transmission test shows that the incorporation of the ESO or the ESOME leads to a difference in transparency, where the transmission of light decreased with the increase of the rate of the latter in the plasticizer system. In conclusion, the mixtures of ESO and ESOME with DEI and with ATBC derived from renewable resources, show plasticization efficiency and can be applied as alternative plasticizers for conventional plasticizers based on a fossil source.

**Keywords:** Polymer, PVC, Biobased plasticizers combinations, Sunflower oil, Thermal stability.

## POSTER SESSIONS

**Id-1386**

### **Analytical and Numerical Analysis of Twin Helical Spring With Circulaire Cross Section**

Nacera Benghanem<sup>1</sup>, Abdelhamid Becheur<sup>1</sup>, Karim Rezouali<sup>1</sup>

<sup>1</sup>Laboratoire de Physique Théorique, Faculté des Sciences Exactes, Université de Bejaia, 06000 Bejaia, Algérie

Corresponding author: benghanem@yahoo.fr

**Abstract:** The filaments of incandescent halogen lamps are often considered as indispensable elements in the lighting industry. They consist in a tungsten wire wound in a structure configured either in simple, twin or triple helical spring shapes (THS and TRHS). Under function, the combined effects of the high temperature and their own weight, induce that the filament creeps by becoming plastically deformed in a permanent and a continuously manner until the rupture. This is the cause of early mortality of a considerable number of lamps. The design and verifications of such complex structures (twin and triple) can be carried out either analytically either numerically by finite element method. However, the behaviour of THS and TRHS filaments seem to be more complex to be studied by the theoretical methods. On the other hand, the finite element simulations allow not only to obtain several behaviour law responses of the filament but also stress distributions are provided in each cross section of the wire. For the present paper, we will limit ourselves to the twin helical spring numerical analysis that will be completed in some cases by analytical results.

**Keywords:** circular cross section, twin helical springs, own weight, temperature effect, inclination with gravity, finite element simulation

## POSTER SESSIONS

Id-1411

**Influence of cholesterol on the physico-chemical properties of phospholipid membranes**Nelly Drinova<sup>1</sup>, Julia Genova<sup>1</sup>, Hassan Chamati<sup>1</sup>, Minko Petrov<sup>1</sup><sup>1</sup>Institute of Solid State Physics, Bulgarian Academy of Sciences, Sofia, Bulgaria

Corresponding author: n\_drinova@issp.bas.bg

**Abstract:** Phospholipids are the building blocks of biological membranes. Due to their amphiphilic structure they form bilayer structures into which various functional constituents (proteins, cholesterol, hydrocarbons, etc.) are being incorporated. SOPC (1-stearoyl-2-oleoyl-sn-glycero-3-phosphocholine) is a synthetic phospholipid that resembles the natural egg yolk lecithin and is widely used for experiments with model lipid systems and liposomal drug delivery applications.

One of the primary roles of cholesterol in the biological cell is to modulate the physical properties of the bilayer phospholipid membrane. The effect of cholesterol on the properties of the lipid structure is strongly dependent on its concentration. The presence of cholesterol in the membrane is vital for the cell's adaption to changes in the environmental temperature. Incorporation of cholesterol in membranes induces diverse changes in the bilayer properties, including alteration of the bilayer thicknesses and changing in lipid order.

The structural properties of the lipid membranes are studied using Fourier transform infrared (FT-IR), polarization micro-Raman spectroscopies and Scanning electron microscopy (SEM) aiming to discover the specific physical characteristics of the doped with cholesterol lipid membrane in a wide range of concentrations (0- 50 mol%). Differential scanning calorimetry studies of SOPC/cholesterol mixtures in the above mentioned concentration range are performed to trace the influence of cholesterol on the phase behaviour of the phospholipid bilayer. The analysis of the far FT-IR spectra shows that hydrogen bonds exist between the hydroxyl group of cholesterol and the phosphate head group of phospholipid. Besides the trivial H-O hydrogen bond, the complex hydrogen bonds involving C and N elements in the complex bilayer membrane is detected. The evaluation of the standard physical parameters, like enthalpy, energy, entropy and strength of the hydrogen bonds (responsible for the bilayer structure and function modification) gives us possibility to apply molecular dynamic simulation for assignment of the new physical and structural characteristics of the complex lipid membrane.

Thermally induced shape fluctuations of giant quasi-spherical lipid vesicles are used to study the influence of the cholesterol, incorporated in the lipid membranes, on the bending elasticity modulus of the lipid membrane. The dependence of the bending elasticity modulus on the concentration of cholesterol in the lipid membrane is obtained in a same interval of concentrations as the DSC and FT-IR and Raman spectroscopy. At low concentration of cholesterol in the SOPC membrane (10 mol %) a decrease of the bending elasticity modulus is observed, compared to pure SOPC membrane. At high cholesterol content (50mol% and above) a twofold increase of the bending modulus is obtained.

**Keywords:** DSC and FT-IR and Raman spectroscopy, SEM, cholesterol, phospholipid membranes

**Acknowledgements** The authors acknowledge support from the Ministry of Education and Research, Bulgaria (National Science Fund, Grant DN 08-02/2016).

## POSTER SESSIONS

Id-1413

### Physico-chemical Study of Lipid Membranes, Containing Functionalized and Non-Functionalized Single Wall Carbon Nanotubes

Julia Genova<sup>1</sup>, Nelly Drinova<sup>1</sup>, Hassan Chamati<sup>1</sup>, Minko Petrov<sup>1</sup>, Peter Rafailov<sup>1</sup>

<sup>1</sup>Institute of Solid State Physics, Bulgarian Academy of Sciences, Sofia, Bulgaria

Corresponding author: julia.genova@issp.bas.bg

**Abstract:** Studies of carbon nanotubes, inserted in phospholipid bilayers show that the nanotubes affect the local structure and dynamic properties of biomembranes, as well as their toxicity and ability to promote trans-membrane channel formation depending on their size, shape, and surface modification. However the dominant forces of the influence of these structures on the conformational states and functions of biomembranes remain not clarified.

The main goal of our study is the investigation of the thermal and conformational structure characteristics of 1-stearoyl-2-oleoyl-sn-glycero-3-phosphocholine (SOPC) phospholipid at variation of the pristine (nonfunctionalized) and amide functionalized single walled carbon nanotubes (SWCNTs) in various concentrations. For that purpose we use the methods differential calorimetric analysis and Fourier transform Infrared (FT-IR) spectroscopy. In the present work we study the influence of incorporated in the membrane nanotubes (pristine or amide functionalized SWCNTs) on the phase transition temperatures and enthalpies of SOPC phospholipid and discuss the possible physical mechanism driving the energetic and structural states of the bio-nano-composites.

The results of our study show that the addition of non-functionalized and functionalized SWCNTs (0.5 - 1mg) sufficiently increase the  $A_{C=O\text{bonded}}/A_{C=O\text{free}}$  ratio. A further increase in SWCNTs content, however, showed a minor influence on the population of H-bonded C=O conformers ( $A_{C=O\text{bonded}}$ ). We found that embedded in the phospholipid functionalized SWCNTs promote hydrogen bonding with C=O carbonyl group of the polar –apolar interface of the membrane, detach the gel  $L_{\beta}$  and  $L_{\alpha}$  liquid crystal phases and depress the intermediate temperature range. Such a phenomenon gives us possibility to control the effect of the van't Hoff enthalpy and control the  $L_{\beta}$ - $L_{\alpha}$  phase transition. Our DSC analysis indicated a novel effect: gel-liquid crystal phase transition driven by van't Hoff enthalpy, pointing to an intermediate, partially cooperative phase transition.

**Keywords:** Fourier transform Infrared spectroscopy (FT-IR), Lipid Membranes, Single Wall Carbon Nanotubes

**Acknowledgements:** The authors acknowledge support from the Ministry of Education and Research, Bulgaria (National Science Fund, Grant DN 08-02/2016).

## POSTER SESSIONS

**Id-1414**

### **The Transfer of Charges in Composite Cellulose-Mineral Oil-Water Nanoparticle**

Konrad Kierczynski<sup>1</sup>

<sup>1</sup>Department of Electrical Devices and High Voltage Technology, Lublin University of Technology, 38a,  
Nadbystrzycka Str., 20-618 Lublin, Poland

Corresponding author: k.kierczynski@pollub.pl

**Abstract:** The study investigated the DC conductivity of cellulose impregnated with insulating oil with different moisture content. Cellulose materials are often used as a solid component of paper-oil insulation of power transformers. In paper it was found that dependence of conductivity on the moisture is far stronger than linear dependence described in ion conductivity models. In this paper it was clearly demonstrated that in damp pressboard impregnated with insulation oil DC conductivity is determined by the moisture and occurs due to hopping (tunnelling) of electrons. The result opens opportunity to determine the problem of the level of humidity in oil impregnated cellulose.

In studies, the results are presented in this paper, used the electrical pressboard production company Weidman with a thickness of 1 mm. This sample was dried in a vacuum chamber for 72 hours at 80 °C. Next, pressboard was saturated with humidity from free air, and thus overlap with the increase in its mass. After obtaining the set moisture value pressboard immersed in insulating oil to the impregnation. The time of the impregnation process was about 6 months.

PDC method (Polarization Depolarization Current) was used for the study on the measurement stand. Three-electrode measurement system with a sample of pressboard is placed in the climatic chamber. In the work was calculated the average number of water molecules in nanodrop, which amounts to  $n \approx 220$ . Diameter of those nanodrops is around 1.5 nm. Our experiments show that in environment of cellulose impregnated with insulating oil, water creates nanodimensional clusters – nanodrops.

## POSTER SESSIONS

**Id-1415**

### **Thermo-gravimetric Analysis of $(\text{FeCoZr})_x(\text{CaF}_2)_{(100-x)}$ Nanocrystalline Layers**

Tomasz Koltunowicz<sup>1</sup>

Department of Electrical Devices and High Voltage Technology, Lublin University of Technology, 38a,  
Nadbystrzycka Str., 20-618 Lublin, Poland

Corresponding author: t.koltunowicz@pollub.pl

**Abstract:** In this paper thermos-gravimetric analysis (DTG/DSC) result for samples of nanocomposite metal-dielectric  $(\text{FeCoZr})_x(\text{CaF}_2)_{(100-x)}$  with different metallic phase content  $x$  are presents.

The analysis showed that the mass of the nanocomposite changes into two stages. In the first stage, starting from 25°C and up to approx. 400°C, the mass gradually decreases from the 25.19 mg to the 24.47 mg. This is related to the evaporation of moisture and other volatiles from the surface of the sample that settle on it during storage. In the second stage, a rapid increase in mass begins and achievement maximum value of over 29 mg, almost 16% more than weight of the dried sample. This is related to the oxidation of the metallic phase particles by the oxygen that diffuses into the layer from the air.

Annealing of samples of the nanocomposite  $(\text{FeCoZr})_x(\text{CaF}_2)_{(100-x)}$  while getting higher temperatures causes, initially, the formation of oxide layers on the surface of the metallic phase nanoparticles, then leads to their increasing oxidation until complete oxidation. At the same time, the number of oxygen atoms per atom of the metallic phase increases.

A structural-phase model of the state of nano-grain layers after high-temperature treatments was proposed. The model assumes that there are three types of nanoparticles in the nanocomposite. The first of these are nanoparticles from a metal alloy, the second is a metallic phase nanoparticle with the coating of oxides of these metals on the surface and the third type – completely oxidized nanoparticles of the metal phase.

## POSTER SESSIONS

Id-1416

## Influence of Thermal Treatment on the Electric Properties of the Nanocomposite on the base of Ferromagnetic Alloy FeCoZr and Dielectric Matrix CaF<sub>2</sub>

Vitali Bondariev<sup>1</sup>

<sup>1</sup>Dept. of Electric Devices and High Voltage Technology, Lublin University of Technology, 38a, Nadbystrzycka Str., 20-618 Lublin, Poland

Corresponding author: v.bondariev@pollub.pl

**Abstract:** To study the effect of annealing on the electrical properties the sample of the nanocomposite (CoFeZr)<sub>x</sub>(CaF<sub>2</sub>)<sub>1-x</sub> with metallic phase content produced by ion sputtering with beam of argon and oxygen was selected. The analysis was made on the basis of frequency-temperature dependences of the conductivity  $\sigma(f, T)$ . Studies carried out by stand to measuring of AC electrical properties of nanocomposites and semiconductors. The measurements have been performed using alternating current within the frequency range of 50 Hz – 1 MHz for measuring temperatures ranging from 77 K to 373 K. Each time, immediately after completing the measurements, the sample was subjected to 15-minute isochoric heating in a tubular furnace in atmospheric air, starting from 398 K to 773 K with a step of 25 K.

For the nonannealed sample, it was observed that the conductivity  $\sigma$  almost does not change its value in the whole frequency range (Fig. 1a). After annealing at  $T_a = 598$  K, the conductivity changes its value and decreases by 4 orders of magnitude at lower frequencies (Fig. 1b). But as the frequency increases, its value increases and reaches similar values as for the sample before annealing.

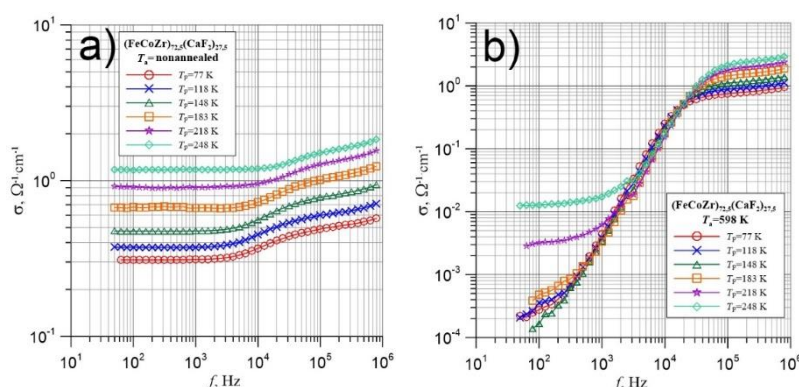


Fig. 1. Frequency dependence on the conductivity  $\sigma$ : a) nonannealed sample, b) annealing temperature  $T_a = 598$  K for nanocomposite (CoFeZr)<sub>72.5</sub>(CaF<sub>2</sub>)<sub>27.5</sub> obtained in the atmosphere Ar and O<sub>2</sub> for selected measuring temperatures  $T_p$

Lowering the value  $\sigma$  after annealing at 548 K can be caused by the oxidation of the surface of the nanoparticles of the metallic phase during the diffusion of oxygen from the air.

**Keywords:** Thermo-gravimetric analysis; nanocomposites, thin layers, electrical properties

## POSTER SESSIONS

**Id-1417**

### **Quantum Supersymmetry Applied to a Linear Energy Dependent Potential: Projection Method**

Rabia Yekken<sup>1</sup>, Elhadj Hocine<sup>1</sup>

<sup>1</sup>Département de Physique Théorique, Faculté de Physique, Université des Sciences et de la Technologie Houari Boumediene, BP. 32 El-Alia, Bab-Ezzouar, 16111 Alger, Algeria.

Corresponding author: rabia\_yek@yahoo.fr

**Abstract :** We are interested by applying the quantum supersymmetry method “SUSYQM” to a non linear Hamiltonian  $H_n(x, E_n)$  in  $1D$  dimensional space. We consider the class of potentials with a coupling constant depending linearly on energy. After the transformation of  $H_n(x, E_n)$  into an equivalent linear Hamiltonian  $\tilde{H}(x)$ , the corresponding transformed potential is energy independent and non-local because it contains a derivative component.

The correlation between energy dependent potential and non-local one, allows us to extend the supersymmetry rules to a specific class of non-local potentials. The projection of the obtained results in the functional space of the starting Hamiltonian,  $H_n(x, E_n)$ , leads to an another appropriate SUSYQM formalism. The corresponding superpotential and factorization partner operators achieved depend only on the ground state data. The application of this method gives a general and a simple supersymmetric solution for both partner potentials generated in each case.

**Keywords:** Quantum mechanics, Quantum supersymmetry, energy-dependent potentials

## POSTER SESSIONS

**Id-1420**

### **Structural and Optical Study of Thin Films Based on Metal Oxide Nanocomposites ZnO-TiO<sub>2</sub> and NiO-TiO<sub>2</sub>**

Hacene Serrar<sup>1,2</sup>, Yacine Bouachiba<sup>2,3</sup>, Adel Taabouche<sup>2,4</sup>, Abderahmane Bouabellou<sup>2</sup>

<sup>1</sup>Research Center in Industrial Technologies CRTI B.P. Box 64, Cheraga16014 Algiers, Algeria

<sup>2</sup>Thin Films and Interfaces Laboratory, University of Constantine1, 25000 Constantine, Algeria

<sup>3</sup>Department of Materials Science Engineering, National Polytechnic School of Constantine, Nouvelle Ville  
Universitaire Ali Mendjeli, Algeria

<sup>4</sup>Faculty of Hydrocarbons and Renewable Energies and Earth and Universe Sciences, University Kasdi Merbah,  
30000 Ouargla, Algeria

Corresponding Author: h.serrar@crti.dz / serrarhacene@gmail.com

**Abstract:** In this work we have studied thin films based on metal oxides: TiO<sub>2</sub> / ZnO and TiO<sub>2</sub> / NiO. TiO<sub>2</sub> / ZnO and TiO<sub>2</sub> / NiO films are successfully prepared by the Sol-gel dip coating method. The layers obtained are characterized by several techniques such as; Raman techniques, m-lines and UV-visible. Raman spectra show that the TiO<sub>2</sub> thin films are characterized by the vibration modes of the Anatase phase. ZnO and NiO induce the reduction of the Raman intensity of TiO<sub>2</sub> vibration modes. The Waveguiding results show that the introduction of ZnO and NiO into pure TiO<sub>2</sub> causes a decreasing refractive index profile. In the same way, the UV-visible analysis shows an increase in the optical band gap due to the Burstein-Moss effect. MB degradation results show that TiO<sub>2</sub> thin films are the best photocatalytic materials. TiO<sub>2</sub>: ZnO and TiO<sub>2</sub>: NiO (T7Z and T7N) are less active as photocatalytic materials, due to the screen effect and the effect of TiO<sub>2</sub> optical gap widening.

**Keywords:** Titanium Dioxide, Zinc Oxide, Nickel Oxide, Waveguiding, Photocatalysis, Sol Gel

## POSTER SESSIONS

Id-1429

## Dimension Effects in Insulating NbTiN Films

Maria Burdastyh<sup>1</sup>, Svetlana Postolova<sup>2</sup>, Alexey Mironov<sup>3</sup><sup>1</sup>Novosibirsk State University, 1 Pirogova Street, Novosibirsk, Russian Federation, 630090<sup>2</sup>Rzhanov Institute of Semiconductor Physics, 13 Lavrentiev Avenue, Novosibirsk, Russian Federation, 630090Institute for Physics of Microstructures of the Russian Academy of Sciences, GSP-105, Nizhny Novgorod,  
Russian Federation, 603950<sup>3</sup>Rzhanov Institute of Semiconductor Physics, 13 Lavrentiev Avenue, Novosibirsk, Russian Federation, 630090

Corresponding author: mburdastyh@gmail.com

**Abstract:** Superinsulating state emerging at the insulating side of the superconductor-insulator transition is a subject of an intense current attention. The characteristic features of a superinsulator are hyperactivated temperature dependence of the resistance, threshold-like current-voltage characteristics, and the peculiar magnetic field dependence of the resistance. It is believed that the superinsulating state is a state in which Cooper pairs are localized and the electrostatic potential of the charges is screened by the Bose condensate of vortices. A fundamental consequence of the Cooper pair localization is asymptotic freedom of Cooper pairs, i.e., disappearance of the confinement hence superinsulating properties on short spatial scales. Therefore, the experimental study of the evolution of superinsulator properties with the geometric characteristics of the system is required.

We investigate the electronic transport in disordered polycrystalline 10-nm NbTiN film as a function of the effective system size along the current direction. The film was obtained by the atomic layer deposition at temperature 350°C and was placed at the insulating side of the disorder-driven superconductor-insulator transition. The low-temperature measurements were carried out on the device comprising the parts of the same film but with different distances between measuring electrodes. We show that in a zero magnetic field the film demonstrates the main superinsulating features, and the reduction of the system effective size suppresses its insulating and superinsulating properties down to the quasi-metallic saturation of the resistance.

At  $T < 0.8$  K the temperature dependence of the resistance demonstrates hyperactivation growth with decreasing temperature when the distance between electrodes is large enough ( $L > 0.2$  mm). The measured current-voltage characteristics show threshold behavior. The current jumps become less sharp upon shortening the distance between the electrodes. The threshold voltage of I-V curves drops linearly during the decrease of the distance between the measuring electrodes, implying that the threshold electric field is independent on the distance between the electrodes. This linear dependence can be used for experimental measurement of the linear tension of the electric string binding Cooper pairs and anti-Cooper pairs in a superinsulator, e.g., we estimate the maximal energy barrier for charge separation.

We studied a set of NbTiN films grown by the atomic layer deposition method at a temperature of 350°C

The work on transport measurements at Novosibirsk is supported by Russian Science Foundation #18-72-10056. Analysis of the experimental data (V.M. Vinokur) are supported by the U.S. Department of Energy, Office of Science, Basic Energy Sciences, Materials Sciences and Engineering Division.

**Keywords:** Superinsulator, thin films, Cooper pair localization, current-voltage characteristic.

## POSTER SESSIONS

**Id-1436**

### **The Effect of Waste Frying Oil and Waste NBR on Physical Characteristics of Modified Bitumen**

Khedoudia Soudani<sup>1</sup>, Smail Haddadi<sup>1</sup>, El Diouher Bennour<sup>1</sup>

<sup>1</sup>LEEGO, Faculty of Civil Engineering, USTHB, ALGERIA

**Abstract:** The performance of the road pavements depends on the properties of the asphalt and the bitumen which are the only deformable components in the mixture. It has thermal susceptibilities and can become deformed due to weathering, moisture damage, heavy traffic, or embrittlement due to the chemical oxidation (bitumen aging) of functional groups within the asphalt. These limitations can be overcome as their performance characteristics significantly modified by modification with polymeric materials. Using virgin materials is not always possible because of its high cost. Pavement professionals are looking for a new material to strengthen the pavement to achieve economic gains by using waste materials with environmentally friendly consideration. In This study, waste industrial polymer (WNBR) and waste frying oil (WFO) are used as modifier. Different processing conditions were performed and various contents of the modifier were used separately in first, and then by association of the two wastes. Standard laboratory tests were carry out on the original and modified bitumen. It was found that the modifier tends to increase the softness of the bitumen which is preferred for the asphalt intended for hot weather regions like Algeria.

**Keywords:** Modified bitumen, Recycling, Thermal susceptibility, Waste frying oil, Waste NBR.

## POSTER SESSIONS

Id-1448

### Synthesis, Anti-inflammatory Activity of 3-Amino 6-Methoxyl 2-methyl quinazolin-4(3H)-One and 3-Amino 6-Methoxyl -2-methyl of 4H-benzo[d] [1,3]-Oxazine-4-one

Osarumwense Peter Osaradion<sup>1</sup>

<sup>1</sup>Department of Chemical Sciences, Ondo State University of Sciences and Technology, Okitipupa, Ondo State, Nigeria.

Corresponding Author: osaradion.peter@yahoo.com

**Abstract:** Quinazolinone derivatives represent one of the most active classes of compounds possessing a wide spectrum of biological activity. They are widely used in pharmaceuticals and agrochemicals. Looking to the medicinal importance of 4(3*H*)-quinazolinone, we report here the synthesis of a new class of heterocyclic molecules in which all of these moieties are present and try to develop potential anti-inflammatory molecules.

The objective of the present study was to synthesize these quinazolinone derivatives 3-Amino 6-Methoxyl 2-Methyl-4H-benzo[d]-[1,3]-Oxazin-4-one and 3-Amino-6-methoxyl-2—Methyl-3H-Quinazolin-4-One and screened them for their anti-inflammatory activity.

The condensation of 2-amino-methyl 5-dimethoxybenzoate with acetic anhydride yielded the cyclic compound 2-methyl 5-substituted-1, 3-benzo-oxazine-4-one which further produce a novel 2,3-disubstituted quinazolin-4 ones via the reaction with hydrazine hydrate. The compounds synthesized were unequivocally confirmed by means of Infrared, Nuclear Magnetic Resonance (<sup>1</sup>H and <sup>13</sup>C), Gas Chromatography Mass Spectrophotometer and Elemental analysis. The synthesized compounds were screened and evaluated pharmacologically for their in-vivo anti-inflammatory activity by the paw volume of each rat was measured before 1 and after 3 h of Carrageenan treatment with the help of a Plethysmometer.

Compound 1 displayed a singlet signal at:  $\delta$  3.78 attributed to methoxy group and singlet at  $\delta$  3.68 which was due to methyl group. Other singlets appeared at  $\delta$  7.16 and 6.40 attributed to aromatic protons. Also, <sup>1</sup>H NMR spectrum of compound 2 showed a characteristic signal at  $\delta$  2.56 (singlet) corresponding to methyl group and duplet at:  $\delta$  3.90 for methoxy group. Two singlets appeared at  $\delta$  7.41 and 7.10 attributed to aromatic protons. Another signal appeared at 5.80 which was attributed to the protons of the amino group. For the IR spectra. Compound 1 was characterized by absence of  $\nu$  NH<sub>2</sub> and presence of  $\nu$  C-O stretch in 1101 cm<sup>-1</sup> region of the compound. Compound 2 and 4 were characterized by absence of  $\nu$  C-O and presence of  $\nu$  NH<sub>2</sub> in 3301 cm<sup>-1</sup> and 3300 region of the compounds. compound 1, revealed signals at  $\delta$  16.95, 51.93 and 56.13 attributed to methyl and the two methoxy groups respectively, while the aromatic carbon atoms appeared between  $\delta$  values 100.05-168.28 with the carbonyl carbon atom appearing as the highest  $\delta$  value of 168.28. Similarly, compound 2 showed signals at  $\delta$  22.58, 56.63 and 56.80 attributed to methyl and the two methoxy groups respectively, while the aromatic carbon atoms appeared between  $\delta$  values 105.64-160.28, with the carbonyl carbon atom appearing as the highest  $\delta$  value of 160.28. The Compounds were screened for their Anti-inflammatory activity. These compounds

synthesized have a higher anti-inflammatory activity than acetylsalicylic acid, which is a standard analgesic drug.

Compound 2 has a higher Anti-inflammatory activity than Compound 1. These compounds synthesized have a higher anti-inflammatory activity than Indomethacin, standard anti-inflammatory drug.

**Keywords:** Anti-inflammatory activity, Quinazoline-4(3H)-One, 6-methoxyl 2-methyl 4H-benzo[d][1,3]-oxazine-4-One, Nucleophile, Synthesis, 3-Amino 6-methoxyl -2-Methyl Quinazolin-4(3H)-One.

## POSTER SESSIONS

**Id-1451**

### **Thermal Configuration Modeling of a mc-Si Ingot Growth Furnace for Photovoltaic**

Djamel Ouadjaout<sup>1</sup>

<sup>1</sup>Centre de Recherche en Technologie des Semi-conducteurs pour l'Energétique. CCPM division

Corresponding author: douadjaout@yahoo.fr

**Abstract:** Multicrystalline silicon (mc-Si) is the dominant material in photovoltaic owing to its interesting properties. Compared with other solar energy materials, mc-Si ingots grown via directional solidification are of higher quality. The ingot growth requires a careful control of a myriad of parameters during the process. The modeling of this type of problem is made particularly difficult because of the existence of non-linear phenomena, the problem of monitoring the solidification front, and finally the multi-scale nature of the crystal growth furnace. The present work study the process of elaboration of mc-Si ingots for photovoltaic. A numerical model is developed to understand the effect of heat transfer on solidification, and to quantify thermal losses in the experimental setup. The simulations carried out made it possible to visualize the structure of the convection movements in the melt phase, in order to determine their influence, to adjust the geometry of the furnace and to adapt the thermal gradients necessary for a stable directed growth, finally to contribute to the improvement of the material quality.

**Keywords:** MC-Silicon, Directional Solidification, Numerical Modeling

#### **References**

- [1]. D. Ouadjaout, Growth of mc-Si ingots for photovoltaic, 20th EUPVSEC (2005)
- [2]. J. Li, Y. Chen and R. Hong Modeling and optimization of the feedstock melting for industrial photovoltaic mc-Si ingot, *Solar Energy* 139 (2016) 108
- [3]. K. Moon, Growth of mc-Si by improved directional solidification process based on numerical simulation, *Sol. Energy Mat. Sol. Cells* 95 (2011) 3059
- [4]. Computational study of heat transfer on molten silicon during directional solidification for solar cells application, *Solar Energy* 139 (2016) 108
- [5]. G. Anbu Modeling on Modified Heater Design of DS System for Improving the Quality of mc-Si Ingot, *Silicon* (2018)
- [6]. T. Lin, Chung H. and C.-Y. Chen Numerical analysis of steady and transient processes in a directional solidification system, *Coupled Systems Mechanics*, Vol. 5, No. 4 (2016) 341-353

#### **Acknowledgments**

This work was realized in the frame of CMMO/CCPM research and development project.

This work is financially supported by the National Fund of Research FNR/CRTSE/DGRSDT

## POSTER SESSIONS

**Id-1470**

### **Electrochemical Oxidation of Glucose by Ni-Fe Nanoparticles Dispersed on Polyaniline Thin Films**

Delloula Lakhdari<sup>1,2</sup>, Abedarrahim Guittoum<sup>2</sup>, Nassima Benbrahim<sup>3</sup>, Ouafia Belgherbi<sup>1</sup>, Nadjem Lakhdari<sup>4</sup>

<sup>1</sup>Research Center in Industrial Technologies CRTI, P.O. Box 64, Cheraga 16014, Algiers -Algeria.

<sup>2</sup>Nuclear Research Centre of Algiers, 2 Bd Frantz Fanon, Bp 399, Alger-Gare, Algiers, Algeria.

<sup>3</sup>Laboratoire de physique et chimie des matériaux, Université Mouloud MAMMERY de Tizi-Ouzou

<sup>4</sup>National School of Biotechnology "Toufik Khaznadar" University City Ali Mendjeli, BP E66 25100. Constantine - Algeria

Corresponding author: d.lakhdari@crti.dz

**Abstract:** In this work we describe the electrodeposition of Ni–Fe nanostructures on polyaniline (PANi) as templates. The conditions and parameters influence in the morphology and electrochemical activity of the electrodeposited of Ni–Fe nanoparticles. The electrocatalytic properties of Ni–Fe polyaniline-modified electrode toward the glucose oxidation were analyzed via cyclic voltammetry and amperometry. The studies showed that Ni–Fe /PANi electrode displayed the highest electrocatalytic activity, attributed to the high density of Ni–Fe nanoparticles deposited on the polyaniline vibreuse nanotubes support. A low detection limit of 0.5  $\mu$  M glucose with a good sensitivity of 539,78  $\mu$ A mM<sup>-1</sup> cm<sup>-2</sup> was obtained for electrochemical detection at Ni–Fe deposited on PANI /FTO.

**Keywords:** Ni–Fe nanoparticles, Glucose, Polyaniline, Cyclic Voltammetry, Electrocatalytic Oxidation

## POSTER SESSIONS

**Id-1470**

### **Anti-icing Property of Nano-ZnO Superhydrophobic Surface Prepared via Radio Frequency Magnetron Sputtering on Aluminum Alloy**

Guoyong Liu<sup>1</sup>, Yuan Yuan<sup>1,2</sup>

<sup>1</sup>State Key Laboratory of Power Transmission Equipment and System Security and New Technology, Chongqing University, Chongqing, China

<sup>2</sup>School of Material Science and Engineering, Chongqing University, Chongqing, China

Corresponding author: yuany@cqu.edu.cn

**Abstract:** Ice accumulation on transmission lines may lead to disastrous consequences for power system. Superhydrophobic (SHP) surface has promising application in anti-icing field. In this work, ZnO SHP surfaces were prepared on aluminum alloy by radio frequency (RF) magnetron sputtering. The Morphology, structure, wettability, and chemical composition of the SHP surfaces were investigated by using corresponding methods. The anti-frosting/anti-icing performance of the ZnO SHP surface was investigated. It's indicated that sputtering time from 5 min to 30 min affected the morphology and roughness of the ZnO SHP surface. The contact angle of as-prepared SHP surface is more than 160°. The anti-frosting/anti-icing results shows that the rough structure compose densely gathered nanoclusters exhibited great anti-frosting/anti-icing property due to the superhydrophobicity and self-transfer behavior of condensed micro-droplets. The freezing of water droplet was delayed for about 2 h, frosting was delayed for approximately 5.5 h at the temperature of -10 °C. A structure with large undulation and pore space reduced the anti-frosting/anti-icing property of the SHP surface. This work provides direction for the design and preparation of anti-icing surfaces for power transmission lines.

**Keywords:** Anti-icing, Superhydrophobic, anti-icing, ZnO nanoclusters

## POSTER SESSIONS

**Id-1472**

### **Effect of Concentration (molarity) on ZnO Properties**

Fayssal Boufelgha<sup>1</sup>, Abderrahmane Bouguelout<sup>1</sup>, Rahima Zellagui<sup>1</sup>, Haydar Dehdouh<sup>1</sup>, Nouredine Brihi<sup>2</sup>,  
Abdelhamide Bouaine<sup>2</sup>

<sup>1</sup> Research Center in Industrial Technologies CRTI, P. O. Box 64, Cheraga 16014, Algiers, Algeria

<sup>2</sup> Laboratoire de Physique de la Matière Condensée et Nanomatériaux (LPMCN), département de physique,  
Faculté des Sciences Exactes et Informatique, Université de Jijel, BP 98, OuledAissa, 18000 Jijel, Algeria.

Corresponding author: boufelghalem@yahoo.fr, f.boufelgha@crti.dz

**Abstract:** In the framework of the optimization of the zinc oxide (ZnO) thin film production conditions for photovoltaic applications, we studied in this work the effect of the molarity on the properties of the ZnO layers, in this framework we developed two solutions the first of a molarity of 0.2M / l and the second 0.4M / l. the RAMAN results show the appearance of ZnO-related vibration modes (formation of a ZnO structure), the SEM imaging shows a dense ZnO structure, the AFM characterization shows a roughness of the layers between 130 and 170 nm.

**Keywords:** Thin films, ZnO, RAMAN, SEM

## POSTER SESSIONS

Id-1491

### Calculation of Electromagnetic Radiation Absorption of a Small Conducting Inhomogeneous Cylindrical Particle Taking into Account the Isoenergetic Surface in the form of an Ellipsoid of Rotation for the Model of Fuchs Boundary Conditions

IRINA KUZNETSOVA<sup>1</sup>, DIMITRY ROMANOV<sup>1</sup>, ALEXANDER YUSHKANOV<sup>2</sup>

<sup>1</sup>Demidov Yaroslavl State University, Yaroslavl, 150000 Russia

<sup>2</sup>Moscow Region State University, Moscow, 105005 Russia

Corresponding author: romanov.yar357@mail.ru

**Abstract:** To obtain an analytical solution to the problem of the electric dipole section of the absorption of a small conducting inhomogeneous cylindrical particle taking into account the isoenergetic surface having the form of an ellipsoid of rotation for the model of Fuchs boundary conditions. A small conducting cylindrical particle of length  $L$  consists of a dielectric core  $R_1$ , surrounded by a shell of conductive material of radius  $R_2$ , placed in the field of a plane electromagnetic wave of frequency  $\omega$ .

To analyze the results, it is convenient to go to dimensionless parameters:

$F$  - dimensionless absorption cross-section is the ratio of the absorption cross-section of a particle to the absorption cross-section of a massive sample,

$x_0$  - the dimensionless radius of a particle is the ratio of the outer radius  $R_2$  of the particle to the free path,

$y_0$  is the dimensionless frequency of the incident electromagnetic wave is the product of the field frequency  $\omega$  on the relaxation time,

$K$  is the ratio of the inner radius of the conductive shell  $R_1$  to the outer radius  $R_2$ ,

$q_1$  - the reflectivity coefficient of the inner surface of the conductive shell,

$q_2$  - the mirror coefficient of the outer surface of the conductive shell.

The isoenergetic surface of some semiconductors (silicon, germanium) is approximated by an ellipsoid of rotation, the shape of which depends on the longitudinal  $m_{\parallel}$  and transverse  $m_{\perp}$  effective mass of charge carriers. We consider the dependence of the dimensionless absorption cross-section  $F$  on the dimensionless transverse effective mass  $k_{\perp} \sim m_{\perp}$  (fig. 1).

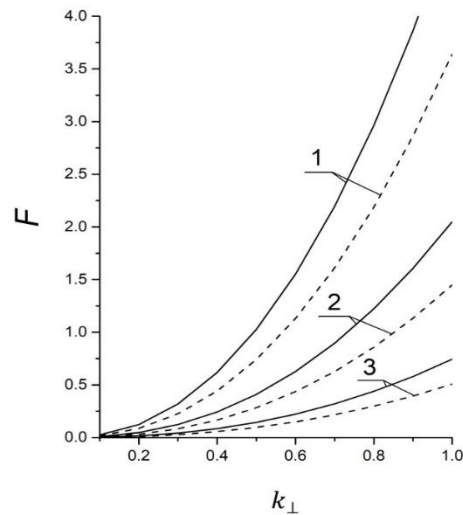


Figure 1 – Dependence of the dimensionless absorption cross section  $F$  on the dimensionless transverse effective mass  $k_{\perp}$  at  $x_0 = y_0 = 0.1$ ,  $q_1 = 0.5$ ,  $q_2 = 0.6$ . The solid, dotted curves correspond to the cases of degenerate semiconductor and non-degenerate semiconductor. Curves 1 –  $K = 0.1$ ; curves 2 –  $K = 0.6$ ; curves 3 –  $K = 0.8$ .

The dimensionless section increases with the growth of  $k_{\perp}$ , and the relative difference between degenerate and non-degenerate cases decreases. This is due to an increase in the velocity of the charge carriers along the particle axis and, consequently, a decrease in the intensity of the surface scattering of the charge carriers, i.e. the effect of surface scattering on the electrical conductivity and the absorption cross section decreases.

This study allows us to describe the optical properties of composite materials. The absorption cross-section spectrum can be used to determine the shape of an ellipsoidal isoenergetic surface of a semiconductor

**Keywords:** Kinetic Boltzmann equation, diffuse-mirror boundary conditions, absorption cross-section, inhomogeneous cylindrical conducting particle, ellipsoidal isoenergetic surface

**Acknowledgments:** The reported study was funded by RFBR, project number 19-31-27001.

## POSTER SESSIONS

**Id-1492**

### **The Lubrication Mechanism of Graphene as an Antiwear Additive at Elevated Temperatures**

Ning Kong<sup>1</sup>, Hongbo Li<sup>1</sup>, Jie Zhang<sup>1</sup>

<sup>1</sup>School of Mechanical Engineering, University of Science and Technology Beijing, Beijing 100083, China

Corresponding author: kongning@ustb.edu.cn

**Abstract:** In this work, the graphene was introduced as a novel antiwear additive into the polyphosphate, which was used to strengthen the existed lubricant for its high temperature application in the steel/steel friction pair. The tribological test, Raman spectroscopy, scanning electron microscopy (SEM) and X-ray photoelectron spectroscopy (XPS) were carried out to study the lubrication mechanism of the proposed lubricant with graphene additives. The results indicated even a small proportion of graphene can dramatically enhance the lubrication performance of the polyphosphate at elevated temperatures. Compared with dry sliding condition, the coefficient of friction and the wear were obviously held down while the surface quality of high temperature friction pair was enhanced effectively with the graphene strengthened polyphosphate lubricant. The detection of worn surfaces of both discs and balls was carried out by using SEM and the XPS was adopted to analyse the elemental distribution. The lubricant reacted with steel pair and inhibited the oxidation between contact interfaces due to the formation of tribofilm during the friction process. These enabled the lubrication mechanism of graphene as an antiwear additive to be understood at high temperatures. It will also contribute to expand the application area of graphene in the materials and mechanical field.

**Keywords:** Graphene; lubrication mechanism; elevated temperatures

## POSTER SESSIONS

**Id-1494**

### **Experimental Research Regarding the Decontamination of Toxic Compound Aqueous Solutions by Plasma Treatment**

Nicoleta Petrea<sup>1\*</sup>, Razvan Petre<sup>1</sup>, Tudor Viorel Tiganescu<sup>2</sup>, Gabriel Epure<sup>1</sup>, Claudiu Lazaroaie<sup>1</sup>, Andrada Pretorian<sup>1</sup>, Sorin Vizireanu<sup>3</sup>

<sup>1</sup>Scientific Research Centre for CBRN Defense and Ecology, Bucharest, Romania

<sup>2</sup>Military Equipment and Technologies Research Agency, Clinceni, Romania

<sup>3</sup>National Institute for Laser Plasma & Radiation Physics, Magurele, Romania

Corresponding author: nicoleta.petrea@yahoo.com

**Abstract:** This paper presents experimental laboratory research regarding the decontamination of aqueous solutions contaminated with toxic compounds like organophosphorous pesticides and organic dyes, using different types of plasma sources. The spreading of these compounds, used in the agriculture field and in different industries, affects the environment and creates long term problems. These compounds pollute the soil and water either because of their intentional use or their accidental propagation.

The organophosphorous pesticides are compounds with similar structures to those of neurotoxic warfare agents (GA, GB, GD, Vx), but are relatively less toxic than these. The dyes are organic compounds used in many industries: textiles, leather, plastics, rubber, drugs, some foods, etc.

Researchers from all around the world are concerned with finding effective and safe methods for destroying these toxic compounds, as well as for protecting the environment. Plasma-based decontamination is an unpolluting technology which acts as a two-step system: first as a detoxification reactor (the plasma arc), then as a decomposing reactor (as a burner or a catalytic oxidant).

**Keywords:** contaminated waters, organophosphorous pesticides, organic dyes, plasma sources

**Acknowledgements:** This work was supported by a grant of the Romanian National Authority for Scientific Research, CNDI-UEFISCDI project number PN-III-P1-1.2-PCCDI-2017-0637.

## POSTER SESSIONS

**Id-1495**

### **Testing the Sensitivity, Selectivity and Time of Response of Some Polymeric Sensors in the Presence of Toxic Compounds Vapours**

Nicoleta Grigoriu<sup>1\*</sup>, Constantin Nicolae Toader<sup>1</sup>, Tudor Viorel Tigănescu<sup>2</sup>, Gabriel Epure<sup>1</sup>, Claudiu Lazaroaie<sup>1</sup>,  
Nicu Scarisoreanu<sup>3</sup>, Cristian Vrespe<sup>3</sup>, Raluca Elena Gînghină<sup>1</sup>, Nicoleta Petrea<sup>1</sup>

<sup>1</sup>Scientific Research Center for CBRN Defense and Ecology, Bucharest, Romania

<sup>2</sup>Military Equipment and Technologies Research Agency, Clinceni, Romania

<sup>3</sup>National Institute for Lasers, Plasma & Radiation Physics, Magurele, Romania

Corresponding author: nico.grigoriu@gmail.com

**Abstract:** The paper presents the results of the testing of new sensors based on active composite materials obtained by matrix-assisted pulsed laser evaporation (MAPLE), SAW-type sensors having a quartz piezoelectric substrate. The sensors were subjected to the action of nerve agents simulants: Dimethylmethyl phosphonate (DMMP) and Diisopropyl methylphosphonate (DIMP).

**Keywords:** Chemical detection, surface acoustic wave sensor, MAPLE, nerve agents simulants, detection limit.

**Acknowledgements:** This work was supported by two grants of the Romanian National Authority for Scientific Research, CNDI-UEFISCDI, projects number PN-III-P1-1.2-PCCDI-2017-0637 and PN-III-P1-1.2-PCCDI-2017-0395.

## POSTER SESSIONS

**Id-1498**

### **Effect of *Streptomyces sp.* GBTUV5 on the Growth of *Solanum lycopersicum* (tomato)**

Fadime Ozdemir Kocak<sup>1,2</sup>, Dilek Unal<sup>3</sup>, Saadet Gizem Ertekin<sup>2</sup>, Ayten Kumas<sup>2</sup>, Levent Degirmenci<sup>2,4\*</sup>

<sup>1</sup> Department of Nursing, School of Health, Bilecik Seyh Edebali University, Bilecik, Turkey

<sup>2</sup> Biotechnology Application and Research Center, Bilecik Seyh Edebali University, Bilecik, Turkey

<sup>3</sup> Department of Molecular Biology and Genetics, Bilecik Seyh Edebali University, Bilecik, Turkey

<sup>4</sup>Correspondence: Department of Chemical Engineering, Bilecik Seyh Edebali University, Bilecik, Turkey

Corresponding author: levent.degirmenci@bilecik.edu.tr

**Abstract:** The aim of the study was to investigate the potential use of GBTUV5 strain as bio fertilizer, bio stimulator and bio controller. In order to reach this goal, experiments were designed as a series of tests conducted on the strain and plant trials were also conducted with seedlings inoculated with the strain. Indole acetic acid production (IAA), phosphate solubility, nitrogen fixation and caseinase activity tests were applied to strain in the course of study. Plant trials with tomato seedlings were conducted to observe the effect of strain on growth.

The strain indicated bio stimulation potential with positive results towards IAA production, and phosphate solubilization. Strain had also the potential to be utilized as biofertilizer due to its nitrogen fixing ability and caseinase activity. Biocontrol effect of the strain was validated by antifungal activity towards *Fusarium* wilt of tomato. These properties, all in one strain, was a seldom combination among microorganisms used as Plant Growth Promoting Bacteria (PGPB).

Plant trials conducted with soil (peat/vermiculite/perlite mixture) also indicated positive results due to evaluation of the increases in root and shoot dry/fresh weights and seedling vigor values compared to control. Nutrient uptake analyses of the plant indicated an increase in P uptake with inoculation. FT-IR analyses revealed enhancement of lipid biosynthesis. Consequently, a microorganism with fair chance of utilization as a PGPB was introduced to existing database.

**Keywords:** PGP, IAA, phosphate solubility, caseinase, *Fusarium* sp.

## POSTER SESSIONS

**Id-1499**

### **Experimental Research on the Response of a Sensory Detection Block in The Presence of Industrial Toxic Chemicals**

Grigoriu Nicoleta<sup>1\*</sup>, Tudor Viorel Tiganescu<sup>2</sup>, Gabriel Epure<sup>1</sup>, Nicoleta Petrea<sup>1</sup>, Marius Dumitru<sup>3</sup>, Constantin Nicolae Toader<sup>1</sup>, Raluca Elena Ginghina<sup>1</sup>

<sup>1</sup>Scientific Research Center for CBRN Defense and Ecology, Bucharest, Romania

<sup>2</sup>Military Equipment and Technologies Research Agency, Clinceni, Romania

<sup>3</sup>National Institute for Lasers, Plasma and Radiation Physics, Magurele, Bucharest, Romania

Corresponding author: nico.grigoriu@gmail.com

**Abstract:** The means of chemical detection devices are intended to identify toxic chemicals, which are in the atmosphere, in confined spaces or on different surfaces. They are effective means for both military conflicts and acts of terrorism or industrial accidents. The worldwide trend of developing high reliability and easy-to-handle devices that do not require very complex training is becoming more and more important.

The paper presents the experimental research regarding setting the response thresholds at different concentrations of the chemicals of a sensory configuration for air quality monitoring. The sensory block is composed of commercial sensors of "electromotive-force"/SnO<sub>2</sub> semiconductors/electrochemical, those are sensitive to carbon monoxide, ammonia, volatile organic compounds and combustion gases emitted by the functional engines on gasoline and diesel fuel base. The analog signals of the sensors are converted to digital information by the analog/digital converter of the Atmega 8 microcontroller used in the electronic circuit. Digital information is processed by the microcontroller according to the sensor characteristics curve and the calibration curve stored using the test procedures.

The chemical testing follows the steps: from the standard gas cylinder was collected a volume in a bag gas, from which was introduced with a special gas microsyringe an exactly volume into a test chamber, so the desired concentrations are obtained. The test chamber (of a volume of 100 liters) is equipped with temperature and humidity control systems, ventilation systems, as well as air inlet and outlet ports. The sensors were equipped with 4 keys corresponding to the detection thresholds, 3 LEDs and 1 buzzer to indicate the sensor status and to interact with the operator during the experiments.

The sensors block was tested for the action of CO, H<sub>2</sub>S and NH<sub>3</sub> (concentration in  $\mu\text{l}$  versus sensor response in mV) and the gas concentrations were established taking into account the limit value for the protection of human health (the maximum daily value of the average of 8 hours), according to the Following the experiments carried out on the chemical detection sensors, the truth tables have been constructed to detect the compounds on each sensor and alarm thresholds have been established. The alarm thresholds for the carbon monoxide are presented in table 1 and figure 1 shows the response of the sensor block sensitized by carbon monoxide at a concentration level of 1.7  $\mu\text{l}$  in the test chamber.

Table 1. The response of the sensors to different

CO ( $\mu$ l)	Sensors block					
	2600 (mV)	2602 (mV)	825 (mV)	2201D (mV)	2201B (mV)	4161 (mV)
Reference (no chemical)	0.060	0.039	0.063	0.026	0.819	0.011
0.2	0.069	0.039	0.101	0.026	0.819	0.011
0.5	0.070	0.056	0.134	0.026	0.819	0.011
1	0.071	0.057	0.189	0.026	0.819	0.011
1.7	0.176	0.136	0.235	0.026	0.819	0.011
2	0.198	0.165	0.345	0.026	0.819	0.011
2.5	0.230	0.189	0.543	0.026	0.819	0.011



Figure 1. Sensors' response corresponding to the CO concentrations

The sensors configuration can be adapted and optimized for the detection of different toxic chemicals and can be mounted on different platforms that have the purpose of monitoring the air quality in different spaces.

**Keywords:** Chemical detection, block sensors, air quality monitoring

**Acknowledgements:** This work was supported by two grants of the Romanian National Authority for Scientific Research, CNDI-UEFISCDI, project number PN-III-P1-1.2-PCCDI-2017-0637 and PN-III-P1-1.2-PCCDI-2017-0419.

**POSTER SESSIONS****Id-1504****Structural Acrylate Adhesive Joints for Civil Engineering Use**Klara Vokac Machalicka<sup>1</sup>, Miroslav Vokac<sup>1</sup><sup>1</sup>Klokner Institute, Czech Technical University in Prague

Corresponding author: klara.machalicka@cvut.cz

**Abstract:** Adhesives for structural applications have opened up new possibilities of using adhesive connections in civil engineering, e.g. in façade applications. Facades have to fulfil not only architectural requirements but there are also construction and material technology requirements, as well as functionality. Connections between substructure and façade cladding can be advantageously designed as an adhesive joint. In dependence on the particular application, adhesive bonding provides higher efficiency of workmanship in comparison with bolted connection and esthetical qualities, e.g. the smooth, flat surface of façade cladding without visual interruption of bolts. An important benefit of adhesive joints in facades is elimination of local thermal bridge in comparison with bolted connections and the possibility of stress peak reduction in dependence on adhesive and substrates stiffnesses and geometrical arrangement of the joint. Despite wide usage of relatively low strength and elastic silicone sealants for a long period of time in façades, there is a lack of information about semiflexible and semi-rigid adhesives with higher strength and reasonable elongation at break. The building facade is a very specific type of usage for adhesive connections due to the requirements on durability, strict geometrical imperfections and joining of unconventional materials often used in the façade design. The paper reports on an experimental analysis focused on determining the mechanical characteristics of two types of acrylate adhesives applied in double lap connection loaded by shear. The study comprises two basic substrate materials often used in facades both for cladding and for substructure – aluminium and galvanised steel. Both materials are applied with a smooth and mechanically roughened surface to compare adhesion in relation to laboriousness of surface preparation. Except for blank aluminium, anodized aluminium was also used. Material and surface treatment has a great influence not only on adhesion and hence strength of the joint but also on failure mode, behaviour and safety of a particular joint. Moreover, every necessary surface treatment creates higher labour intensity, higher time consumption and thus increased costs. Our results showed different behaviour of both chosen acrylate adhesives in spite of their similar chemical base. The first acrylate, two-part structural methacrylate, showed shear strength from 12 to 17 MPa in dependence on substrate material with shear strain between 0.6 and 1.2. The best adhesion was observed at roughened galvanized steel substrates. The second acrylate adhesive, two-part structural adhesive based on acrylic double performance polymer technology (ADP), proved shear strength from 8 to 9 MPa for aluminium substrates and less than 6 MPa for galvanized steel substrates. ADP adhesive also showed higher shear strain values (approx. 2.8). The experimental study proved that a choice of the adhesive has a great influence on mechanical properties of adhesively bonded joint as well as on adhesion to a particular substrate even in the case of the similar chemical base of adhesives.

**Keywords:** adhesive joint, acrylate, civil engineering, mechanical properties, adhesion, metalsubstrates

**POSTER SESSIONS****Id-1506****Estimation of Systematic Errors Committed When Approximating Length of Grain Boundaries Using Edges of Various Grid Patterns of EBSD Maps**Piotr Bobrowski<sup>1</sup><sup>1</sup>Institute of Metallurgy and Materials Science of Polish Academy of Sciences, 25 Reymonta Str., PL 30-059  
Kraków, Poland

Corresponding author: p.bobrowski@imim.pl

**Abstract:** The Electron Backscatter Diffraction (EBSD) is a widespread technique in Scanning Electron Microscopy (SEM) utilized for detailed microstructural characterization of crystalline materials. Apart from the analysis of common microstructural parameters such as crystallite size or crystallographic texture, it can also be used to detect boundaries between grains (GB) or phases, and to calculate their density. However, the choice of the method for detecting and drawing grain boundaries can noticeably influence the obtained results [1-3]. The current work is aimed at explaining the reason for the differences in the case of regular grid approach.

One of the most popular methods for detecting interfaces in EBSD maps is based on drawing boundaries between pixels which differ according to certain criterion (eg. phase or crystallographic orientation). However, grain boundaries approximated as segments of discrete mesh will tend to appear torn and wavy, and therefore, longer than they actually are. The average error for GB length overestimation was calculated for rectangular, hexagonal and kiskvadriille meshes, reaching values of 27.32%, 27.32% and 5.48%, respectively.

The calculations were confronted with experimental results. For this purpose, a 1x1 mm map of crystallographic orientation distribution was acquired from commercially pure copper sample (M1E grade). Subsequently, grain boundary networks were reconstructed basing on rectangular, hexagonal grid patterns, as well as the marching square approach.

For the possibly most accurate GB reconstruction basing on the EBSD data, a novel algorithm was developed. In principles it is similar to the approach utilized in the OIM Data Analysis software and joins triple points found in the EBSD map with straight lines which are subsequently divided into shorter sections for better resemblance of the real microstructure.

The comparison of the mathematical calculations with experimental results showed that the values of the average errors may be used as correction coefficients to adjust experimental results towards more accurate numbers.

**Acknowledgements:** The work was financed by the Polish National Science Centre upon decision 2015/19/D/ST8/00823.

**References**

- [1]. P. Bobrowski, M. Faryna, Z. Pędzich: Investigation of grain-boundary geometry and pores morphology in dense and porous cubic zirconia polycrystals, *Mater. Res. Bull.* 57 (2014) 203-209, <https://doi.org/10.1016/j.materresbull.2014.06.004>.

- [2]. P. Bobrowski, Z. Pędzich, M. Faryna: Three-dimensional microstructural characterization of porous cubic zirconia, *Micron* 78 (2015) 73-78, <https://doi.org/10.1016/j.micron.2015.07.004>.
- [3]. P. Bobrowski, M. Faryna, Z. Pędzich: Microstructural characterization of yttria-stabilized zirconia sintered at different temperatures using 3D EBSD, 2D EBSD and stereological calculations, *J. Mater. Eng. Perform.* 26 (2017) 4681-4688, <https://doi.org/10.1007/s11665-017-2794-4>.

## POSTER SESSIONS

**Id-1508**

### **Experimental Researches Regarding the Treatment of Industrial Wastewater Using Unconventional Techniques**

Raluca Elena Ginghina<sup>1</sup>, Dionezie Bojin<sup>2</sup>, Petrisor Iordache<sup>1</sup>, Tudor Viorel Tigănescu<sup>3</sup>, Iulian Vasile Antoniac<sup>2</sup>,  
Nicoleta Grigoriu<sup>1</sup>, Nicoleta Petrea<sup>1</sup>

<sup>1</sup>Scientific Research Centre for CBRN Defense and Ecology, Bucharest, Romania

<sup>2</sup>Politehnica University of Bucharest, Bucharest, Romania

<sup>3</sup>Military Equipment and Technologies Research Agency, Clinceni, Romania

Corresponding author: nicoleta.petrea@yahoo.com

**Abstract:** This paper presents the results of laboratory experimental research regarding the depollution of wastewater resulted from the leather industry, using a cellulosic adsorbent material.

Over the last decades, the large-scale discharge of untreated water from power plants, industrial installations, households and commercial waste has significantly increased the level of pollution in water bodies. Due to this fact, the water from fresh water sources has been affected by a high level of toxic chemicals, making it unsuitable for human consumption. An average of 80% of the global wastewater, which rises to 95% in some low-developed countries, is released into the environment without any treatment. Over the years, a traditional technique used for reusing the water, was to release the wastewater from industrial processes directed to the rivers, and downstream the diluted wastewater was treated and reused for municipal purposes.

In order to control the environmental pollution, the authorities in the field have increased the rigor of pollution prevention rules, and the local and national governments have made efforts to implement several policies favorable to recycling, including supporting markets for wastewater recycling and reusing, and the research and development of alternative / unconventional technologies. The market for wastewater treatment technologies it has, at the moment, a strong potential for growth and income generation.

**Keywords:** wastewater depollution, unconventional techniques, cellulosic adsorbent material

**Acknowledgements:** This work was supported by a grant of the Romanian National Authority for Scientific Research, CNDI–UEFISCDI project number PN-III-P1-1.2-PCCDI-2017-0637.

## POSTER SESSIONS

**Id-1513**

### **Statistic Model of Mobile Services Channel Power Density Estimation for RF Energy Harvesting**

Zhijian Liang<sup>1\*</sup>, Jie Yuan<sup>1</sup>

<sup>1</sup>Department of Electronic and Computer Engineering, Hong Kong University of Science and Technology, Clear Water Bay, Hong Kong

Corresponding author: zliangal@ust.hk

**Abstract:** RF energy harvesting provide power for various devices of perpetual operation without placement constrain and battery change. To ensure a reliable performance, the channel power density estimation is a key component for the optimized design of the RF energy harvesters. In this paper, we derive a statistic model of mobile services channel power density estimation for RF energy harvesting. The proposed model of kernel density estimation matches well with the measurement results and reveal the characteristic of the channel power density with detailed value. The measured total channel power of indoor is about 3.8  $\mu$ W and that of outdoor is about 35.6  $\mu$ W. The numerical analysis and strategy followed by modelling are useful for the RF energy harvesters design.

**Keywords:** Statistic model, channel power density estimation, RF energy harvesting, RF energy harvesters design.

#### **References**

- [1]. R. Dayal and L. Persa, "Low-power low-voltage AC–DC converters for electromagnetic energy harvesting with efficient indirect feedback scheme," *IET Power Electronics*, vol. 5, no. 9, pp. 1923-1933 (2012).
- [2]. J.A. Hagerty, F.B. Helmbrecht, W.H. McCalpin, R. Zane and Z.B. Popovic, "Recycling ambient microwave energy with broad-band rectenna arrays," *IEEE Trans.Microwave Theory Tech.*, vol. 52, no. 3, pp. 1014-1024 (2004).
- [3]. V. Kuhn, C. Lahuac, F. Seguin and C. Person, "A multi-band stacked RF energy harvester with RF-to-DC efficiency up to 84%," *IEEE Trans.Microwave Theory Tech.*, vol. 63, no. 5, pp. 1768-1778 (2015).
- [4]. C. Song, Y. Huang, J. Zhou, P. Carter, S. Yuan, Q. Xu and Z. Fei, "Matching network elimination in broadband rectennas for high-efficiency wireless power transfer and energy harvesting," *IEEE Trans.Ind.Electron.*, vol. 64, no. 5, pp. 3950-3961 (2016).

## POSTER SESSIONS

**Id-1520**

### **Viscoelastic Properties of Selected PVB Interlayers for Laminated Glass**

Miroslav Vokac<sup>1\*</sup>, Tomas Hana Klara<sup>1</sup>, Klara Machalicka<sup>1</sup>, Martina Eliasova<sup>2</sup>

<sup>1</sup>Klokner Institute, Czech Technical University in Prague

<sup>2</sup>Faculty of Civil Engineering, Czech Technical University in Prague

Corresponding author: miroslav.vokac@cvut.cz

**Abstract:** Laminated glass is a structural element used very extensively in the contemporary architecture. It is sought-after because of its transparency and its smooth reflective surface. When using laminated glass as a glass staircase, balustrades, transparent flooring, facades or even structural elements, it is advisable to consider the interaction of the individual glass panes in the cross-section. A conservative approach where glass pane shear interaction is not considered is uneconomical. The shear interaction of the glass pane layers depends on the properties of the polymeric interlayers used for lamination process. Various commercial products based on PVB (polyvinyl butyral), EVA (ethylene vinyl acetate), ionomer, or thermoplastic polyurethane (TPU) are used. Polymers stiffness depends on temperature and duration of a load. Interlayers exhibit the viscoelastic properties and temperature dependency described usually by the generalized Maxwell model and WLF model (Williams-Landel-Ferry). The parameters of these models are most effectively determined by Dynamic Mechanical Temperature Analysis (DMTA), where the material is cyclically loaded at different frequencies and temperatures.

Material parameters were found by DMTA for 2 types of PVB interlayers (Trosifol Extra Strong and Trosifol BG-R-20). In addition, experimental quasi-static loading tests were performed in shear at different loading rates and at various temperatures. The testing arrangement was as single lap shear test in both cases. The experimental stress-strain diagrams from static tests were compared with the theoretical diagrams derived from material parameters based on DMTA testing.

Although both materials are PVB-based, shear stiffness and temperature dependence are considerably different due to additives added to the PVB feedstock (usually Butvar). These considerable differences in material behaviour are very important because, in the design of glass constructions, the actual material properties have to be taken into account.

**Keywords:** Viscoelastic Properties, Laminated glass, Trosifol Extra Strong and Trosifol BG-R-20, PVB

## POSTER SESSIONS

**Id-1521**

### **Numerical Estimation of Nuclear Decay Heat from Induced Neutron Fission of $^{235}\text{U}$ and $^{239}\text{Pu}$**

Amir Al-Ramady<sup>1\*</sup>, Sherif Nafee<sup>1</sup>, Ahood Alshammary<sup>1</sup>

<sup>1</sup>King Abdulaziz University, Saudi Arabia

Corresponding author: ameerkamel@hotmail.com

**Abstract:** In this paper, Joint Evaluated Fission and Fusion (JEFF) Nuclear Data Library has been used to calculate the nuclear decay heat after a fission burst of both  $^{235}\text{U}$  and  $^{239}\text{Pu}$  for shutdown time up to  $10^5$  sec. This estimation is based on the numerical solution of the linear differential equations that describe buildups and decays of the fission products. The code was written in MATLAB, which is fast and easy-access, platform. The verification of the current code is carried out by comparing the numerical results with experimental well-known cases. Comparisons with the measurement results and the evaluated results using the Evaluated Nuclear Data File (ENDF) Nuclear Data Library, show the reliability of the current calculation.

**Keywords:** Fission yield, Nuclear Decay heat, and Nuclear Data Library

## POSTER SESSIONS

Id-1536

### Cu(I) Complexes Having Propionitrile and Pyridine Moieties: In-Vitro Biological Study

ZIYAD TAHA<sup>1\*</sup>, AHMED HIJAZI<sup>1</sup>, NISREEN ABUHAMAD<sup>1</sup>, WALEED MOMANI<sup>2</sup>

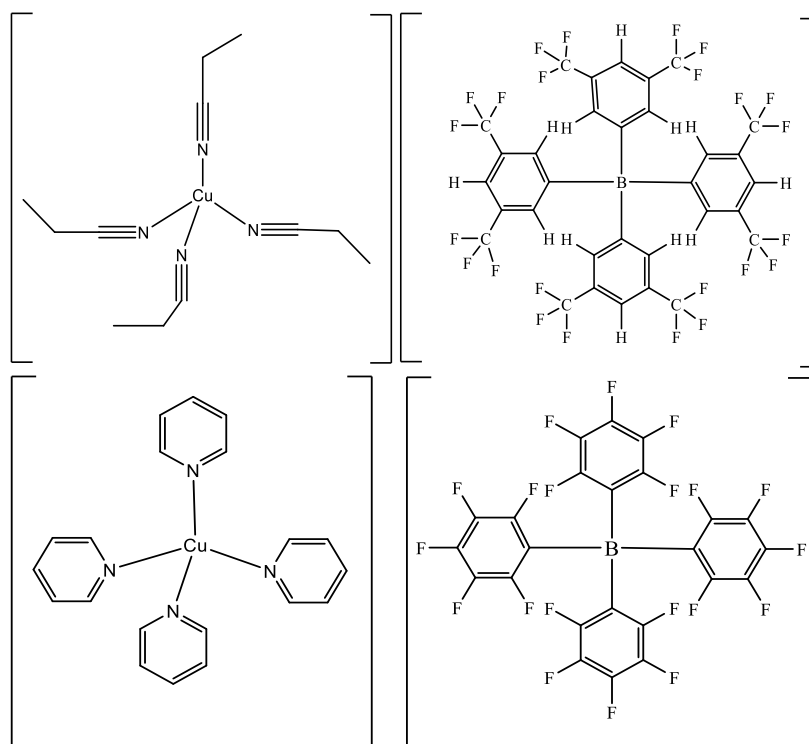
<sup>1</sup>Chemistry Department, Faculty of science and Arts, Jordan University of Science and Technology, Irbid, Jordan

<sup>2</sup>Department of basic Medical Sciences, Faculty of Medicine, Yarmouk University, Irbid, Jordan

Corresponding author: tahaz33@just.edu.jo

**Abstract:** Cu(I) complexes of general formula  $[\text{Cu}(\text{C}_2\text{H}_5\text{CN})_4][\text{A}]$  and  $[\text{Cu}(\text{C}_5\text{H}_5\text{N})_4][\text{A}]$  where A: counter anion =  $\text{B}(\text{C}_6\text{F}_5)_4^-$  and  $\text{B}\{\text{C}_6\text{H}_3(\text{m}-\text{CF}_3)_2\}_4^-$  have been synthesized from the reaction of CuCl and silver salt of the corresponding counter anion. The complexes were characterized in the solid state and in solution using elemental analysis, <sup>1</sup>H-NMR, <sup>11</sup>B-NMR, FT-IR Spectroscopy, UV-Visible spectroscopy and thermogravimetric analysis (TGA). The complexes can be obtained in good yields and are moderately sensitive to air. All complexes are used to study biological activities against different types of bacteria (Gram-negative and Gram-positive). Complex 4 showed the greatest activity of against *Proteus mirabilis* (Gram-negative) while complexes 2, and 3 showed the lowest activity against *Pseudomonas aeruginosa* (Gram-positive).

**Keywords:** Antimicrobial, weakly anions, bio-inorganic materials



## POSTER SESSIONS

Id-1537

### Biological Properties of Some Transition Metal(II) Complexes Having a Pyridine Moiety

Ahmed Hijazi<sup>1\*</sup>, Mohammad El-khateeb<sup>1</sup>, Noor Khwaileh<sup>1</sup>, Waleed Momani<sup>2</sup>

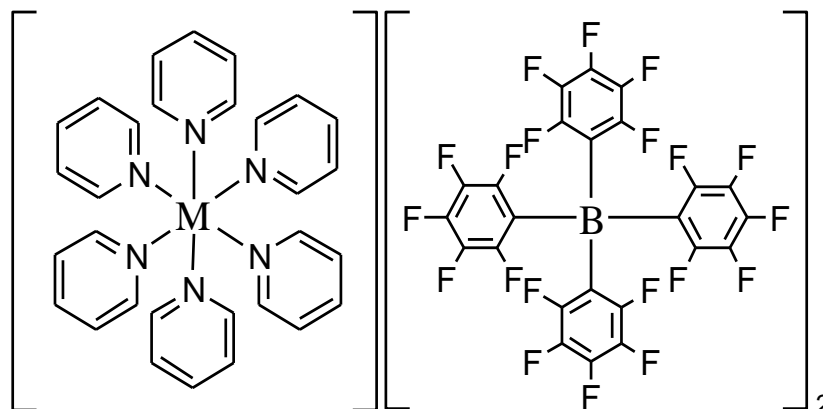
<sup>1</sup>Chemistry Department, Faculty of science and Arts, Jordan University of Science and Technology, Irbid, Jordan

<sup>2</sup>Department of basic Medical Sciences, Faculty of Medicine, Yarmouk University, Irbid, Jordan

Corresponding author: akhijazi@just.edu.jo

**Abstract:** Metal(II) complexes of the general formula  $[M^{II}(NC_5H_5)_6][B(C_6F_5)_4]_2$  where ( $M^{II} = Mn, Fe, Co, Ni, Cu, Zn$ ) have been synthesized by direct reaction of their metal halides and silver salt  $Ag[B(C_6F_5)_4]$ . The complexes were characterized in solid state and in solution using elemental analysis (EA), electron paramagnetic resonance (EPR), thermogravimetric analysis (TGA), ultraviolet-visible (UV-Vis) spectroscopy, <sup>11</sup>B-NMR, <sup>1</sup>H-NMR and fourier-transform infrared (FT-IR) spectroscopy. All complexes can be prepared and obtained in high yields and are moderately sensitive to air. The biological properties against different types of bacteria (gram-negative and gram-positive) were studied for all prepared complexes. Complex **6** showed the highest antibacterial activity against (*streptococcus pyogenes*) while complexes **3**, **5** and **6** showed the lowest activity against (*pseudomonas aeruginosa*, *eschereshia coli* and *klebsiella pneumonia*), respectively.

**Keywords:** Bio-inorganic materials, pyridine, WCA



## POSTER SESSIONS

**Id-1547**

### **Production of Enantioselective Alcohols by Phosphinite Ligands and Their Ruthenium(II) Complexes**

Khadichakhan Rafikova<sup>1,2</sup>, Alexey Zazybin<sup>1,2</sup>, Murat Aydemir<sup>3</sup>, Nermin Meric<sup>3</sup>, Cezmi Kayan<sup>3</sup>, Sholpan Islam<sup>2</sup>

<sup>1</sup>Kazakh-British Technical University, School of Chemical Engineering, Tole-bi 70, 05000, Almaty, Kazakhstan

<sup>2</sup>Satbayev University, School of Chemical & Biochemical Engineering, Satpayeva 22, 05000, Almaty, Kazakhstan

<sup>3</sup>University of Dicle, Department of Chemistry, Faculty of Science, Diclekent, 010205, Diyarbakir, Turkey

Corresponding author: hadichahan@mail.ru

**Abstract:** Novel optically pure phosphinite ligands were synthesized and their ruthenium complexes proved to be excellent catalyst for the enantioselective hydrogenation of ketones, affording products up to 99% ee.

An increasing number of chiral compounds and enantiomerically pure drugs are prepared through transition metal-catalyzed asymmetric reactions. Because hydrogen transfer reactions are mild techniques for reduction of ketones in which a substrate-selective catalyst transfers hydrogen between the substrate and a hydrogen donor or acceptor, respectively (donor (e.g. 2-propanol) and the acceptor (e.g. a ketone) are environmentally friendly [1]).

**Keyword:** catalysts, alcohols, phosphinite, complexes

**Acknowledgements:** Partial supports of this work by Project numbers: **FEN.17.019** and **FEN.17.023** and IRN: **AP05132833**, **BR05236800** is gratefully acknowledged.

#### **References**

- [1]. J.S.M. Samec, J.E. Backwall, P.G. Andersson, P. Brandt, Mechanistic aspects of transition metal-catalyzed hydrogen transfer reactions, Chem. Soc. Rev. 35 (2006) 237-248.

## POSTER SESSIONS

Id-1554

**Rheological Characterization of Hydrogel-like N, N, N-trimethyl Chitosan-Based Polyelectrolyte Complexes**Zuzana Bayerova<sup>1</sup>, Eva Cerna<sup>1</sup>, Marjan Marinsek<sup>2</sup>, Janez Carar<sup>\*2</sup><sup>1</sup>Brno University of Technology, Faculty of Chemistry, Purkynova 118, CZ-612 00 Brno, Czech Republic<sup>2</sup>University of Ljubljana, Faculty of Chemistry and Chemical Technology, Večna pot 113, SI-1000 Ljubljana, Slovenia

Corresponding author: janez.cerar@fkk.uni-lj.si

**Abstract:** Polysaccharide-based hydrogels are over the past few decades intensively studied for numerous practical applications, predominantly in the field of medicine and pharmaceuticals. In this study, we prepared several novel hydrogel-like materials based on N, N, N-trimethyl chitosan (TMC) and characterized them with regard to their rheological properties. Series of polyelectrolyte complexes being composed of TMC as a polycation and of different (poly)anions (polystyrene sulfonate, polyanethol sulfonate, alginate, 7 $\alpha$ -fullerenehexamalonate, 1-decanesulfonate, 1-octanesulfonate) were obtained by mixing 1% aqueous solution of N, N, N-trimethyl chitosan chloride and aqueous solution of a sodium salt containing the corresponding polycation. Precipitated polyelectrolyte complexes were centrifuged to obtain hydrogel-like material. Rheological properties of these hydrated precipitates were determined using Anton Paar MCR 302 rheometer. Strain amplitude sweep tests showed that in the linear viscoelastic (LVE) region the storage modulus ( $G'$ ) of all the studied samples was higher than the loss modulus ( $G''$ ); the ratio  $G'/G''$  being typically around 3. The shape of the curves was typical for concentrated microgel dispersions. In the absolute sense, the highest consistency of these hydrated polyelectrolyte complexes was found for TMC complexes with 7 $\alpha$ -fullerenehexamalonate, polyanethol sulfonate, and 1-decanesulfonate, respectively. Both the charge density and/or hydrophobic properties of the (poly)anion consisting polyelectrolyte complex contribute to increased consistency of these materials. Nevertheless, the absence of transitive increase of loss modulus at the high-end of the LVE region testifies that despite significantly higher values of  $G'$  than  $G''$  in the LVE region the samples do not behave as true physical hydrogels. This can be attributed to the lack of ability of these polyelectrolyte complexes to form a three-dimensional network. Examination of Scanning Electron Microscope micrographs of the freeze-dried samples confirmed poor ability of these polyelectrolyte complexes to establish consistent three-dimensional network over larger distances.

**Keywords:** Hydrogels, N, N, N-Trimethyl chitosan, Rheology, Polyelectrolyte Complexes

## POSTER SESSIONS

**Id-1556**

### **Ferromagnetism of two dimensional MoO<sub>3</sub> doped with Te**

Dong Jin Lee<sup>1\*</sup>, Sejoon Lee<sup>2</sup>, Deuk Young Kim<sup>1,2</sup>

<sup>1</sup> Quantum-Functional Semiconductor Research Center, Dongguk University, Seoul, Korea

<sup>2</sup> Department of Semiconductor Science, Dongguk University, Seoul, Korea

Corresponding author: jin514rin@naver.com

**Abstract:** Two dimensional Te doped MoO<sub>3</sub> nanoflakes( $\alpha$ -MoO<sub>3</sub>:Te) were prepared by vapor phase epitaxy assisted with e-beam evaporator. The  $\alpha$ -MoO<sub>3</sub>:Te nanoflakes revealed a strong Raman peak from the A<sub>g</sub> band, which represents a symmetric stretching mode of  $\nu(\text{Mo}-\text{O}_3-\text{Mo})$  along the a- axis of 2D-like ultrathin  $\alpha$ -MoO<sub>3</sub>:Te. Due to the intentional incorporation of smaller Te<sup>6+</sup> ions into bigger Mo<sup>6+</sup> sites, the pentacoordinated Mo<sup>5+</sup> ions and their corresponding VO defects were effectively formed in  $\alpha$ -MoO<sub>3</sub>:Te. Since the randomly distributed magnetic Mo<sup>5+</sup> ions (i.e., Mo<sup>5+</sup>: [Kr] 4d<sup>1</sup>) create the overlapped bound magnetic polarons (BMPs) via coupling with the charged VO defects, the degree of long-range ferromagnetic ordering could be enhanced in the  $\alpha$ -MoO<sub>3</sub>:Te solid state system. This enables us to demonstrate enhanced room-temperature ferromagnetism in ultrathin  $\alpha$ -MoO<sub>3</sub>:Te nanoflakes.

**Keywords:** MoO<sub>3</sub>, vapor phase epitaxy, ferromagnetic, nanoflakes

## POSTER SESSIONS

**Id-1560**

### **Investigation of Shielding Properties of Strontium-Bismuth Borate Glasses Doped DMSO and PMMA Smart Polymers for Gamma and Heavy Ions**

Derya Yilmaz Baysoy<sup>1</sup>

<sup>1</sup>Istanbul Aydin University, Electronic and Automation Department, 34295, Istanbul, Turkey

Corresponding author: dyilmazbaysoy@gmail.com

**Abstract:** In this study, gamma-ray shielding performance for mixtures obtained by adding 0.15SrO-(0.35-x) Bi<sub>2</sub>O<sub>3</sub>-xB<sub>2</sub>O<sub>3</sub> (x=0.10, 0.15, 0.20, 0.25 and 0.30) glass material to dimethyl sulfoxide (DMSO) and polymethyl methacrylate (PMMA) smart polymers were investigated. For this purpose, mass attenuation coefficients ( $\mu/\rho$ ), half-value and tenth value layers, mean free paths of ten mixtures were calculated in the photon energy range from 1 keV to 100 GeV and compared with. Also, the results of Monte Carlo simulations which were obtained by using MCNPX code for photon energies of 0.084, 0.511, 0.662, 1.173 and 1.332 MeV were found to be compatible with the XCOM data. Besides, the projected range and deposited energy values were calculated for heavy ions such as H, He and C using the SRIM code to examine some charged particle interactions.

**Keywords:** Shielding, DMSO, PMMA, Strontium Bismuth Borate Glasses, MCNP, XCOM, SRIM

## POSTER SESSIONS

**Id-1562**

### **Current State of Critical Raw Materials for Turkish Construction Sector**

Hamdi Tekin<sup>1</sup>, Ismail Cengiz Yilmaz<sup>2</sup>

<sup>1,2</sup>Istanbul Arel University, Istanbul, Turkey

Corresponding author: hamditekin@arel.edu.tr

**Abstract:** Depletion of natural resources leads majority of sectors seek new sources to reach raw materials. In addition to finding sustainable solutions, using raw materials efficiently is important. Critical Raw Materials (CRMs), which are determined and listed by European Commission, are of great importance for the continuity and future of the economy. Therefore, replacing such materials with alternative materials should be much more concerned. Construction sector drives many other sectors and leads the economy in many countries. In this study, a qualitative study has been conducted to highlight the current state of raw materials in construction sector in Turkey. Interviews have been held with experts working in a variety of construction fields. The aim of the study is to determine which raw materials are crucial, whether there is a problem for reaching raw materials, if research and development studies are conducted for replacing current raw materials for construction sector. In addition to this focus, the future role of CRMs for construction sector has been discussed. In conclusion, it has been apparently seen that the importance given to recycling processes for raw materials has increased, but measures especially against harms of concrete structures, which contribute to CO<sub>2</sub> emission and energy consumption considerably, are very limited. A number of big companies have some projects for energy efficiency and replacement of raw materials, but most of the stakeholders do not have any action. Turkey is especially rich in boron, magnesium, antimon, phosphate and graphite. CRMs play important role on construction materials and minimizing their usage and replacement is essential for the construction sector in order to keep the existing capacity and take action against future probable raw material problem.

**Keywords:** Critical Raw Materials (CRMs), Construction Sector, Construction Materials, Recycling

## POSTER SESSIONS

**Id-1566**

### **Weakly Nonlinear Gravity-Capillary Short Crested Interfacial Waves**

Allalou Nabil<sup>1</sup>, Debiane Mohammed<sup>2</sup>, Boughazi Dalila<sup>3</sup>

<sup>1</sup>Faculté de Physique, BP 32 El Alia, USTHB, Alger, ALGERIE

<sup>2</sup>Faculté de Physique, BP 32 El Alia, USTHB, Alger, ALGERIE

<sup>3</sup>Faculté des Sciences, Université de Boumerdes, ALGERIE

Corresponding author: n\_allalou2004@yahoo.fr

**Abstract:** Internal waves develop at the interface of two fluids of different densities. They are enjoying renewed interest in the international scientific community. This is directly related to the current limitations of ocean models. The understanding of internal waves at the fundamental level has gone through a phase of idealization where two-dimensional shapes have long been considered as a basic model to describe these waves. However, this is generally not the case in reality and the study of three-dimensional wave fields is essential for a more realistic description. The simplest form of these waves is the one resulting from the interaction of two wave trains of the same characteristics. The resulting wave field is periodic in two directions distinct from the horizontal plane. This work deals with the calculation of the properties of interfacial short crested gravity-capillary waves. To solve the problem, the perturbation method will be used, which offers the advantage of the possibility of highlighting harmonic resonances. We show that the resonance condition is function of the ratio of densities, surface tension, and thicknesses of the two layers as well as the angle of reflection. We focused on studying resonant solutions. They are characterized by the formation of wavelets giving an irregular structure to the wave.

**Keywords:** Gravity-capillary waves; Short crested waves; Harmonic resonance

## POSTER SESSIONS

**Id-1567**

### **Crystal Structure, Hirshfeld Surfaces, Optical and Thermal Behavior of Two $\alpha$ -Hydroxyphosphonate**

Louiza Quksel<sup>1\*</sup>, Riadh Bourzami<sup>2</sup>

<sup>1</sup>Laboratoire d'Electrochimie des Matériaux Moléculaires et des complexes (LEMMC), Département de génie des procédés, Faculté de Technologie Université Ferhat Abbas, Sétif-1, 19000. Algeria

<sup>2</sup>Emerging Materials Research Unit, Ferhat Abbas University Sétif-1, 19000. Algeria

Corresponding author: louksel2014@gmail.com

**Abstract:** The two  $\alpha$ -hydroxyphosphonate DHPMP and DH4MPMP have been synthesized and characterized successfully. A single crystal X-ray investigation of the two compounds revealed that the hydrogen bonding plays a key role in the formation of the elementary structure. Hirshfeld surface analysis was used to visualize the fidelity of the crystals structures. This method permitted the identification of individual types of intermolecular contacts and their impact on crystal packing. Molecules are linked by a combination of C H...H and C...H contacts, which have clear signatures in the fingerprint plots. The UV-Visible absorption spectrum shows that the crystal exhibits a good optical transmission in the visible domain, and strong absorption in middle ultraviolet one. The vibrational frequencies of various functional groups present in DHPMP and in DH4MPMP crystals have been deduced from FT-IR spectra and then compared with theoretical values performed with DFT (B3LYP) method using 631G (p, d) basis sets. Chemical and thermodynamic parameters such as ionization potential (I), electron affinity (A), hardness ( $\sigma$ ), softness ( $\eta$ ), electronegativity ( $\chi$ ) and electrophilicity index ( $\upsilon$ ), are also calculated using the same theoretical method. The thermal decomposition behavior of DHPMP and DH4MPMP, studied by using thermogravimetric analysis (TDG), shows a thermal stability until to 125°C.

**Keywords:** Hydroxyphosphonate, Single crystal, Hirshfeld surface, DFT calculation, TDG.

## POSTER SESSIONS

**Id-1572**

### **The Development and Applications of Nanostructural and Monocrystals Materials in Medical X-ray Technique**

Nikita Golovin<sup>1</sup>, Michail Taubin<sup>1,2</sup>, Natalya Koltunova<sup>1</sup>

<sup>1</sup>Federal State Unitary Enterprise "Science Research Institute "LUCH", Zheleznodorozhnaya st, Podolsk, Moscow region, 142100, Russia

<sup>2</sup>National Research Nuclear University MEPhI (Moscow Engineering Physics Institute), Kashirskoe highway 31, Moscow, 115409, Russia

Corresponding author: taubin@sialuch.ru

**Abstract:** Monocrystals and nanostructural materials using is allow getting a high value of X-ray radiation source operational and dozing characteristics.

Well known, that refractory metals, such as molybdenum, tungsten, rhenium and its alloys is widely using for cathodes and anodes in X-ray technique.

The fabrication of miniature X-ray radiation source (diameter of miniature X-ray tube is about 10-20 mm) and the apparatuses is based on them is one of the promising areas of modern x-ray technology development. Obviously, that reducing the size of x-ray sources leads to increased requirements for the performance of their designs elements. Therefore, when developing such sources, it is necessary to use materials with increased properties.

In this paper, a comparative analysis of the mechanical, emission and thermophysical characteristics of poly-and single-crystals refractory materials was held. It is shown that monocrystalline tungsten has a work function 4.4 eV, which allows to reduce the cathode operating temperature by a value of about 100 °C. At the same time, the monocrystalline materials characteristic features, such as density (close to theoretical), low concentration of impurity atoms contribute to reducing gas emission and increasing thermal conductivity in operating conditions, and their high resistance to high-temperature creep increases the performance characteristics.

Also it is shown that a single crystal of alumina oxide with high dielectric properties (electrical strength is about 30 kV/mm) can be used as a structural material for the miniature x-ray tubes body.

The research results of tungsten nanocomposite high temperature deformation in comparison with W-Ta single-crystal alloy at 2200 °C was presented.

Shown significantly high creep resistance of the tungsten nanocomposite, making it a preferred material for the X-ray tubes cathodes.

The presented materials were used in the development and manufacture of miniature x-ray tubes for medical purposes.

**Keywords:** X-ray tube, refractory materials, single crystalline, nanocomposite

**ALL SUBMISSIONS & TOPICS**

<b>Condensed Matter Physics</b>	Id 1319 - Heat Resistance of Conductive Filler-polymer Composites Evaluated by Dynamic Tensile Modulus under Electric Field and Dielectric Measurement
	Id 1422 - Effects of Perforation on Thin Superconducting Films
	Id 1429 - Dimension Effects in Insulating NbTiN Films
	Id 1502 - Effects of Material Constituent and Magnetic Field on Mechanical Properties of Magnetorheological Elastomers
<b>Crystallography</b>	Id 1410 - Challenges of the Inverse Problem of the X-ray Diffraction Tomography. Theory, Formulas and Computer Iterative Algorithms towards The 3D Recovery of Elastic Static Displacement Field around the Point-Defects in a Crystal
	Id 1539 - Syntheses, Spectroscopic and Crystallographic Characterizations of the Tetrapiperidino-2-pyridyl(N/O)spirocyclotriposphazene and Its Phosphazanium Salt
	Id 1540 - Syntheses, Spectroscopic and Crystallographic Characterizations of Protic Ionic Liquids (PILs) Containing 2-pyridyl Pendant Arm
	Id 1567 - Crystal structure, Hirshfeld Surfaces, Optical and Thermal Behavior of Two $\alpha$ -Hydroxyphosphonate
<b>Semiconductors Physics and Devices</b>	Id 1217 - Affinity-based Performance Analysis of Heterojunction p-i-n PV Cells
	Id 1257 - Simulation of Hole Transient Photocurrents
	Id 1443 - Photovoltaic Cells and Modules for Future Energy Systems
	Id 1491 - Calculation of Electromagnetic Radiation Absorption of a Small Conducting Inhomogeneous Cylindrical Particle Taking into Account the Isoenergetic Surface in the form of an Ellipsoid of Rotation for the Model of Fuchs Boundary Conditions
	Id 1499 - Experimental Research on the Response of a Sensory Detection Block in the Presence of Industrial Toxic Chemicals
<b>Ferroics and Multiferroics</b>	Id 1373 - Tunnel Electroresistance in Superconducting/Ferroelectric Junctions
	Id 1525 - Multiferroic Domain Walls in Ferroelastic Materials

<b>Magnetic Materials</b>	Id 1219 - Stress-induced Magnetic Anisotropy Enabling Engineering of Magnetic Softness and Domain Wall Dynamics of Fe-rich Amorphous Microwires
	Id 1228 - Magnetic Materials Based on Dinuclear Copper(II) Trimethoxybenzoates
	Id 1358 - Theoretical Study on Anisotropic Magnetoresistance Effect for Ferromagnets
	Id 1389 - Nanostructured Lanthanum Manganite Films Grown by Pulsed-injection MOCVD: Tuning the Magnetoresistive Properties for Magnetic Field Sensors Applications
	Id 1404 - Ferromagnetic Resonance Detection in Magnetic Single Objects via a Novel Microresonator and Microantenna Approach
	Id 1423 - Magnetic Catalysts and Their Applications
	Id 1556 - Ferromagnetism of Two Dimensional MoO <sub>3</sub> Doped with Te
<b>Computational Solid State Physics</b>	Id 1245 - Deformation Effect on the Structural and Energy Characteristics of Intermetallic NiAl and Ni <sub>2</sub> AlNb
<b>Nanoscience and Nanotechnology</b>	Id 1194 - Unraveling the Acoustic Exciton-phonons Interaction in a Single GaN/AlN Quantum Dot
	Id 1197 - Low field Microwave Absorption in Metal Nanoparticles Embedded Conducting Polymers
	Id 1200 - Magneto Transport in Metal Nanoparticles Embedded Conducting Polymer Nano Fibres
	Id 1324 - Blister Formation in Tungsten by Deuterium Ion Irradiation: Energy and Fluence Dependent Study
	Id 1353 - Transition Metal Oxide Materials with a Nonstoichiometry
	Id 1375 - The Influence of Twinning on the Tensile Properties of Nanocrystalline Light Weight Aluminum Alloys
	Id 1378 - Synthesis and Structural Characterization of Erbium Electrodepositing on Silicon Nanowires
	Id 1414 - The Transfer of Charges in Composite Cellulose-mineral oil-water Nanoparticle
	Id 1415 - Thermo-gravimetric Analysis of (FeCoZr) <sub>x</sub> (CaF <sub>2</sub> ) <sub>(100-x)</sub> Nanocrystalline Layers

	Id 1416 - Influence of Thermal Treatment on the Electric Properties of the Nanocomposite on the Base of Ferromagnetic Alloy FeCoZr and Dielectric Matrix CaF <sub>2</sub>
	Id 1519 - Modified TiO <sub>2</sub> Based Nanostructures for Photocatalysis
<b>Graphene and 2D Materials</b>	Id 1199 - Excitonic Properties in the Vertical Heterobilayer Semiconducting Transition Metal Dichalcogenides MoS <sub>2</sub> -WSe <sub>2</sub> within Wannier Mott Model
	Id 1478 - Uniaxial Compression and Buckling of Graphenes
	Id 1492 - The Lubrication Mechanism of Graphene as an Antiwear Additive at Elevated Temperatures
	Id 1507 - Introducing 2D Materials for Magnetic Tunnel Junctions
<b>Multifunctional Nanomaterials</b>	Id 1345 - Novel Types of Additively Manufactured Micro-architected Multifunctional Shell-based Cellular Materials
	Id 1557 - Mesoporous Silica Nanocomposites for Advanced Luminescent Chemosensor Materials: Design, Synthesis, Fabrication and Applications
<b>Nanoelectronics and Information Technology</b>	Id 1196 - ReRAM Based on Water Soluble Polymer Nano Composite
<b>Nanobiotechnology</b>	Id 1411 - Influence of Cholesterol on the Physico-chemical Properties of Phospholipid Membranes
	Id 1413 - Physico-chemical Study of Lipid Membranes, Containing Functionalized and Non-functionalized Single Wall Carbon Nanotubes
	Id 1421 - Comparison of Nanoscale Adhesion Energies, Forces, Pull-off Distances and Repulsion Energies Measured between Bacterial Cells and Silicon Nitride under Water by AFM
	Id 1468 - Electrochemical Oxidation of Glucose by Ni-Fe Nanoparticles Dispersed on Polyaniline Thin Films
	Id 1498 - Effect of Streptomyces sp. GBTUV5 on the Growth of Solanum Lycopersicum (Tomato)
<b>Layered and Composite Nanostructures</b>	Id 1472 - Effect of Concentration (Molarity) on ZnO Properties
<b>Nanofabrication</b>	Id 1361 - Self-assembly of Colloidal Nanoparticles Ag <sub>2</sub> S in Water Solution
	Id 1184 - Topology States of Iso-frequency Surfaces of a Hypercrystal with Ferrite and Semiconductor Layers

<b>Optical Physics, Quantum Electronics and Photonics</b>	Id 1348 - Enhancement of the RE <sup>3+</sup> Ions Luminescence in RE-Ag Co-doped Borate Glasses
<b>Materials Science &amp; Engineering</b>	Id 1138 - Investigating the Effects of Temperature on the Mechanical Properties of Austempered Ductile Iron Castings
	Id 1166 - Mechanical Properties of Austenitic Stainless Steel Welded by Laser and TIG
	Id 1167 - Evaluation of Harmless Crack Size using a Uniformized Equation Considering the Nonlinear Region of the Crack Tip
	Id 1171 - Environmental-friendly Composites Based on Natural Rubber and Plasticized Starch Obtained by Electron Beam Irradiation in the Presence of Polyfunctional Monomers
	Id 1172 - Flocculants for Water Treatment Obtained by Electron Beam Irradiation
	Id 1190 - Self-propagating High-temperature Synthesis of Fe <sub>2</sub> TiSn <sub>1-x</sub> M <sub>x</sub> (M= Hf, V, Zr, Si) Heusler Alloys with Following Spark Plasma Sintering
	Id 1193 - Effect of Rubber Crumb on the Behavior of Concrete Sand
	Id 1211 - The Boriding Treatment of XC38 Steel: Characterization and Optimization of the Paste Composition for Wear Resistance
	Id 1212 - Mechanical Behavior and Microstructure of Gas Pipelines Welded Joints Achieved with Hybrid Welding Process
	Id 1253 - Electrodeposition of Vanadium Oxides Films, for Lithium-ion Insertion
	Id 1263 - Enhanced Sensitivity of H <sub>2</sub> Gas Sensor Based on Nanostructured Amorphous Methylated Silicon Films
	Id 1296 - Designing Domain Walls in Bismuth Ferrite by Controlling the Type and Concentration of Defects
	Id 1372 - Molecular Dynamics Simulations of Separation Membrane Based on Super Carbonaceous Materials for Small Gas Molecules
	Id 1427 - Piezoelectric Nanogenerators Based on PVDF-HFP/ZnO-Mesoporous Silica Nanocomposites for Self-powering Devices
	Id 1436 - The Effect of Waste Frying Oil and Waste NBR on Physical Characteristics of Modified Bitumen
Id 1450 - Machining Challenges and Solutions to Aerospace Grade Composite-Titanium Stacks	

	Id 1460 - Improvement of the Sulfur Corrosion Resistance of Copper Windings by Using Grain Boundary Engineering (GBE) and Its Effect for Oil-Paper Insulation
	Id 1515 - Methods to Improve Fly Ash Reactivity and Increase Its Reuse Potential in Construction Materials Industry
	Id 1547 - Production of Enantioselective Alcohols by Phosphinite Ligands and Their Ruthenium(II) Complexes
	Id 1554 - Rheological Characterization of Hydrogel-like N, N, N-trimethyl Chitosan-based Polyelectrolyte Complexes
	Id 1572 - Development and Application of Nanostructural and Monocrystals Materials in Medical X-ray Technique
<b>Surfaces, Interfaces and Colloids</b>	Id 1376 - Giant Thermally Modulated and Stable Step Bunching on Epitaxially Grown SrTiO <sub>3</sub> Thin Films on Vicinal MgO (100) Terraces
	Id 1470 - Anti-icing Property of Nano-ZnO Superhydrophobic Surface Prepared via Radio Frequency Magnetron Sputtering on Aluminum Alloy
<b>Sol-gel Technology</b>	Id 1162 - Synthesis of Uvarovite Garnet Using Different Synthesis Routes
	Id 1379 - Structural and Optical Properties of Silicon Carbide Nanoparticles Produced by Sol-gel Method
<b>Thin Film Technology</b>	Id 1295 - Growth and Characterization of Cu <sub>2</sub> SnSe <sub>3</sub> Single Crystal by the Melting Method for Thin Film Solar Cells
	Id 1420 - Structural and Optical Study of Thin Films Based on Metal Oxide Nanocomposites ZnO-TiO <sub>2</sub> and NiO-TiO <sub>2</sub>
<b>Polymers and Amorphous Materials</b>	Id 1140 - $\beta$ -Relaxation Governs Damping Stability of Phenol/Acrylate Hybrids
	Id 1216 - Vortex Motion of an Incompressible Polymeric Liquid
	Id 1301 - Preparation of Synthetic Copper-oxidases Mimics by Molecular Imprinting within Suspension and Precipitation Polymers
	Id 1366 - Polymeric Micelles Based on Pluronics as Flavonoids' Nanocarriers
	Id 1385 - Thermal, Physicochemical and Rheological Properties of Biobased Plasticizers Combinations Used in Poly (Vinyl Chloride)
	Id 1469 - Advanced Polymeric Materials and Preserving of Polymer Objects
	Id 1485 - Advances in Polymer Enriched Concrete for Strengthening Concrete Roads and Airfields. _The Case of Green Overlays

	Id 1548 - Functional Block Copolymer Nanocarriers of Natural Polyphenols
<b>Ceramics and Glasses</b>	Id 1155 - The Influence of Dislocations on Crack Propagation in a Glass Material
	Id 1260 - Elaboration and Characterization of Porous Hydroxyapatite Materials via the Reaction-sintering of Phosphate and Aluminium Powder
	Id 1336 - Ageing Effect of DBD Activated Ceramic Powders: The Impact of Storage Humidity on the Electrophoretic Deposition Rate
	Id 1337 - Thermal Desorption Spectroscopy Investigation of DBD Plasma Modified Aluminium Oxide Submicron Powders
	Id 1446 - Optimizing the Migration Behavior of Vitreous Enamel Coatings
	Id 1447 - Investigation of Nickel Effects on Matt Cast Iron Enamel
	Id 1453 - Compositional Engineering of (Ba, Ca)TiO <sub>3</sub> -based Solid-solution Plates: Piezoelectric Characteristics and Phase Transitions Behaviour
	Id 1477 - Processing, Characterisation and Testing of Environmental Barrier Coatings for SiC/SiC CMCs
	Id 1555 - Formation Mechanism, Structure, Magnetic and Photocatalytic Properties of Aluminate and Ferrite Spinels
<b>Biomaterials</b>	Id 1428 - Production of Biodegradable Plastic Polyhydroxyalkanoates from Low-cost Substrates for Industrial Applications
	Id 1536 - Cu(I) Complexes Having Propionitrile and Pyridine Moieties: In-vitro Biological Study
	Id 1537 - Biological Properties of Some Transition Metal(II) Complexes Having a Pyridine Moiety
<b>Powder Metallurgy</b>	Id 1354 - Study on Microstructure and Properties of High-entropy Alloys Prepared by Powder Metallurgy
	Id 1355 - Microstructure and Properties of Ti(C,N)-TiB <sub>2</sub> -FeCoCrNiAl High-Entropy Alloys Composite Cermets
<b>Heat treatment</b>	Id 1527 - Measurement of Heat Transfer Coefficient in Interaction Zone of Multiple Liquid Jet Impingements
<b>Mechanical Behavior of Materials</b>	Id 1222 - About Rock Strength Certificate
	Id 1308 - Porous Lime Pastes with Improved Mechanical Properties after Addition of Synthetic Aragonite
	Id 1364 - Wave Propagation Behavior of Friction Welded Rods

	Id 1487 - Development of Computational Simulation Tools for Fatigue and Creep-fatigue Crack Growth in Metallic Alloys at Elevated Temperatures
	Id 1524 - Effect of Dynamic Strain Aging on Thermomechanical Response of High Strength Steels
<b>Science and Technology Composite Materials</b>	Id 1371 - Prediction and Modeling of the Mechanical Properties of the Laminate Hybrid Composite Material
<b>Nondestructive Evaluation of Materials</b>	Id 1356 - Fault Diagnosis Based on Enhancement of Barkhausen Noise Using Hybrid Method Empirical Mode Decomposition-Savitzky-Golay Filter
	Id 1254 - Morphological and Optical Parameters of Monolayers and Multilayers Porous Silicon Studied by Spectroscopic Ellipsometry
	Id 1352 - A Computational Model of Chemical Reactions Occurring During Thermal Desorption Spectroscopy
	Id 1357 - Dielectric and Thermal Analysis of a Leaf of Vegetation for the Modeling of Forest Fires
	Id 1374 - Micrographic and Chemical Characterization of Timimoun Quartz Deposits (Algeria)
	Id 1439 - Neutron Diffraction Analysis of Cold Rotary Swaged Tungsten Heavy Alloys and Other Engineering Materials at CANAM Infrastructure
<b>Computational Materials Science and Engineering</b>	Id 1154 - Computational Design of Novel High-capacity Mg-based Materials for Hydrogen Storage
	Id 1303 - On the Choice of the Geometrical Extrapolation Models for the Mg-Al-Sr System: Experimental Investigation
	Id 1335 - Prediction of Fatigue Lives of Aluminum Alloys Using Crystal Plasticity Framework
	Id 1451 - Thermal Configuration Modeling of a mc-Si Ingot Growth Furnace for Photovoltaic
<b>Engineering and Industrial Physics, Instrumentation Metrology and Standards</b>	Id 1506 - Estimation of Systematic Errors Committed when Approximating Length of Grain Boundaries Using Edges of Various Grid Patterns of EBSD Maps
<b>Advances in Instrumentation and Techniques</b>	Id 1495 - Testing the Sensitivity, Selectivity and tTme of Response of Some Polymeric Sensors in the Presence of Toxic Compounds Vapours

<b>Applied Non-linear Physics</b>	Id 1566 - Weakly Nonlinear Gravity-capillary Short Crested Interfacial Waves
<b>Separation and Purification Processes</b>	Id 1494 - Experimental Research Regarding the Decontamination of Toxic Compound Aqueous Solutions by Plasma Treatment
	Id 1508 - Experimental Researches Regarding the Treatment of Industrial Wastewater Using Unconventional Techniques
<b>Finite Element Analysis</b>	Id 1322 - Modal Analysis and Natural Frequencies for Helicopter Rotor Blade
	Id 1386 - Analytical and Numerical Analysis of Twin Helical Spring with Circulaire Cross Section
<b>Quantum, Atomic and Nuclear Physics</b>	Id 1417 - Quantum Supersymmetry Applied to a Linear Energy Dependent Potential: Projection Method
<b>Radioactivity and Radiochemistry, Radiation Protection and Safety Issues</b>	Id 1247 - Radionuclide Characterization of Tritiated Water Using NMR Spectrometry
	Id 1248 - Determination of Tritium Contents in Stainless Steel Samples Using full Combustion Method
	Id 1255 - Determination of Radioactive Concentration of Tritiated Water Using EPR Spectrometry
	Id 1262 - X-ray Exposure Configuration and Dose Measurements at Different Thicknesses of Water Layer Using Individual Dosimeter
	Id 1560 - Investigation of Shielding Properties of Strontium-Bismuth Borate Glasses Doped DMSO and PMMA Smart Polymers for Gamma and Heavy Ions
<b>Nuclear Sciences and Engineering</b>	Id 1225 - Crystallization and Properties Degradation in Ultrathin Amorphous HfO <sub>2</sub> Films Induced by Swift Heavy Ions
	Id 1227 - Irradiated Effects in Few- and Mono-layer MoS <sub>2</sub> Induced by Heavy Ions
	Id 1249 - Gamma-rays Shielding Properties of Heavy Concrete with Barite and Tungsten Aggregate
	Id 1521 - Numerical Estimation of Nuclear Decay Heat from Induced Neutron Fission of U-235 and Pu-239
<b>Plasma Physics, High-energy Physics and Particle Physics</b>	Id 1142 - The Effects of Superstatistics on Nonthermal and Suprathermic Distributions
	Id 1380 - Mass Spectrum of Charmonium Meson Using an Energy-dependent Potential and the Quantum Supersymmetry

<b>Pharmacology</b>	Id 1448 - Synthesis, Anti-inflammatory Activity of 3-Amino 6-Methoxyl 2-methyl quinazolin-4(3H)-One and 3-Amino 6-Methoxyl -2-methyl of 4H-benzo[d] [1,3]-Oxazine-4-one
<b>Materials &amp; Steel</b>	Id 1151 - Valuation of Mill Scale as Anticorrosive Pigment
	Id 1562 - Current State of Critical Raw Materials for Turkish Construction Sector
<b>Chemical Manufacturing</b>	Id 1338 - A Comparative Electrochemical Study on Corrosion Inhibition by Méthoxy Carbonyl Triphenyl Phosphonium Bromide in Acid Media HCl 1M
<b>Electronics</b>	Id 1363 - Electromagnetic Wave Propagation of Double Walled Wires
<b>Energy, Utilities &amp; Environment</b>	Id 1158 - Numerical Comparison between Single and Twin Jets
	Id 1179 - Effects of Rotary Tubes on Aerodynamic Forces in Tube Bundles
	Id 1346 - Dynamic Analysis of the Effect of a Wall on the Wake Behaviour in the Fluid Flow behind Cylindrical Obstacle
	Id 1397 - Modeling and Optimization of Experimental Parameters for the Removal of Heavy Metal and Production of Porous Adsorbents by RSM and ANN Techniques
	Id 1513 - Statistic Model of Mobile Services Channel Power Density Estimation for RF Energy Harvesting
<b>Engineering</b>	Id 1323 - Determination of the Natural Frequencies for a Light Aircraft Engine Suspension
	Id 1493 - Role of Auxetic Composites in Protection of Building Materials and Structures
	Id 1504 - Structural Acrylate Adhesive Joints for Civil Engineering Use
	Id 1520 - Viscoelastic Properties of Selected PVB Interlayers for Laminated Glass